THERMAL CONDUCTIVITY OF DENSE FLUIDS

A thesis presented for the Degree of
Doctor of Philosophy
in the Faculty of Engineering
University of London

by

Rafael Kandiyoti, B.S.

Department of Chemical Engineering
and Chemical Technology,
Imperial College
of Science and Technology,
London S.W.7.

August 1969.

ABSTRACT

The transient hot wire cell technique has been used to build an apparatus for measuring the thermal conductivity of liquids, at pressures up to 7000 atmospheres, in the temperature range 25-100°C. Measurements have been made on toluene with an estimated accuracy of 2 to 5% over the pressure range. The analysis of the data has been developed by solving the heat conduction equation assuming variable physical properties for the test fluid. In the solution of this non-linear equation, the Kudryashev-Zhemhov transformations have been used.

The theory of Horrocks and McLaughlin, on the thermal conductivity of simple liquids has been extended to chain molecules and the model compared with data on the normal paraffin homologous series.

The Chapman-Enskog theory, on the transport coefficients for binary mixtures of dense systems has been combined with the Lebowitz radial distribution functions derived in the Percus-Yevick approximation. The kinetic, collisional and distortional contributions have been factorized and the model compared with real systems.

Acknowledgements

It is a pleasure to thank Professor A. R. Ubbelohde, C.B.E., F.R.S., for his interest in this work.

I wish to thank Dr. E. McLaughlin, for his supervision, help and advice.

I would also like to thank Mr. Russell Harris, Mr. John Oakley, Mr. Len Tyley and the staff of the Departmental workshop for their constant help and cooperation.

Last but not least I wish to thank Miss. C. Thurlow for her typing and help.

A paper based on Chapters 8 and 9 of this work

has been accepted for publication by Molecular Physics.

CONTENTS

CHAPTER 1
INTRODUCTION

The thermal conductivity of liquids is a subject of interest both for the scientist and the engineer. Data is required for engineering design purposes, and for testing the validity of statistical mechanical models of dense fluids. At present, there is need in science and technology for more data as well as for more accurate data.

In the measurement of the thermal conductivity coefficient, there still seems to be problems that have not been solved or avoided satisfactorily. So far none of the various techniques utilized for measurements of thermal conductivity can be claimed to have completely isolated the conductive contribution to heat transfer from the radiative and convective contributions. Also in measurements on mixtures, there is the complicating effect of thermal diffusion.

On the other hand, theoretical predictions of thermal conductivity are far from perfect; agreement to 15% is considered reasonable. This does not mean however that the present levels of accuracy in thermal conductivity measurements are adequate so far as theory is concerned. A great deal of information can be obtained from comparing calculated and experimental values of rates of change

of the conductivity with temperature and density; there available data is in many cases deficient.

A great deal of information on liquid structure can also be obtained by extending the data range to high pressures, which affords the evaluation of structural models over wide ranges of density. In particular the change of sign from negative to positive, of the temperature coefficient of thermal conductivity, at high densities is an important index of the success or failure of thermal conductivity theories.

The transient hot wire cell chosen here for thermal conductivity measurements at high pressure has several advantages over other techniques of measurement. While no attempt will be made here to compare in detail charachteristics of the various techniques, as relative merits have been discussed extensively by Ziebland (Ref. 1) and Pittman (Ref. 2), two advantages of the transient hot wire cell which have not been discussed before must be mentioned here. The first is the adaptability of the hot wire cell to high pressure techniques. The physical size and limiting dimensions of the hot wire cell are such that the one designed for this work was accommodated in

a conventional 1.5" ID, 6" OD pressure vessel with a range of up to 7000 atmospheres. Co-axial cylinder and particularly flat plate techniques require rather larger pressure vessels. This complicates problems related to construction and sealing.

The second advantage of the technique is its suitability for measurements on mixtures. Approach to the state in the presence of a temperature gradient leads to the setting up of concentration gradients because of thermal diffusion. It is to be expected that the short duration of the experiments with the transient hot wire cell (20 - 30 seconds) will go a long way to prevent partial separation from affecting the measured thermal conductivity values.

In this work, the apparatus designed and constructed for high pressure measurements will be described and data on toluene for pressures up to 6250 atmospheres over a temperature range of 30 to 90°C presented. The analysis of the data is based essentially on the work of Horrocks and McLaughlin (Ref. 5) and Pittman (Ref. 2). Here however, in analyzing the data, effects relating to the temperature dependance of the thermal conductivity coefficient, and the change in power supplied to the system are treated as part of the mathematical statement describing the

system. This implied solving a non-linear partial differential equation. The method used for this particular application was also examined as a tool for solving partial differential equations with temperature dependent physical properties.

While on the one hand an apparatus has been designed, constructed and tested for measuring thermal conductivities of pure and mixed liquids, and certain improvements made in the analysis of the data, attention has also been paid to the theory of transport properties of liquids.

The hot wire technique can be used for measuring the thermal conductivity of non-polar, non-conducting liquids. (The method has also been extended to gases; that however is beyond the scope of this work.) The most important single group among these is the normal paraffin homologous series. Here the Horrocks and McLaughlin model (Ref. 3) for the thermal conductivity of simple liquids has been extended to liquids composed of chain molecules by using Prigogine's cell model for pure polymers. (Ref. 4). As will be seen, the thermal conductivity, in this approximation, is a function only of the molecular force constants and the density. Hence calculation of λ as a function of pressure follows from data on high

pressure densities for the homologous series. Results for atmospheric pressure calculations will be presented here, but not those for high pressure, as data is not available for comparison. It must be said however that the temperature coefficient of thermal conductivity does not go through a sign inversion for calculations up to 10,000 atmospheres.

As mentioned before, the fact that the hot wire method is a transient one makes it particularly useful for measurement on liquid mixtures. This is because for a mixture in a non-uniform temperature field, there exists a velocity of diffusion in the direction of the temperature gradient. The mass flux is then given by

$$J_M = D_{12} \frac{\partial x_1}{\partial r} + D_T \frac{\partial \ln T}{\partial r}$$

where x_1 is the mole fraction of component 1

r is the position variable

D_{12} is the mutual diffusion coefficient.

and D_T is the thermal diffusion coefficient.

The potential availability of a technique for satisfactory thermal conductivity measurements on liquid mixtures raises the question of the state of theories on the transport properties of dense fluid mixtures. The most general theory to date has been

that of Chapman and Enskog (Ref. 6). The derived equations have been generalized to dense fluid mixtures by Thorne (Ref. 6a). The work is based on the rigid sphere interaction potential and as such, can be combined with the radial distribution functions of Lebowitz (Ref. 7) derived by using the Percus Yevick approximation (Ref. 8).

This analysis was first used on mutual diffusion in binary mixtures by McLaughlin (Ref. 9). Here it is extended to thermal conductivity, viscosity and thermal diffusion. While the treatment, on the whole, does broadly reproduce charachteristics of liquid mixtures observed experimentally, better quantitative agreement must wait for the treatment to be applied to more realistic intermolecular interaction potentials.

The Lebowitz radial distribution functions were also used in recalculating results from the theory of Longuet-Higgins, Pople and Valleau (Ref. 10), for isotopic mixtures. While for the mutual diffusion, thermal conductivity and viscosity coefficients, equations resulting from the two theories are at least partly related, for thermal diffusion there seems to be no correspondance. Furthermore neither one of the two theories gives satisfactory results when compared with experiment. This is to be expected as the thermal diffusion coefficient is particularly sensitive to the form of the intermolecular interaction potential.

CHAPTER 2

Theory of the Transient Hot Wire Cell

1 Introduction

The experimental technique is based on the measurement of the voltage change across a thin wire carrying a current and immersed in a test fluid. The wire is joined to thick current leads, top and bottom, and at distances conveniently removed from its ends, welded to two voltage taps.

In order to determine the thermal conductivity of the test fluid from this system, the heat conduction equation appropriate to the system will be obtained, and solved for the temperature profiles in the thermal conductivity cell; the temperature profiles will then be related to electrical measurements. In addition, any approximations made in the derivation of the heat transfer equation and the solution will be examined.

2. The General Equations of Heat Transfer

The equation of thermal energy (Ref 1) in the absence of radiative heat transfer is given by

$$\rho \frac{DU}{Dt} = - (\nabla \cdot \underline{q}) - P(\nabla \cdot \underline{v}) - (\tau : \nabla v), \qquad (1)$$

where the rate of gain of internal energy equals the sum of three terms which are successively:

1) heat input by conduction

2) reversible energy increase by compression and,

3) irreversible energy increase by viscous dissipation.

In order to reduce equation (1), to the desired form, the following ralationship, derived from the first and second laws of thermodynamics is used:

$$\rho \frac{DU}{Dt} = \left[-P + T\left[\frac{\partial P}{\partial T}\right]_v \right] \rho \frac{DV}{Dt} + \rho C_v \frac{DT}{Dt}. \qquad (2)$$

Here the operator D/Dt is defined by

$$\frac{D}{Dt} = \frac{\partial}{\partial t} + v_x \frac{\partial}{\partial x} + v_y \frac{\partial}{\partial y} + v_z \frac{\partial}{\partial z} \qquad (3)$$

Combining eq. (2) with the Equation of Continuity

$$\frac{D\rho}{Dt} = - \rho (\nabla \cdot v) \qquad (4)$$

equation (1) can be written in the form

$$\rho\, C_v \frac{DT}{Dt} = -\,(\underline{\nabla}\cdot\underline{q}) - T\left(\frac{\partial P}{\partial T}\right)_v (\underline{\nabla}\cdot\underline{v}) - (\underline{\tau}:\underline{v}) \quad (5)$$

which in turn can be reduced by the substitution of Newtons and Fourrier's Laws to

$$\rho\, C_v \frac{DT}{Dt} = \underline{\nabla}\cdot(\lambda\underline{\nabla}T) - T\left(\frac{\partial P}{\partial T}\right)_v (\underline{\nabla}\cdot\underline{v}) + \chi \quad (6)$$

where χ is called the dissipation function (Ref 1). Equation (6) can be further reduced by using

$$\left(\frac{\partial P}{\partial T}\right)_v = \frac{\alpha}{\beta_T} \quad ; \quad C_p - C_v = \frac{\alpha^2 T}{\rho\, \beta_T}$$

and

$$-d\rho = -\rho\,\beta_T\, dP + \rho\,\alpha\, dT$$

where

$$\alpha = +\frac{1}{V}\left(\frac{dV}{dT}\right)_p \quad , \quad \beta_T = -\frac{1}{V}\left(\frac{\partial V}{\partial P}\right)_T$$

to

$$\rho\, C_p \frac{DT}{Dt} = \underline{\nabla}\cdot(\lambda\underline{\nabla}T) + T\,\alpha\,\frac{DP}{Dt} + \chi \quad \cdot (7)$$

(Ref. 2)

Equation (7) describes the behaviour of the experimental system but is mathematically intractable. It is therefore further reduced by using physical arguments.

As heat is supplied to the central wire, expansion of the liquid around the heated section gives rise to

radially symmetric free convection. Hence the operator D/Dt reduces to

$$\frac{D}{Dt} = \frac{\partial}{\partial t} + v_z \frac{\partial}{\partial z}$$

where z is the axis along the length of the wire. Furthermore due to the existence of a heating section below the bottom voltage tap, the rising liquid surrounds the mid-section of the heating wire, still retaining the temperature distribution that would have existed in the absence of convection, until cold liquid rising from below the heated section reaches the bottom tap. Hence before cold liquid reaches the bottom tap

$$\frac{\partial T}{\partial z} = 0 \text{ and } \frac{DT}{Dt} = \frac{\partial T}{\partial t}$$

Clearly, this simplification imposes a time limit on the duration of the experiment.

Using a set of assumptions fully discussed in a later section of this chapter, the velocity of the fluid along the z-axis has been calculated (Ref. 3 and Ref. 4a). Using these results and toluene properties it has been shown in Appendix 1A that the term $T \alpha DP/Dt$ can be neglected. It has also been found (Ref. 4b) that the viscous dissipation term χ is negligible, under the relevent conditions. Equation (7) then reduces to

$$\rho C_p \frac{\partial T}{\partial t} = \underline{\nabla} \cdot (\lambda \underline{\nabla} T) \qquad (8)$$

3. Solution of the Heat Conduction Equation for the Hot Wire Cell.

In order to relate the temperature changes in the cell to the thermal conductivity that is being measured, it is necessary to solve the heat conduction equation. In the first approximation the following is assumed:

a) Free convection and viscous dissipation effects are negligible.

b) The heat source is of infinite length and zero diameter (line source). This assumption will be removed as more refined solutions to equation (8) are derived.

c) The fluid medium is externally unbounded, and the limiting value of the temperature, sufficiently far away from the heat source, is zero.

d) Physical properties of the test fluid are temperature independent.

e) Power dissipation, q_1, per unit length of heat source is constant. The last two assumptions will also be subsequently removed. Lastly

f) Radiative heat transfer is negligible.

The solution of eqn. (8) under these conditions is well known (Ref. 5a).

$$T(r,t) = -\frac{q_1}{4\pi\lambda} \quad Ei\left[-\frac{r^2}{4kt} \right] \tag{9}$$

where $-Ei\ (-x) = \int_x^{\infty} \frac{e^{-u}}{u}\, du$

and $K = \frac{\lambda}{\rho C_p}$. Clearly, $T(r,t)$ is referred to the initial temperature. For large t, eqn. (9) reduces to

$$T(r,t) = -\frac{q_1}{4\pi\lambda} \left[\ln \frac{4Kt}{Cr^2} \right] \tag{10}$$

where $C = \exp(\gamma)$ and γ is Euler's constant.

If the heat source is assumed to be a cylinder of infinite length, uniform diameter and infinite thermal conductivity the solution becomes (Ref. 5b)

$$T(a,t) = \frac{q_1}{4\pi\lambda} \left[\ln \frac{4\tau}{C} + \frac{1}{2\tau} + \left(\frac{\alpha-2}{\alpha} \right) \frac{1}{2\tau} \ln \frac{4\tau}{C} + \ldots \right] \tag{11}$$

where $\alpha = 2(\rho' C_p' / \rho C_p)$ and $\tau = \frac{Kt}{r^2}$

In obtaining equation (11) surface resistance to heat conduction is assumed to be negligible.

4. Temperature Dependent Physical Properties

We now remove assumption (d) as well as (b), and assume linear temperature dependences for thermal conductivity, density and specific heat.

$$\lambda = \lambda_1(1 + \lambda_2' T) \quad ; \quad \lambda_2' = \frac{1}{\lambda_1} \frac{d\lambda}{dT} \tag{12a}$$

$$\rho = \rho_1(1 + \rho_2' T) \quad ; \quad \rho_2' = \frac{1}{\rho_1} \frac{d\rho}{dT} \tag{12b}$$

$$C_p = C_{p1}(1 + C_{p2}' T) \quad ; \quad C_{p2}' = \frac{1}{C_{p1}} \frac{dC_p}{dT} \tag{12c}$$

where the subscript 1 denotes the properties at the initial temperature. The problem can now be stated follows:

$$\rho \; C_p \; \frac{\partial T}{\partial t} = \underline{\nabla} \cdot (\lambda \; \underline{\nabla} \; T) \tag{13}$$

with initial conditions

$$\left.\begin{aligned} T(r, 0) &= 0 \\ \frac{dT}{dr}(r, 0) &= 0 \end{aligned}\right\} \quad r \geq a \tag{14a, 14b}$$

and boundary conditions (Ref. 6)

$$2\pi a\lambda \left.\frac{\partial T(a,t)}{\partial r}\right. + q_l = \pi a^2 \rho' C_p' \frac{\partial T(a,t)}{\partial t} , \tag{15}$$

where ρ' and C_p' are the density and specific heat of the wire respectively, and

$$T(a, t) = f(t), \tag{16a}$$

$$\lim_{r \to \infty} T(r, t) = 0 \quad \text{for finite } t. \tag{16b}$$

f(t) is obtained as data during the experiment. Given equations (12), the problem stated above is nonlinear.

We will now use a set of linearization transformations (Ref. 7) to obtain the linear analog of the problem, the solution to which, of course, is similar to eqn. (11), and then invert the solution.

Consider the specific enthalpy, as referred to the initial temperature

$$dh = C_p \, dT$$

and define through h, the quantity ϕ such that

$$\phi = \int_0^h \frac{\lambda}{\rho C_p} \, dh.$$

Using the last two equations

$$d\phi = \frac{\lambda}{C_p} \, dh = \lambda dT \tag{17}$$

from which it follows that

$$\frac{d\phi}{dr} = \lambda \frac{dT}{dr} \text{ and } \underline{\nabla}^2 \phi = \underline{\nabla} \cdot (\lambda \, \underline{\nabla} T) \tag{18}$$

Furthermore, we define the quantity ξ, such that

$$\xi = \int_0^t \frac{\lambda}{\rho C_p} \, dt \; ; \; d\xi = \frac{\lambda}{\rho C_p} \, dt \; . \tag{19}$$

Through equations (17) - (19), equation (13) can be transformed to

$$\frac{\partial \phi}{\partial \xi} = \nabla^2 \phi \tag{20}$$

The initial and boundary conditions are also transformed:

$$\phi\,(r,\,0) = 0\;;\;\phi'\,(r,0) = 0 \qquad (21)$$

$$\lim_{r \to \infty} \phi\,(r,\,\xi) = 0 \qquad (22)$$

and

$$2\pi a\,\frac{d\phi}{dr} + q_1 = \frac{2\pi a^2}{\alpha}\,\frac{d\phi}{d\xi}\;;\quad r = a\,. \qquad (23)$$

Here α is assumed to be constant with temperature. This is further discussed in Appendix 2.

So far we have used a set of transformations to linearize the nonlinear system of equations (12) - (16). The linearized problem has been solved by the Laplace Transform technique (Ref. 5b):

$$\phi(r,\,\xi) = \frac{q_1}{4\pi}\left[\ln\frac{4\tau}{C} + \frac{1}{2\tau} + \left(\frac{\alpha-2}{\alpha}\right)\frac{1}{2\tau}\ln\frac{4\tau}{C} + \ldots\right] \qquad (24)$$

where $\tau = \xi/r^2$. With the exception of τ and absence of λ, this is identical to equation (11). We must now perform the back-transformation.

Combining equations (12a) and (18) we have

$$\frac{d\phi}{dr} = \lambda_1\,\frac{dT}{dr} + \lambda_2\,T\,\frac{dT}{dr}\,, \qquad (25)$$

where

$$\lambda_2 = \lambda_1\,\lambda'_2 = \frac{d\lambda}{dT}$$

Integrating both sides from r to ∞

$$\phi(\infty, \xi) - \phi(r, \xi) = \lambda_1 [T(\infty,t) - T(r,t)] + \frac{\lambda 2}{2} [T^2(\infty,t) - T^2(r,t)] \quad (26)$$

Using equations (15b) and (21)

$$\phi(r, \xi) = \lambda_1 T(r,t) + \frac{\lambda 2}{2} T^2(r,t) \quad (27)$$

where $\phi(r, \xi)$ is given by equation (23). In particular

$$\phi(a, \xi) = \lambda_1 T(a,t) + \frac{\lambda 2}{2} T^2(a,t). \quad (28)$$

Throughout the treatment ξ is given by

$$\xi = \int_0^t \frac{\lambda}{\rho C_p} \, dt.$$

Using equations (12a) - (12c) and letting r = a

$$\xi = \frac{\lambda_1}{\rho_1 C_{p1}} t + \int_0^t \frac{\lambda_2 T(a,t)}{[1 + \rho_2 T(a,t)][1 + C_{p2} T(a,t)]} \, dt \quad (29)$$

The second terms on the right hand side of equations (28) and (29) constitute the total correction for the case of variable physical properties, under the given set of assumptions. Neglect of these terms would reduce the set of equations (24), (28) and (29) to equation (11).

An upper limit to the value of the integral in the rhs of equation (29) can be calculated by making use of the physical properties of toluene and the magnitude of the temperature rise in the cell. This calculation is presented

in Appendix 1.B, and shows that neglect of the integral introduces an error of the order of .01% into the thermal conductivity measurement. For this application then

$$\xi = (\lambda_1/\rho_1 C_{p1})\, t = Kt \qquad (30)$$

where K is the thermal diffusivity. Combining equations (24), (28) and (30) we get

$$\frac{q_1}{4\pi}\left[\ln\left(\frac{4\tau}{C}\right)+\frac{1}{2\tau}+\left(\frac{\alpha-2}{\alpha}\right)\frac{1}{2\tau}\ln\left(\frac{4\tau}{C}\right)+\ldots\right] = \lambda_1 T(a,t)+\frac{\lambda_2}{2}T^2(a,t),$$

where

$$\tau = \frac{Kt}{a^2}$$

5. The Case of a Time Dependent Heat Source

In the previous section the heat conduction equation has been solved with the assumption that heat input into the system is constant throughout the experiment. As the current remains substantially the same, and the wire resistance changes by about .01 to .02 ohms during a run, we know that q_1 ($=I^2 R/l$) is a weak function of time. We will now assume this dependence to be of quadratic form,

$$q_1 = q_1 + q_2 t + q_3 t^2 \qquad (31)$$

and solve the heat transfer problem of equations (12) - (16)

with the altered boundary condition:

$$2\pi a \frac{\partial \phi}{\partial r} + (Q_1 + Q_2 \xi + Q_3 \xi^2) = \frac{2\pi}{\alpha} \frac{d\phi}{d\xi}; \quad r = a \qquad (32a)$$

where

$$Q_i = \frac{q_i}{K^i} \qquad (32b)$$

It must be noted that in equations (32a) and (32b) the approximation of equation (30) has been used.

The derivation of the temperature profiles under these conditions is rather lengthy and will be presented here only in outline form; the full treatment may be found in appendix 2.A.

After linearizing the problem as before, the Laplace-transform of the heat conduction equation and the boundary conditions are taken:

$$\frac{\partial^2 \bar{\phi}(r,s)}{\partial r^2} + \frac{1}{r} \frac{\partial \bar{\phi}(r,s)}{\partial r} = r\bar{\phi}(r,s) \qquad (33)$$

$$2\pi a \frac{\partial \bar{\phi}(a,s)}{\partial r} + \frac{Q_1}{s} + \frac{Q_2}{s^2} + \frac{2Q_3}{s^3} = \frac{2\pi a^2}{\alpha} s\bar{\phi}(a,s) \qquad (34)$$

$$\lim_{r \to \infty} \bar{\phi}(r,s) = 0. \qquad (35)$$

Here s is the complex variable of the transformation, $\bar{\phi}(r,s)$ is the Laplace transform of $\phi(r,t)$, and α, as before, is assumed to be constant. Solving equations (33) - (35) for $\bar{\phi}$ we obtain

$$\bar{\phi}(r,s) = \frac{(Q_1 + Q_2/s + 2Q_3/s^2)}{2\pi as} \frac{K_o(r\beta)}{[\beta K_1(\beta a) + \frac{as}{\alpha} K_o(\beta a)]} \qquad (36)$$

By inverting equation (47) back into the real plane, using equations (28) and (30), dropping small terms in the second and third brackets, and rearranging, we have

$$\lambda_1 T(a,t) + \frac{\lambda_2}{2} T^2(a,t) = \qquad (37)$$

$$\frac{q_1}{4\pi}\left[\ln\frac{4Kt}{Ca^2} + \frac{a^2}{2Kt} + \frac{\alpha-2}{\alpha}\frac{a^2}{2Kt}\ln\frac{4Kt}{Ca^2} + \cdots\right]$$

$$+ \frac{q_2}{4\pi}\left[t\left[\ln\frac{4Kt}{Ca^2} - 1\right] + \cdots\right]$$

$$+ \frac{q_3}{4\pi}\left[t^2\left[\ln\frac{4Kt}{Ca^2} - 3/2\right] + \cdots\right]$$

Again by setting q_2, q_3 and λ_2 equal to zero, equation (11) can be obtained.

In deriving equation (37), some of the simplifying assumptions of section 3. have been dropped. We must now go on to examine the remaining ones.

6. Effect of the External Boundary

Equation (37) has been derived with the assumption that an infinite medium surrounds the central cylinder. The duration of the experiment, then is limited to times beyond which heat loss to the outer walls significantly distorts the temperature profile in the cell. The equation of heat conduction has been solved (Ref. 8) for a bounded medium, under the following conditions:

a) A non-convecting medium is bounded internally and externally by two infinitely long concentric cylinders, with radii a and b respectively.

b) Power is dissipated from the central cylinder, at the constant rate of $q_1/2\pi a$ for $t \geq 0$.

c) The external cylinder is held at the initial temperature.

d) Physical properties are assumed to be temperature independent over the temperature rise in question.

The solution of the heat conduction equation is then given by

$$T(a,t) = \frac{q_1}{4\pi}\left\{ \ln \frac{b}{a} + \pi \sum_{n=1}^{\infty} \exp\left[-\left(\frac{Kx_n}{a}\right)^2 t\right] \frac{J_0(x_n)Y_1(x_n) - Y_0(x_n)J_1(x_n)}{x_n\left\{\left[\frac{J_1(x_n)}{J_0(x_n\sigma)}\right]^2 - 1\right\}} \right\}$$

where $\sigma = \frac{b}{a} > 1$, n is the running index n = 1, 2, ...

and the x_n satisfy the equation

$$J_o(\sigma x_n)\, Y_1(x_n) - Y_o(\sigma x_n)\, J_1(x_n) = 0 \qquad (39)$$

where J_k and Y_k are Bessel functions of the first and second kinds, of order k respectively. For large values of t, equation (38) reduces to

$$T(a,t) = \frac{q_1}{2\pi\lambda}\left\{ \ln\frac{b}{a} - 2\sum_{n=1}^{\infty} \frac{\exp -(Kx_n/a)^2 t}{x_n\left[\left(\frac{J_1(x_n)}{J_o(x_n\sigma)}\right)^2 - 1\right]} \right\} . \qquad (40)$$

When b>> a, using (Ref. 8 and Ref. 9).

$$\lim_{z\to 0} J_k(z) \doteq (\tfrac{1}{2}z)^k / \Gamma(k+1)$$

$$\lim_{z\to 0} Y_k(z) \doteq -(\frac{1}{\pi})\, \Gamma(k)(\tfrac{1}{2}z)^{-k}$$

where for k an integer

$$\Gamma(k) = (k-1)! \quad ,$$

along with equation (39) leads to

$$\frac{J_o(\sigma x_n)}{Y_o(\sigma x_n)} = -\frac{\pi}{4} x_n^2 \qquad (41)$$

and

$$J_1(x_n)\, Y_1(x_n) = -\frac{1}{\pi} \quad . \qquad (42)$$

Combining equations (39) - (42) leads to

$$T(a,t)=\frac{q_i}{2\pi\lambda}\left\{\ln\frac{b}{a}-2\sum_{n=1}^{\infty}\frac{\exp-(Kx_n/a)^2t}{\left[\frac{2}{\pi J_o(\sigma x_n)}\right]^2-x_n^2}\right\} \qquad (43)$$

where in this approximation $x_n\sigma$ satisfy the transcendental equation

$$J_o(x_n\sigma)=0.$$

(Ref.8).

Equation (43) will be referred to, when cell design requirements are considered.

7. End Effects.

The assumption of infinite wire length must now be examined. Heat generated in the small diameter, high resistance section of the wire is conducted away by the current and potential leads. Heat loss through the former may be rendered negligible by leaving a suitable length of heating wire between the ends of the section where voltage changes are monitored, and the thick leads leading out of the cell. The following method has been used to estimate this length. (Ref. 10a and Ref. 5c).

The two ends of the wire, of length 2L, are assumed to be kept at zero temperature, and also surrounded by an

enclosure at zero temperature. The temperature distribution, in the steady state, along the length, $0 \leq x \leq 2L$, for constant power, q_l, supplied to the wire is then given by

$$T_f(z) = \frac{q_l}{2\pi a H} \left\{ 1 - \frac{\cosh M(L - z)}{\cos ML} \right\} \tag{44}$$

where H is the heat transfer coefficient given by (Ref. 4c)

$$H = 2\lambda / a \ln \frac{4\tau}{C} \quad ; \quad \tau = Kt/a^2 \tag{45}$$

and

$$M = (2H/\lambda_w a)^{\frac{1}{2}} \tag{46}$$

where λ_w is the thermal conductivity of the wire. In equation (45) the steady state temperature at the wall has been approximated by the "line source" solution of equation (10). The value of δ for which

$$T_f(L) - T_f(2L - \delta)$$

is much less than .01% of $T_f(L)$ has been calculated (Ref.10a) to be about 1 cm; the error rises rapidly to .6% for $\delta = .2$ cm. (Ref. 4d).

Heat conduction away from the potential leads had initially been treated (Ref. 12) as cooling fins and the error neglected. Pittman estimated the error in the thermal conductivity measurement due to these losses, on a scaled up model (Ref. 4e)

for an essentially stationary fluid. The resulting calculation shows that for toluene measurements, errors would be about .3 - .4% over the pressure range. This seems to be an underestimation, for reasons to be discussed in the next chapter. Still, however it is possible to minimize this error by extrapolating λ vs. t data to zero time, as the error due to end effects grows with time.

8. Convection.

While in the reduction of the equation of energy transfer, convective heat transfer and viscous dissipation were neglected, it is to be expected that the presence of a radial temperature gradient along only the middle part of the fluid, will give rise to free convection.

By using steady state methods it was previously found (Ref. 10b and Ref. 13) that for the Rayleigh number, $R < 1000$, convective effects could be assumed negligible.

$$R = g\,\rho\alpha\Delta T d^3/\mu K < 1000.$$

Here g is the gravitational constant

ρ, α, μ, K are the physical properties of the medium and

$d = b-a$ is the charachteristic dimension of the system

The velocity profiles of the convecting fluid have subsequently been investigated. Pittman (Ref. 4a) numerically solved the equation for the velocity distribution (Ref. 3) within the cell, with the following assumptions:

1) A cold front of fluid begins to rise from the lower edge of the heating section, as soon as heat is supplied to the central cylinder.

2) The radial temperature distribution is assumed to be that of the stagnant fluid, and to give rise to density gradients which determine the velocity field.

3) The velocity along the r-axis is zero.

4) Heat conduction from the warm region into the cold front is neglected.

The equation describing this system has been solved numerically by Pittman (Ref. 4d)

$$\frac{\partial^2 v}{\partial r^2} + \frac{1}{r}\frac{\partial v}{\partial r} + \rho g \frac{\alpha T}{\mu} = \frac{1}{r}\frac{\partial v}{\partial t} \qquad (47)$$

with the initial condition

$$v(r,0)=0$$

and boundary conditions

$$v(a,t) = 0$$

$$\lim_{r \to \infty} (r,t) = 0$$

The calculated velocities are 10 to 15% lower than those observed (Ref. 14) by interferometric techniques (Ref. 4f). As mentioned in section 2., the viscous dissipation term, is calculated by using velocites obtained by this method.

9. Heat Transfer by Radiation.

So far, radiative heat transfer has been neglected. For systems where radiation effects are important equation (8) becomes

$$\rho\, C_p \frac{\partial T}{\partial t} + \epsilon_n = \nabla \cdot (\lambda \nabla T) \qquad (48)$$

where, ϵ_n is called the net emission,

$$\epsilon_n = K\left[\epsilon_{bb}(r,t) - \epsilon^{\circ}(r,t)\right] \qquad (49)$$

and

K is the absorptivity coefficient

ϵ_{bb} is the black body emission function.

ϵ° the absorption function. (Ref. 15)

The difficulty in the analysis of radiative heat transfer is twofold: firstly the absorption function is a very complicated function of the geometry of the system, and has been constructed here only through use of simplifying assumptions; secondly even the simplified form of ϵ_n involves integrations over the

temperature and equation (48) then becomes an intractable integro-differential equation, as will be presently shown. Approximations at various levels have been made to overcome these difficulties, a good survey of which will be found in Ref. 4g. In relation to the hot wire experiment it had been suggested (Ref. 10c) that the emission from a central cylinder into a black enclosure would yield a good estimate of the radiative heat losses from the central wire; the error calculated in this way had been found to be of negligible magnitude. Other estimates of these losses for measurements on toluene were as high as 2%. (Ref. 11, 16-18).

It is assumed here, that since the central cylinder is of infinite length (see section 3) radiation emission from it and from concentric shells of surrounding fluid may legitimately be taken as having no component along the axis of the central cylinder. The equation for monochromatic radiation intensity, I_ν, in cylindrical coordinates, is then given by (Ref. 15)

$$\frac{dI_\nu(r,t)}{dr} + \left[\frac{1}{r} + K_\nu\right] I_\nu(r,t) = E_\nu \qquad (50)$$

where

$$E_\nu = E_\nu(T) = n^2 K_\nu I_{bb,\nu}(T) \qquad (51)$$

$K_\nu = K_\nu(T)$

n = the index of refraction

$$I_{bb,\nu} = \frac{2\,c^2 h}{\nu^5 \left[\exp \frac{ch}{\nu KT} - 1\right]} \quad , \tag{52}$$

and

c = speed of light.

h = Planck's constant.

ν = wavelength of radiation.

k = Boltzmann's const., and finally

T = the absolute temperature.

Equation (50) can be solved by the integrating factor method:

$$I_\nu (r,t) = \frac{1}{u(r)} \int_{ro}^{r} E_\nu (T)\, u(r) dr \tag{53}$$

where the integrating factor u(r) is given by

$$u(r) = \exp - \int_{ro}^{r} \left(\frac{1}{r'} + K_\nu\right) dr' \tag{54}$$

Here r_o is the radius of the central cylinder and r' is the variable of integration. All terms in equation (53) are functions of position, wavelength and temperature; the latter in turn is a function of position and time. An obvious simplification of equation (53) is to adopt a suitable average value of K_ν over the infra red region which is relevant for radiative heat transfer. We may then write

$$I(r,t) = \frac{1}{u(r)} \int_{ro}^{r} E(T)\, u(r)\, dr \tag{55}$$

Since radiative transfer has been assumed to occur only radially, $e^{\circ} = I(r,t)$.

Also using the Stefan-Botzmann law

$$e_{bb}(r,t) = 2\pi n^2 \sigma (\Delta T)^4; \quad \Delta T = \frac{dT}{dr}(r,t). \qquad (56)$$

Hence

$$e_n = K(T)\left[2\pi n^2 \sigma T^4 - \frac{1}{u(r)} \int_{ro}^{r} E(T)\, u(r^{\circ})\, dr^{\circ} \right] \qquad (57)$$

where

$$u(r) = \exp\left[- \int_{ro}^{r} \left(\frac{1}{r^{\circ}} + K(T)\right) dr^{\circ} \right]. \qquad (58)$$

Due to the form of equations (57) and (58), equation (48) is mathematically intractable. The difficulty could be removed by assuming K, the absorptivity coefficient to be temperature independent. This however would impose time independence on the radiative transfer problem, which would in turn lead to lower levels of outward emission from concentric fluid shells and hence to a smaller correction to the thermal conductivity. Pittman (Ref. 4g) solved the heat conduction equation with a heat sink term representing absorption of radiation by the liquid, with a constant absorptivity coefficient and the boundary condition,

$$- 2\pi a\lambda \frac{\partial T}{\partial r} = q_1 - \delta q(t)$$

where

$$\delta q(t) = 8\pi a \sigma \epsilon T_A^3 T(a,t)$$

σ = Stefan-Boltzmann const.

ϵ = emissivity coefficient

T_A = Absolute temperature

$T(a,t)$ = Temp rise in the wire, from the start of the experiment ,

with the conclusion that for toluene, the error involved is of the order of 1 to 2%. This would seem rather high. The boundary condition assumes a temperature gradient equal to $T(a,t)$, which would lead to overestimating the error; neglecting absorption of radiation by concentric fluid shells would have the same effect. Though due to its approximative nature, this treatment, like previous ones cannot be used for actual corrections to thermal conductivity data, a practical aspect does emerge. The error decreases as time goes to zero; thus a zero time extrapolation of data for each run would lead to a value less affected by radiation losses. (Ref. 4g)

CHAPTER 3

Apparatus, Procedure and Data Handling

1. Introduction

The theory of the hot wire cell presented in Chapter 2 was applied in designing a thermal conductivity cell adapted to high pressure measurements. Here a description of the cell, the pressure system and temperature control system will be given, along with the working equations used in analysing the data. The experimental procedure will also be described, and finally the method of handling and processing the data will be given.

2. The Thermal Conductivity Cell

The cell (Fig. 1) was constructed of EMS stainless steel with dimensions of 1 cm I.D., .98 inch O.D. and 15.7 cm internal length. Four 26 SWG thermopure platinum leads were connected from the sealed electrodes on the high pressure plug to the cell; the two current leads were spotwelded to needles at the top and bottom of the cell, which were insulated from the main body by baked pirophylite beads. The two potential leads which ran down the side of the cell were insulated from it by pyrex capillaries drawn to 3/16" OD. In the cell a spring (Pt + 10% Iridium) was placed between the top current lead and the heating wire in order to prevent the wire from sagging as the experimental temperature was raised. The spring was shunted on both sides with .001" thick, 1/16" wide platinum foil (Ref 1a), as the spring material is of rather high resistance. The heating wire, .001" diameter, die drawn high alpha grade platinum wire supplied by Johnson Mathey Limited, was then connected top and bottom to the spring and lower current lead respectively. The potential leads were then spot welded, about 1 cm away from the spring at the top, and 3 cm away from the current lead at the bottom. After completion, the welds and the heating

FIG. 1

THERMAL CONDUCTIVITY CELL

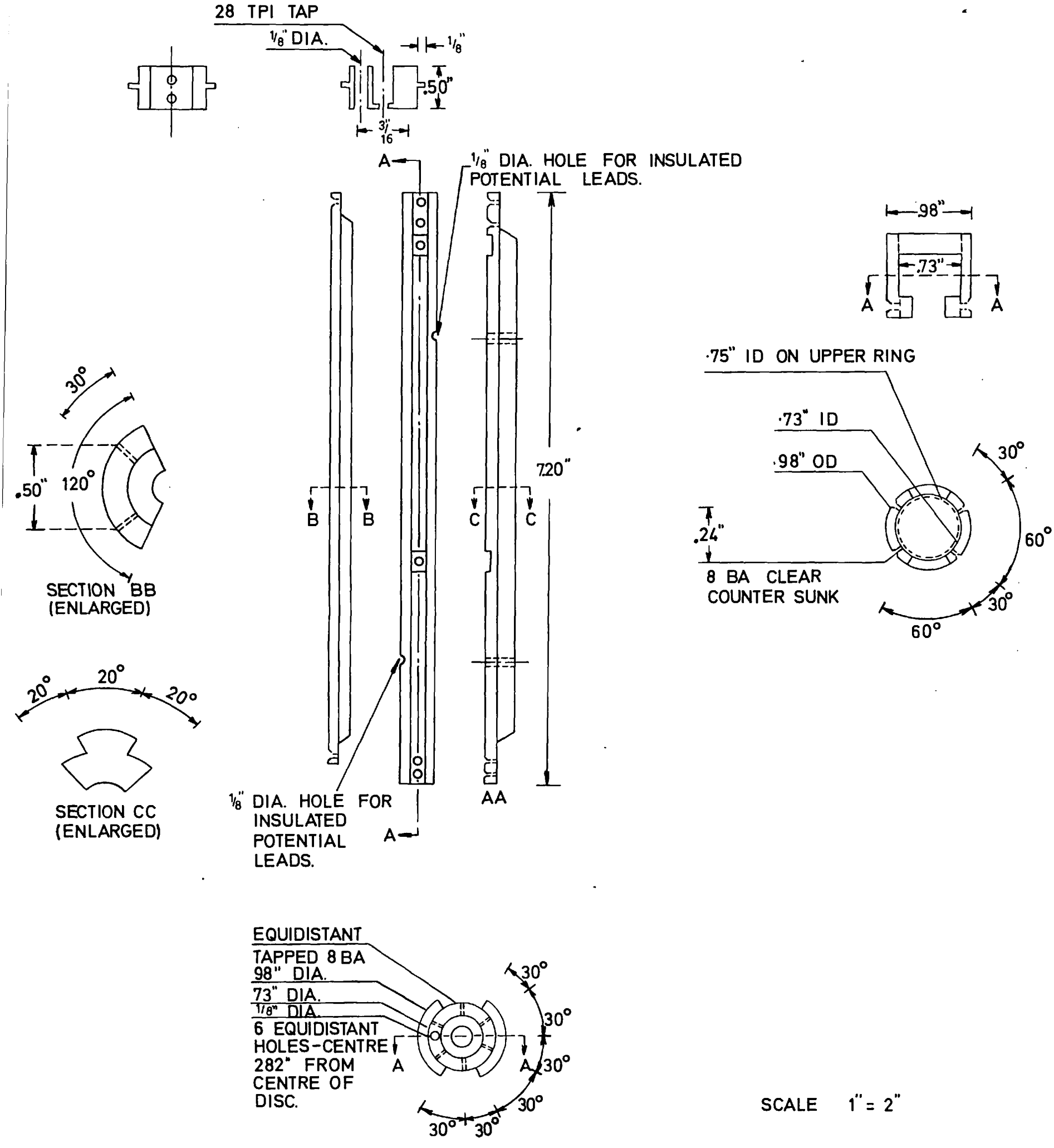

SCALE 1" = 2"

wire were inspected by microscope and found free of kinks or distortions. The potential lead weld regions were found to be partially flattened, up to a distance of 3 or 4 wire diameters.

The design specifications arise from considerations fully discussed in references (1), (2) and (3). These arguments will now be briefly summarised.

i) Effect of the External Boundary.

It has been found (Ref. 1b) that, comparing, in the first approximation, equations (9) and (43) of the previous chapter, agreement is within .01% for $Kt/b^2 < .12$. For toluene at 90°,K, the thermal diffusivity, is about $.7 \times 10^{-3}$. This implies that over 30 seconds are necessary for wall effects to become significant in a 1 cm I.D. cell.

ii) Distance Separating the Potential Taps from Ends of the Heating Wire.

The distance between the top potential tap and the spring is determined by considering conduction away from the heating section by the current lead (and spring). Here leaving approximately 1 cm between the bottom of the spring and the potential tap was found sufficient (see section 2.7).

Other considerations enter in determining the length of wire to be allowed between the voltage tap and the bottom

current lead. Free convection starts as soon as the central wire begins to heat up. Shells of liquid, with the same temperature distribution as for the case of no convection, rise followed by the cold front described in section 2.8 (Ref 4). The experiment can be continued as long as the cold front remains .5 cm away from the bottom end of the heating wire. As mentioned in section 2.2, the duration of the experiment is limited by the length of wire allowed below the bottom potential lead. Clearly the velocity of the cold front also depends on the heating rate: low heat rates would allow longer experiments but lead to low voltage changes and hence less accurate results, where as high heat input rates would necessitate short experiments due to convective and wall effects. It was found (ref 3a) that for a distance of 3-4 cm below the bottom potential lead, heating rates corresponding to 17-25 milliamps cell current would allow the experiment to last up to about 30 seconds. In fact all measurements were completed within the first 20 seconds.

iii) Diameter of the wire - Analysis of initial specific heat effects, end effects and radiation losses, indicate the necessity of using heating wires with the smallest diameter with which it would be possible to build a cell. .001 inch diameter was found to be adequate for this purpose.

iv) Wire length. Two cathetometers, set at right angles relative to each other were used to measure the length of the heating section of the wire, while the cell was clamped down vertically. The wire length was found to be 8.100 ± .002 cm. The measurement was repeated after the thermal conductivity runs and no significant change found.

3. The Cell Casing and Bellows

The case which envelopes the cell is made of three parts (Fig 2). The main body of the case screws into the pressure plug. The middle part, a short cylinder, is argon arc welded to a bellows; this assembly screws into the main body of the case. The middle part has been designed as a separate piece from the main body for easier handling and replacement. The lower end of the bellows was welded to a plug, with a tapped hole for filling. All parts were made of stainless steel and screwed joints were sealed with teflon flat rings.

The bellows, made by Teddington Aircraft Controls Ltd., had ± 1 inch axial movement. This corresponds to about 32% compression of the fluid confined in the cell assembly which is sufficient to raise most liquids to 7000 atmospheres, over the temperature range of 30-95°C.

The assembly (Fig. 3) was filled with the test fluid, under its own vapor pressure, following a "bulb to bulb"

FIG. 2
BELLOWS AND CASING

Mat. EMS Stainless
unless specified

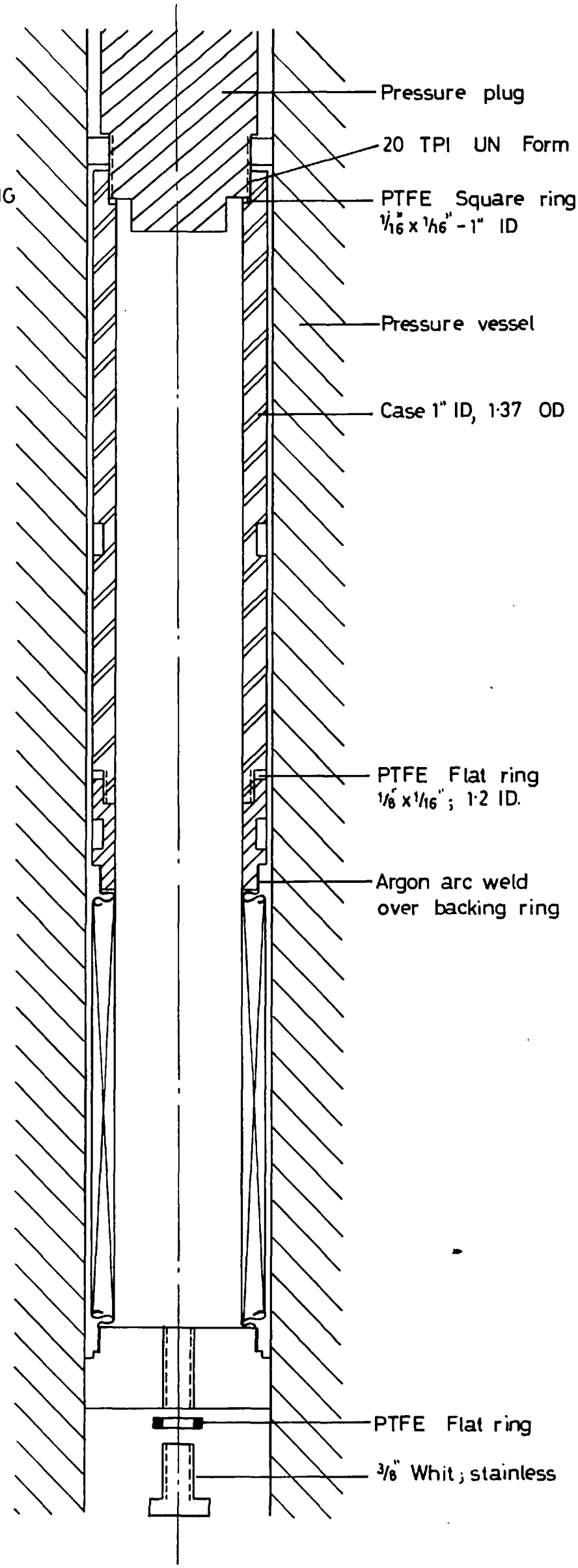

BELLOWS DATA

ID 1·00 ; OD 1·37"
THICKNESS ·005/·0055
MOVEMENT AXIAL ± 1"
FREE LENGTH 3·47"
30 CONVOLUTIONS

FIG. 3

vacuum distillation, where liquid nitrogen was used as coolant. A glass system, Fig. 4, was designed for the purpose, and attached to a standard vacuum system, including a backing pump and an air cooled oil diffusion pump.

4 The Electronic System

A system previously developed (Ref.3b) for atmospheric pressure determinations of thermal conductivity was used for the high pressure thermal conductivity measurements. (Fig. 5).

Basic requirements in the high pressure experiments were similar to those at atmospheric pressure:

i) 20 mA current stable to 1-2 ppm,

ii) Eight readings a second with 1 microvolt resolution in about 20 millivolts,

iii) Stable backoff facility,

iv) Automatic data logging.

The major parts of the curcuit will now be briefly described.

1) Power supply. D.C. voltage standard made by Cohu Electronics, Kintel Division, U.S.A., with voltage range 0-1000 V, provides currents up to 50 mA. This instrument was placed in series with a 10,000 ohm resistor, in a thermostatted oil bath, to provide the cell current. The latter was measured by monitoring the voltage drop across an NPL calibrated 10 ohm

FIG. 4 VACUUM DISTILLATION AND FILLING APPARATUS

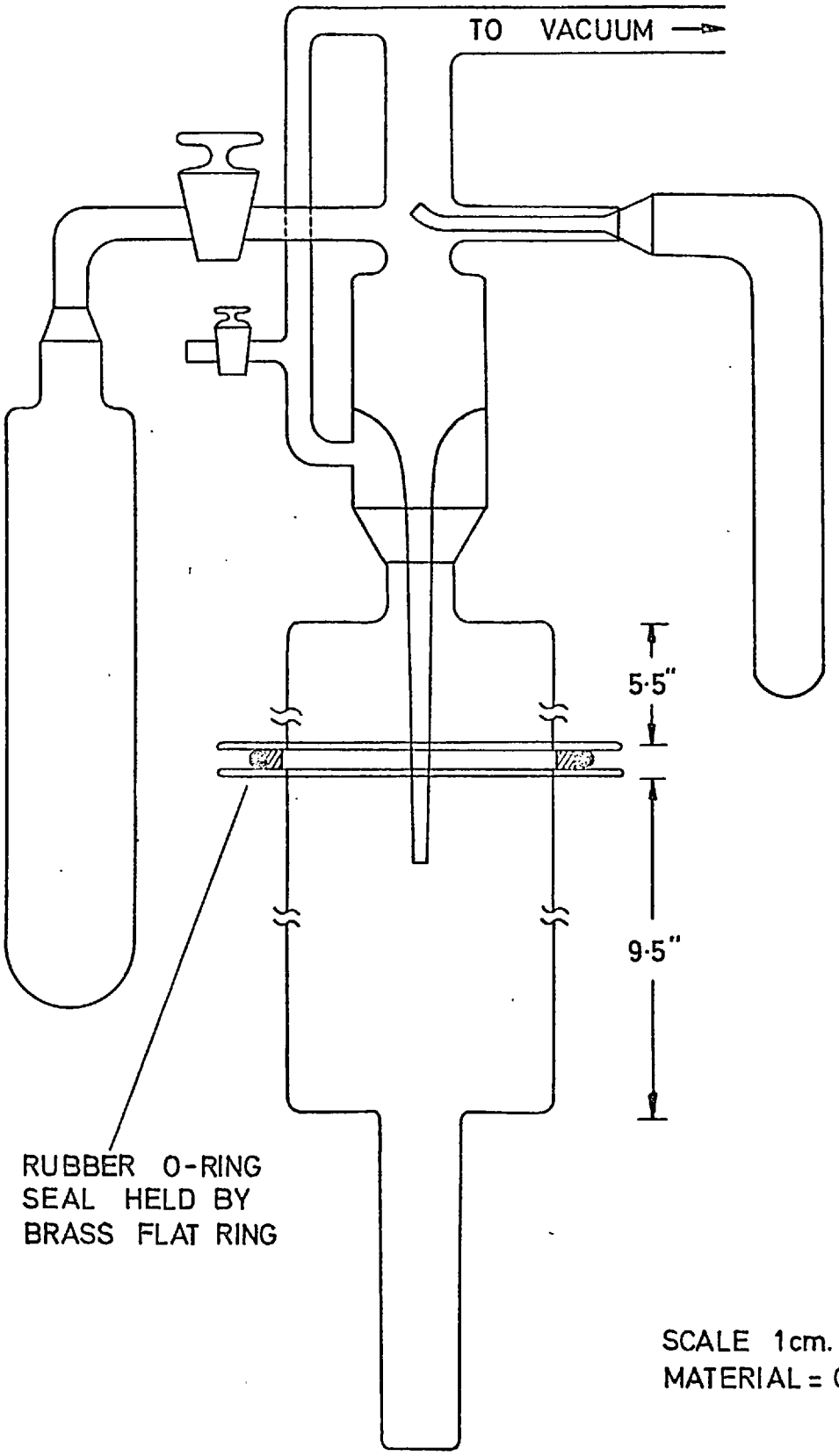

FIG. 5 CURRENT SUPPLY AND VOLTAGE MONITORING SYSTEMS

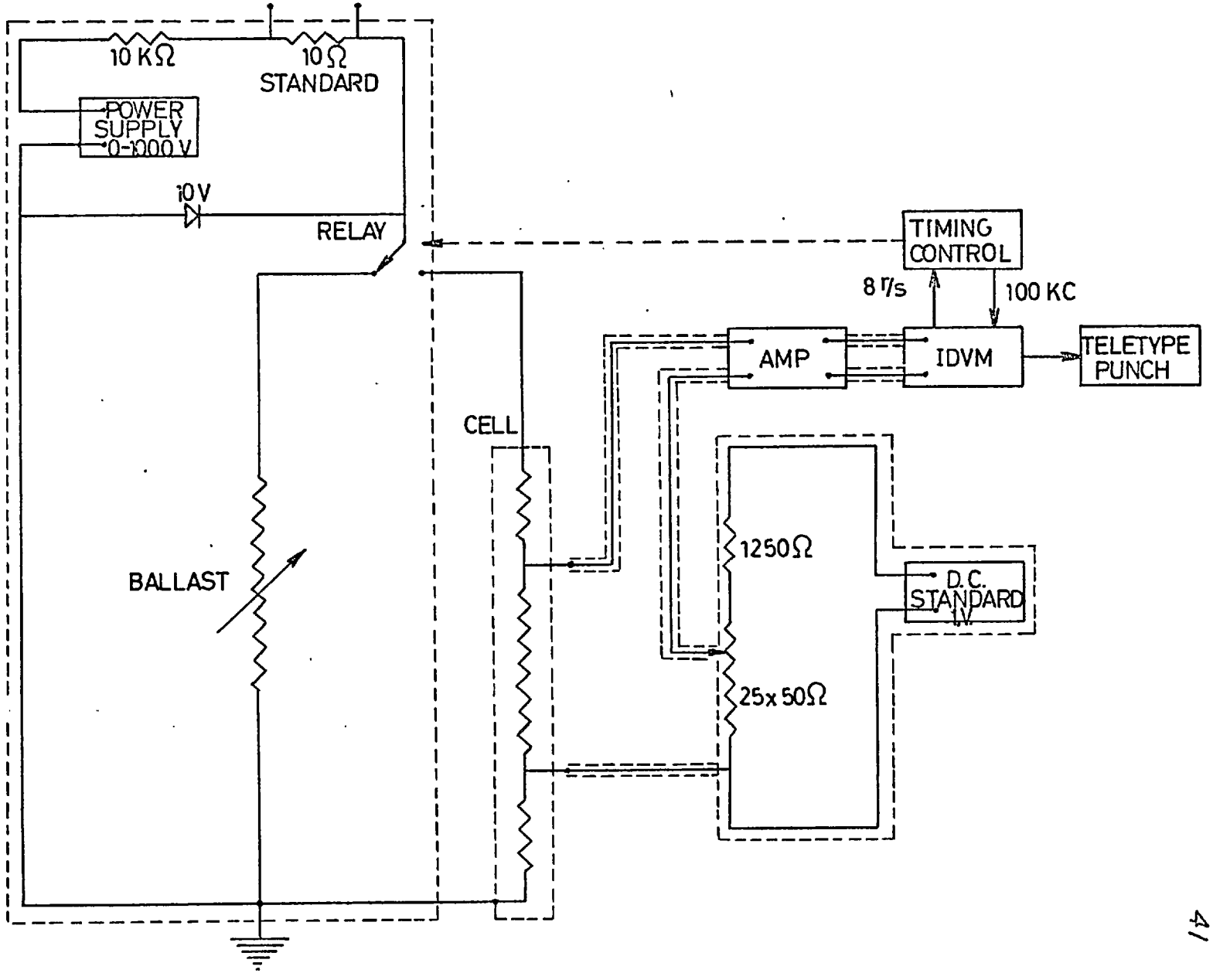

Tinsley standard resistor.

2) Backoff Circuit. A Model 735A D.C. Transfer standard made by Hewlitt-Packard Co., U.S.A. provided the bachoff, through a voltage divider of 2500 ohm total resistance in steps of 50 ohms.

3) Amplifier. Hewlitt-Packard Model DY 2411A amplifier, with gain selection of 1,10, and by-pass, was used in series with the voltmeter. The gain is specified accurate to $\pm$ .007% with temperature coefficient of less than .5 microvolts /^{o}C. Input impedance was 10^{10} ohms.

4) Voltmeter. A Hewlitt-Packard Model DY 2401 C Integrating Digital Voltmeter was used in series with the amplifier. Maximum resolution of the instrument was 1 part in 300 000. When used with a set sampling period of 1 second, resolution was .1 microvolt, and for a sampling period of .1 second, 1 microvolt. Accuracy is better than $\pm$ .025% of the reading. Both the amplifier and voltmeter are guarded and have high common mode rejection.

5) Data-Logging Equipment. Monitored voltage changes across the cell were logged by a Hewlitt-Packard DY 2545 high speed tape punch set with a HRPE II tape punch made by Teletype Corp.

Before a run, the system was allowed to stabilize by passing current through the ballast. This is a 100 ohm, continuously variable resistance introduced in order to avoid transients in the power supply due to changes in the load, when a run is triggered. This was done by a push button which activated a mercury wetted relay. A Zener diode was provided in parallel with the 10K ohm resistor (See Fig. 5), so as to avoid large voltages appearing at relay contacts. The falling edge of the pulse generated across the relay triggers the opening of the gate to a counter circuit available in the voltmeter with a 100 kilocycle signal. This signal provides the timing control for reset pulses externally generated and fed back into the voltmeter. The first integrating period can be delayed by up to $^1/8$ sec. after the opening of the gate; the the delaying period is followed by a reset period of 9.7 milliseconds which is the gap between the reset pulse and the beginning of an integrating period. The integrating periods are 100 milliseconds each separated by 25 milliseconds from each other, the start of each being triggered by an external reset pulse.

The sequence of operations and voltage measurements leading up to a thermal conductivity run, will be described in a later section of this chapter.

5. The Voltmeter Integration Period

Each voltmeter reading is an average value over a

100 millisecond integration period. Hence

$$T_M = \frac{1}{t_2-t_1} \int_{t_1}^{t_2} T_R(t)\, dt \quad , \tag{1}$$

where T_M the measured temperature change is the average value over Δt $(= t_2-t_1)$ of T_R , the real temperature. Equation (37) of the previous chapter must now be modified to take this integration into account. Defining from eqn. (37)

$$\varphi_1 = \frac{q_1}{4\pi}\left[\ln\frac{4Kt}{Ca^2} + \frac{a^2}{2Kt} + \frac{\alpha-2}{\alpha}\frac{a^2}{2Kt}\ln\frac{4Kt}{Ca^2} + \ldots\right] \tag{2}$$

$$\varphi_2 = \frac{q_2}{4\pi}\left[\ln\frac{4Kt}{Ca^2} - 1\right] t + \ldots \tag{3}$$

$$\varphi_3 = \frac{q_3}{4\pi}\left[\ln\frac{4Kt}{Ca^2} - \frac{3}{2}\right] t^2 + \ldots \tag{4}$$

we may write

$$\lambda_1 T_R + \lambda_2 T_R^2/2 = \varphi_1 + \varphi_2 + \varphi_3 \, . \tag{5}$$

Integrating equation (5) with respect to t between t_1 and t_2 and dividing by Δt, we get

$$\frac{\lambda_1}{\Delta t}\int_{t_1}^{t_2} T_R\, dt + \frac{\lambda_2}{2\Delta t}\int_{t_1}^{t_2} T_R^2\, dt = \frac{1}{\Delta t}\int_{t_1}^{t_2}(\varphi_1+\varphi_2+\varphi_3)\, dt$$

and hence

$$T_M = \frac{1}{\lambda_1 \Delta t} \int_{t_1}^{t_2} \left[\varphi_1 + \varphi_2 + \varphi_3 - \frac{\lambda_2}{2} T_R^2 \right] dt \qquad (6)$$

As the variable conductivity correction is expected to be less than .5%, it is permissible to calculate the average value of T^2 from the line source method. Thus by eqn. (10) of the previous chapter

$$T_R^2 \doteq \left[\frac{q_1}{4\pi\lambda} \ln \frac{4Kt}{Ca^2} \right]^2 . \qquad (7)$$

Integrating equations (2)-(4) and (7) with respect to t we get

$$T_M = \frac{1}{\lambda_1} \left[\bar{\varphi}_1 + \bar{\varphi}_2 + \bar{\varphi}_3 - \frac{\lambda_2}{2} \bar{T}_R^2 \right] \qquad (8)$$

where after dropping terms containig $(\Delta t)^2$, $(\Delta t)^3$ etc. ,

$$\bar{\varphi}_1 = \frac{q_1}{4\pi} \left\{ \left[\frac{t_1}{\Delta t} + \frac{a^2}{2K\Delta t} \right] \ln\left[1 + \frac{\Delta t}{t_1}\right] + \ln \frac{4K(t_1+\Delta t)}{Ca^2} - 1 \right.$$
$$\left. + \left[\frac{\alpha-2}{\alpha} \frac{a^2}{4K} \right] \frac{1}{\Delta t} \left[\left[\ln \frac{4K(t_1+\Delta t)}{Ca^2} \right]^2 - \left[\ln \frac{4Kt_1}{Ca^2} \right]^2 \right] \right\} \qquad (9)$$

$$\bar{\varphi}_2 = \frac{1}{\Delta t} \frac{q_2}{8\pi} \left[t_1^2 \ln\left[1 + \frac{\Delta t}{t_1}\right] + 2t_1 \Delta t \ln \frac{4K(t_1+\Delta t)}{Ca^2} - 3t_1 \Delta t + \ldots \right], \qquad (10)$$

$$\bar{\varphi}_3 = \frac{1}{\Delta t} \frac{q_3}{12\pi} \left[t_1^3 \ln\left(1 + \frac{\Delta t}{t_1}\right) + 3t_1^2 \Delta t \ln \frac{4K(t_1+\Delta t)}{Ca^2} - \frac{11}{2} t_1^2 \Delta t + \ldots \right] \qquad (11)$$

and

$$\bar{T}^2 = \left[\frac{q_1}{4\pi\lambda_1}\right]^2 \frac{1}{\Delta t}\left\{ (t_1+\Delta t)\left[\ln\frac{4K(t_1+\Delta t)}{Ca^2}\right]^2 - t_1\left[\ln\frac{4Kt_1}{Ca^2}\right]^2 \right.$$

$$\left. -2t_1 \ln\left(1+\frac{\Delta t}{t_1}\right) - 2\Delta t \ln\frac{4K(t_1+\Delta t)}{Ca^2} + 2\Delta t \right\} . \qquad (12)$$

Here Δt = .1 second.

6. The Working Equation

For fixed a, λ_2 and α equation (8) gives the measured temperature changes as a function of time, at the wire-fluid boundary.

$$T_M(t) = \frac{1}{\lambda_1} F(t) \quad .$$

For any interval, Δt, then

$$\lambda_1 = \Delta F(t) \,/\, \Delta T_M(t).$$

For small temperature changes (Ref. 1)

$$\Delta T_M = \frac{dT_M}{dR} \Delta R \quad \text{where} \quad \Delta R = \frac{\Delta V}{I} - \frac{V}{I^2} \Delta I \ .$$

Therefore

$$\Delta T_M = \frac{dT_M}{dR}\left[\frac{\Delta V}{I} - \frac{V}{I^2} \Delta I \right]$$

and

$$\lambda_1 = \frac{dR}{dT_M}\left[\frac{1}{I}\frac{\Delta V}{\Delta F} - \frac{V}{I^2}\frac{\Delta I}{\Delta F} \right]^{-1} \qquad (13)$$

From equation (8) it can be seen that F(t) is a weak function of λ_1 . Hence an iterative calculation is called for. The computer program written to perform these calculations will be described in a later section.

7. The Pressure System

The pressure system was designed to reach pressures up to 7,000 atmospheres. The accompanying flow sheet, Fig. 6, illustrates the layout.

1) The pressure vessel was manufactured by Pressure Products Inc. (UK) Ltd.; design details may be found in Fig. 7. The vessel was made of EN 25 stainless steel, with $1\frac{1}{2}$" bore and 12" working length, from the tip of the electrode head to the bottom of the vessel. The electrode head was also made of EN 25 steel with initially a beryllium copper-teflon half Bridgman main seal and four electrode seals. The latter consisted of Hilumina insulators (Smith Industries, Ceramics Division) and brass cones, successively lapped in.

It was found during the experiments, that beryllium-copper work-hardened sufficiently to scratch the vessel bore when the plug was being extracted from the vessel. Copper was tried and found to flow too easily and fill the gap between itself and the plug (see Fig. 7). Phosphor bronze was then tried with a larger angle, 6 degrees, between the ring and the plug and found satisfactory, provided a groove was turned off on the outside, as shown in Fig. 7. This groove prevents the O.D. of the ring from flowing flush to the vessel bore which would have increased surface

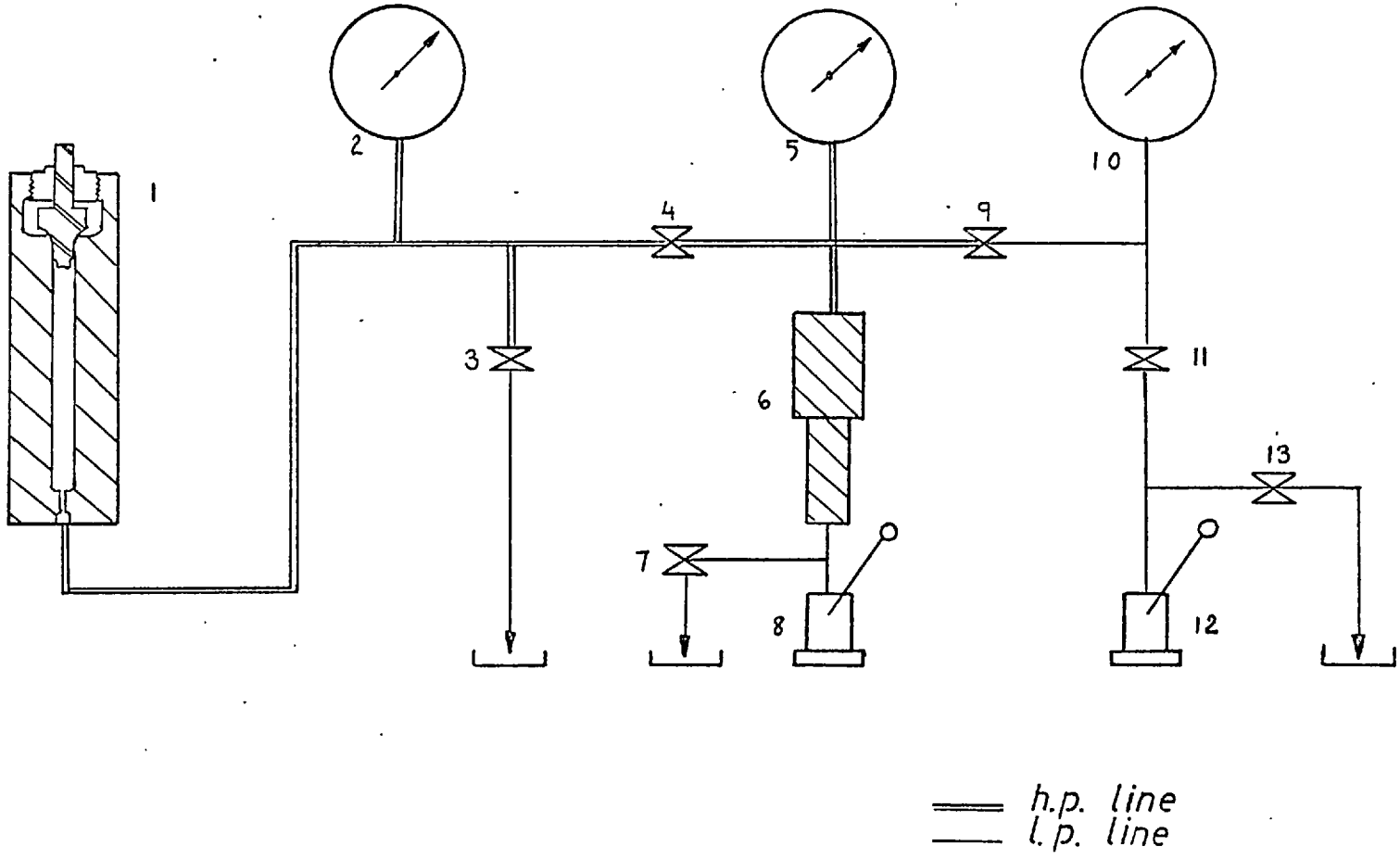

fig 6 .

flowsheet of the pressure system

FIG. 7

PRESSURE VESSEL AND PLUG

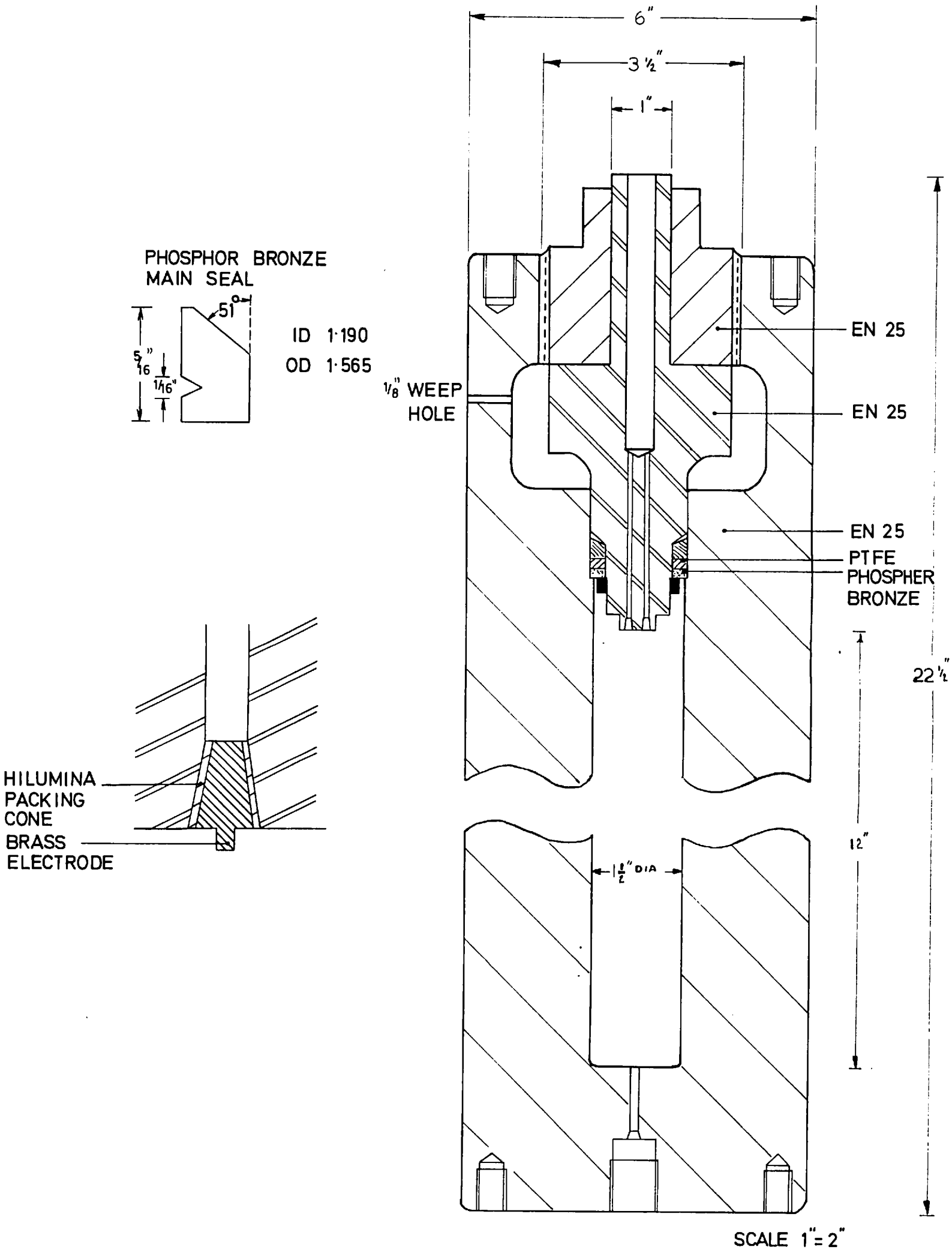

contact and caused leaking. This design was found sufficiently durable over the pressure and temperature cycling that took place during the experiments.

2) 10,000 atmosphere gauge, made by Budenberg Gauge Company, rated to 1% accuracy of full scale deflection.

3) Letdown Valve, with nonrotating spindle, rated to 100,000 psi, was made by Pressure Products Inc.

4) Valve, with same specifications as (3).

5) Gauge, with same specification as (2).

6) Intensifier, rated to 200,000 psi, with intensification factor of 15; model A2.5J made by Harwood Engineering Co., U.S.A.

7) Non-rotating spindle valve, rated at 30,000 psi, made by P.P.I.

8) Pump, stainless steel body, rated at 60,000 psi, made by McCarney Manufacturing Co., U.S.A.

9) Valve, with some specifications as (3).

10) 40,000 psi gauge, made by Budenberg Gauge Company.

11) Non-rotating spindle valve, rated at 60,000 psi, made by P.P.I.

12) Hand pump; same as (8).

13) Valve; same as (11).

The whole pressure system was enclosed in a steel frame and shielded with $\frac{1}{4}$" thick mild steel plate (Fig. 8).

The system is initially pumped up by (12) to about 2,000 atmospheres. Valve (9) is closed off to isolate the low pressure side, and the pressure further raised by pumping (8) on the low

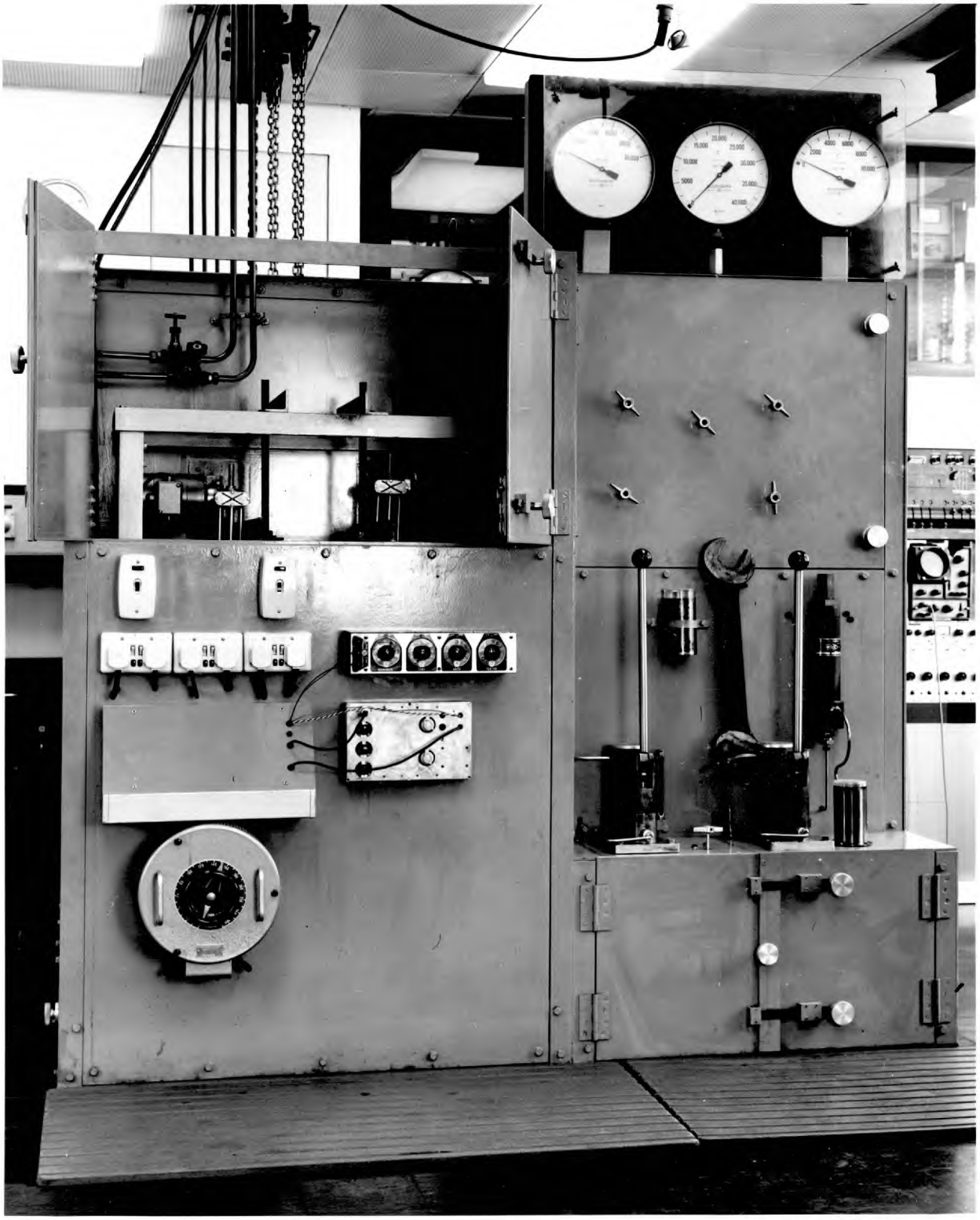

FIG. 8

side of the intensifier (6) until the piston reaches the end of the stroke. Valve (4) is then closed off, valve (7) opened and the pressure between (4) and (9) dropped to about 2,000 atmospheres. Valve (9) is then opened and the intensifier piston pumped down by (12); the pressure is raised again to 2,000 atmospheres, and values (7) and (9) turned off. The pressure between (4) and (9) can then be raised by (8) to the vessel pressure, valve (4) opened and pumping continued. Vessel pressure can normally be raised to the designed maximum during the second stroke of the intensifier. During experiments, (4) is shut to isolate the vessel from the rest of the system.

The pressure calibrations were carried out against an N.P.L. calibrated "dead weight" standard pressure gauge over the range 0-3000 atmospheres. The zero-error of the two 10,000 atmosphere gauges remained, as pressure was raised, and no error exceeding the quoted accuracy (1% of full scale reading) of any of the three gauges was found. The calibration was repeated by reducing the pressure from 3,000 atmospheres, with the same result (Fig. 9). The results were assumed to hold for pressures above 3,000 atmospheres.

8. The Temperature Control System

As the temperature rise of the central wire during the

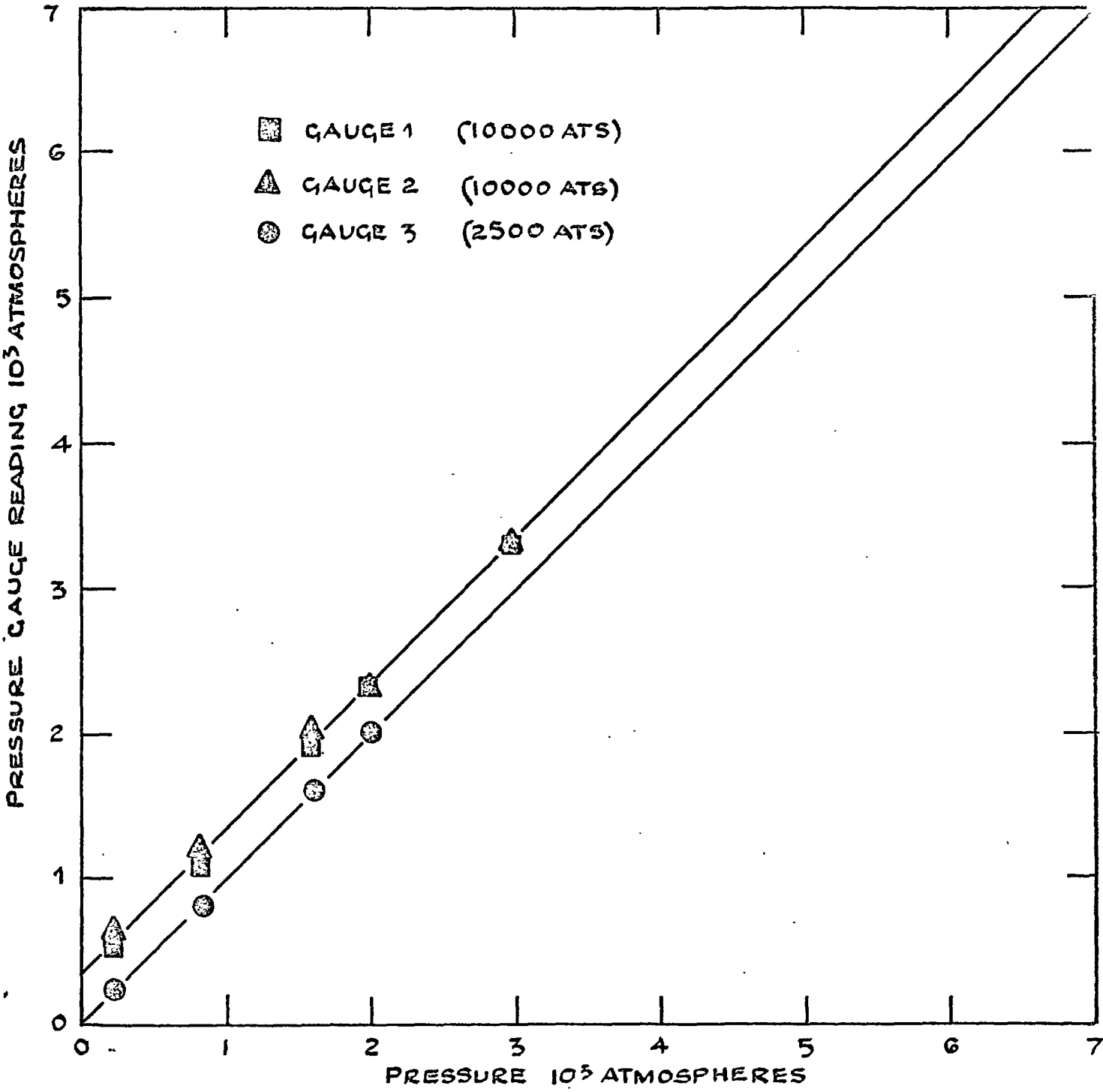

FIG. 9 PRESSURE GAUGE CALIBRATION CURVE

experiment is .3°C, maximum allowable temperature drifts in the cell are on the order of .05°C/hour. In order to achieve this temperature stability the pressure vessel was placed in a temperature controlled, stirred oil bath. (Fig. 10).

1) Tubalox immersion heater, rated 230/50 volts, 3 kw, with no heat dissipation above the surface of the oil. Power to this heater was supplied through a 15 amp variac.

2) 1" thick blockboard case, housing vermicullite insulation.

3) 3" thick layer of vermicullite insulation around and beneath the galvanized iron tank.

4) 1/30 HP induction motors made by Klaxon Ltd; 1425 rpm slowed down by gearboxes and with shafts mounted with 12" long vertical fins as well as 4" diameter brass propellers at the tip.

5) ¼" thick mild steel plate supporting pressure vessel.

6) 1/8" thick duraluminium sheet cylinder, provided lagging by trapping 1" of oil between itself and the pressure vessel..

7) Pressure vessel.

8) 10 gauge galvanized iron tank, 20" long, 14" wide, 35" deep and with 4" flanged top.

9) Tubalox immersion heater, rated 230/250 volts, 500 watts, supplied through the temperature controller.

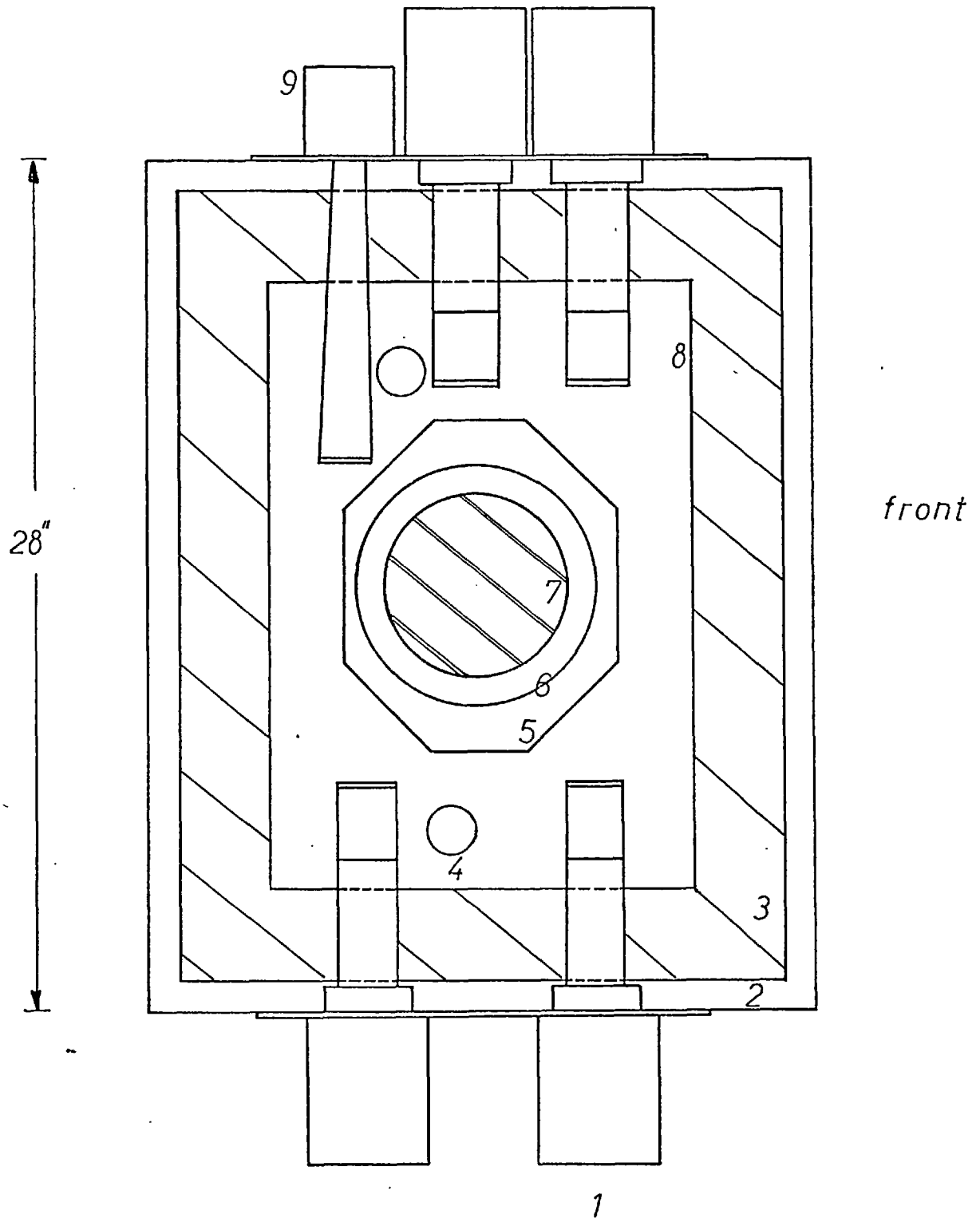

fig 10 Thermostat Bath
plan view

1 cm = 2"

The whole system was provided with a lid made of $\frac{1}{2}$" thick syndanyo plate and 3" layer of vermicullitz, enclosed in cardboard.

The heat transfer fluid used was Shell Voluta Oil 45, a mineral oil based fluid, which can be used at temperatures up to 300°C. The oil was pumped in and out of the thermostat bath, using the oil handling system shown in Fig. 11, which was also used for cooling the system.

A temperature controller was designed and constructed in the departmental electronic workshop for the purpose of providing the required stability, and will be briefly discussed here.

The sensing element, a Degussa, 100 ohm (nominal) resistance thermometer, was used as one arm of the bridge with a PYE, variable resistance box, as the pre-set arm. The bridge was driven by an 18 volt stabilised power supply. The out-of-balance voltage from the bridge is fed into a pre-amplifier, and then into a 3-term unit gain amplifier, the output of which is used to determine what proportion of a second the heater will be turned on.

This signal drives a gate which allows the output of a mains driven zero voltage pulse generator to reach the triac controlling the heater. The latter shuts power off when voltage across it passes through zero, thus breaking circuit at each

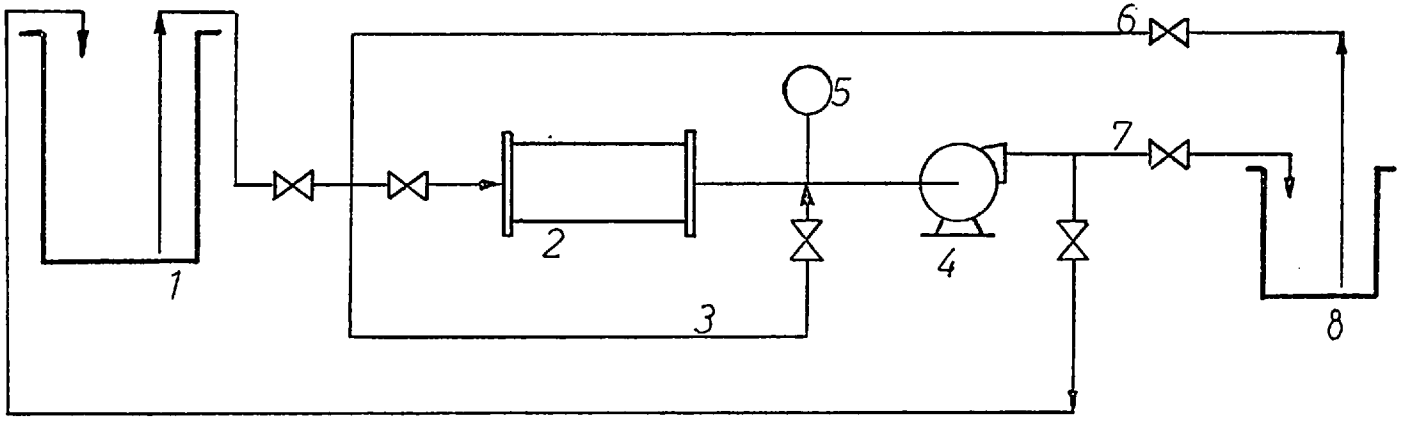

1 Reservoir
2 Heat Exchanger
3 By Pass
4 Pump
5 Temperature Gauge
6 Draining Line
7 Filling Line
8 Thermostat Bath

fig 11 ..... Flowsheet of Oil Handling System

mains half cycle, and being reactivated by the zero voltage reset pulse, as long as the gate remains open.

Temperature stability in the cell was followed over time by measuring the cell resistance, and the system described above was found to drift at rates of less than .05°C/hour after a settling down period of 12 to 18 hours. Furthermore, the vertical temperature distribution in the vessel bore was investigated by vertically moving a resistance thermometer. In the absence of the bath lid and the pressure plug, it was found that a vertical gradient of about .05°C existed. It was assumed that the gradient would be reduced to negligible propertions when the vessel closure and bath lid were replaced.

Finally in order to measure the experimental temperature, an N.P.L. calibrated 25 ohm (nominal) resistance thermometer, made by H.Tinsley and Co. Ltd., was immersed in the bath between the pressure vessel and the cylindrical shell surrounding it. (see Fig. 10). Thermometer resistance was measured to .0001 ohm. The constants of the calibration polynomial were used by a computer program , in order to evaluate the temperature. (see section 10). Experimental temperatures will be quoted here to the nearest tenth of a degree centigrade.

9. Procedure

The thermal conductivity of toluene was measured, at each temperature, first at atmospheric pressure and then at various elevated pressures.

As the pressure is raised by pumping, work is done on the compression oil (DDT 585, Shell) and the test fluid; consequently the temperature in the vessel and the cell rises above the temperature at which the system is being controlled. More than three hours were allowed for this heat to be dissipated. Experiments were carried out only after temperature drifts due to cooling were observed to be indistinguishable from controller drifts for about half an hour.

The criterion of negligibility for errors due to temperature drifts in the cell is that drifts should be less than .1% of the temperature rise over the duration of the experiment. As experiments lasted approximately 20 seconds, and temperature rises were never larger than .3°C, this condition corresponds to drifts of about .07°C/hour. In fact no experiments were carried out with observed drifts above .05°C/hour. These drifts were followed by measuring the cell resistance at short intervals. If before a run cell resistance changes larger than those allowed for

controller drifts were found, this was attributed to cooling due to pressure leaks and the set of runs cancelled.

In theory, two factors must be taken into account in identifying a pressure leak through cell resistance measurements. The first, as indicated above, is the changes of temperature undergone by the system, as the pressure is raised or lowered. This must be distinguished from resistance changes that Pt wire will undergo due to changes of pressure. At 50^{o}C, the pressure-resistance relationship for platinum may be represented by the empirical equation (Ref. 5)

$$R_p = R_o(1+a\,P + b\,P^2) \qquad (14)$$

where

$a = -1.949 \times 10^{-6}$, $b = 7.86 \times 10^{-12}$ and R_o is the resistance at atmospheric pressures.

While, clearly, the two effects change the wire resistance in opposite directions, this in practice does not pose a serious problem as the magnitude of the resistance change due directly to pressure changes, is much smaller than the temperature change due to work done on the liquid.

At each setting of the temperature and pressure, the pressure was raised to a slightly higher value than the desired one, in

order to compensate for drops due to heat dissipation. At each pressure and temperature, three thermal conductivity measurements were made. In addition a run was simulated where the voltage drop across the 10 ohm standard resistor was measured in order to calculate the current change.

An experiment is set up as soon as temperature and pressure stability criteria are satisfied. The power supply is allowed to stabilize at 10 volts output, where the current drawn is about 1 milliamp. The following operations are then carried out.

1) Total cell resistance is measured and the ballast resistance set to the same value.
2) Current is switched into the cell and the voltage drop across the two potential leads measured. Heating due to the 1 milliamp current is negligible.
3) With the current going through the ballast the potential drop across the standard resistor is measured. This allows the calculation of the current flowing in the cell in (2) and consequently the calculation of the cell resistance.

Output from the power supply is then raised to 200 volts, drawing approximately 20 milliamps; the system is allowed to stabilize for five minutes.

4) Necessary backoff voltage is calculated on the basis of allowing about 20 millivolts across the voltmeter; this is set on the voltage divider.

5) With the current flowing through the ballast the potential drop across the standard resistor is measured in order to calculate the initial current. The voltmeter is then set to the .1 second sampling period, the tape punch activated and the current switched into the cell. 50 minutes was allowed between runs.

10. Processing of Data

In order to calculate the thermal conductivity from V v.s. t data, it is necessary to know the temperature coefficient of the cell wire resistance. To this end the cell resistance was measured as a function of temperature at each experimental pressure, over the range 30-95°C.

A computer program was written to execute the following operations:

1) Thermometer resistance data was converted to temperature readings.
2) For each pressure the temperature v.s. cell resistance data was fitted to a straight line.
3) Using the T v.s. R_c fits, pressure v.s. cell resistance data was cross-plotted and fitted to a quadratic.
4) These curves, in turn, are used for fitting straight lines to T v.s. R_c, for each experimental pressure. dR/dT values relevant to the experimental states were then computed.

The source program listing may be found in appendix 3B. The least-squares polynomial fitting subroutine used, was a Program Library deck written by C. Ho, Computation Laboratory G.P.D., I.B.M., Rochester, Minnesota, U.S.A. The same subroutine was used in the main data analysis program, which will now be described.

Data in the form of paper tape produced by the Teletype punch in Atlas autocode was first loaded, without code translation on to magnetic tape by the IBM 1401. The main programme written in Fortran IV was then loaded on the IBM 7094 to perform the following operations.

1) Each data batch consisting of several thermal conductivity runs and a current run, were translated into BCD code*, assigned a decimal point in units of volts and read into the memory.

2) The following information was fed in from data cards, for each run:

- the temperature coefficient of thermal conductivity at the initial temperature
- time delay before the start of the first integration period
- wire and fluid densities and specific heats
- experimental temperature and pressure
- backoff voltage value
- temperature coefficient of wire resistance at the initial

---

* I am indebted to Mr. Richard Beckwith of C.C.A., Imperial College of Science and Technology for the translation routine.

temperature

- voltage drop across the 10 ohm standard resistor with current flowing through ballast and power supply set at 10 V; this value is denoted by SV1, and is used for calculating the current at the 10 volts setting.

- voltage drop across the heating section of the wire, with 10 volts across the circuit, this is denoted by RIVT, and is used for calculating the cell resistance.

- voltage drop across the 10 ohm standard resistor, with power supply set at 200 volts, SV2, used for calculating the initial current in the cell.

3) Calculation of q_1, q_2 and q_3. The heat dissipation per unit length in the active part of the cell is given by

$$q(t) = V(t)\ I(t)\ /\ L$$

where V(t) is the sum of V_B the backoff voltage (measured accurate to 10 microvolts) and the voltmeter reading $V_v(t)$ (accurate to 1 microvolt).

$$V(t) = V_v(t) + V_B.$$

The current changes are measured by monitoring the voltage changes across the standard resistor (the resistance of which is known) during a simulated run. This data is fitted to a quadratic,

$$I(t) = i_o + I_1\ t + I_2\ t^2 \qquad (15)$$

where i_o is the value relative to the backed off voltage. The initial current is then calculated from SV2 and the resistance of the standard resistor. Then

$$I(t) = I_o + I_1 t + I_2 t^2$$

The power dissipation can can now be written as

$$Iq(t) = I(t) V_v(t) + I(t) V_B \qquad (16)$$

The upper limit of the total current change during the experiment is 4 ppm. Taking $V_B \doteq 300$ millivolts, $\Delta V_v \doteq 500$ microvolts, we see that the change in the second term on the rhs of the last equation is much smaller:

$$\frac{(I_f - I_o) V_B}{\Delta q} \doteq .2\% \quad ;$$

here $I_f = I_o + \Delta I$. Hence measuring V_B to 10 microvolts produces negligible error, in the calculation of q_2 and q_3.

Combining equations (15) and (16), with voltage change data as a function of time is sufficient to fit q(t) where the first term q_1 is calculated from the measured initial current and cell resistance. Hence

$$q_1(t) = q(t)/1 = q_1 + q_2 t + q_3 t^2$$

The time averaged power dissipation is given by

$$\bar{q}_1 = q_1 + \frac{q_2}{2} t_{max} + \frac{q_3}{3} t_{max}^2 .$$

4) Calculation of λ_1. The string of voltage changes measured as a function of time are smoothed by fitting to a quadratic in ln t averaged over the integration period.

$$V(t) = A + Bg(t_1) + Cg^2(t_1) ,$$

where

$$g(t_1) = \frac{t_1}{\Delta t} \ln\left[1 + \frac{\Delta t}{t_1}\right] + \ln(t_1 + \Delta t) .$$

Data taken during the first half second where specific heat effects are important is ignored. The first conductivity value is, found by processing readings 5-15 and a conductivity is calculated through an iterative procedure by using 6 more readings each time.

An iteration is initiated by calculating the first approximation to the thermal conductivity by the line source method. This value is used for calculating, through equation (13) a new value, which is fed back into equation (13). The process is continued until the change is successive iterations is less than .01% of the value of λ_1.

A series of apparent conductivities as a function of experimental time are thus calculated, along with corresponding

standard deviations, and differences from the line source method arising from finite wire diameter, variable power and temperature dependent thermal conductivity.

A listing of the source program may be found in appendix 3A.

CHAPTER 4

DATA AND DISCUSSION

1. Introduction

The thermal conductivity of toluene has been measured at three temperatures between 30 and 90 degrees centigrade over a pressure range of up to 6250 atmospheres. In all, a series of approximately 50 measurements has been made. No data could be found for comparison with the high pressure thermal conductivity measurements of this work. Atmospheric pressure measurments were within about 0.5% of previous work by Pittman (Ref.5).

In this chapter, the data will be presented along with results of hot wire dR/dT calculations. A sample calculation for the conductivity will also be given.

2. Toluene Properties

Analar grade toluene (Hopkin and Williams Ltd.) was refluxed over sodium wire for about six hours and distilled. A middle cut was separated and it's refractive index measured. This was found to be 1.4942 $\pm$ .0002 at 25 $\pm$ .1°C.

No high pressure data on the heat capacity and density of toluene are at present available. The heat capacity values at high pressure were taken to be those at the corresponding temperature at 1 atmosphere (Ref.1). Since, in the calculation of the conductivity the heat capacity appears in terms which are rather small, the error arising from this approximation is negligible (see Chapter 3).

Density data for toluene had to be estimated in order to relate the pressure to the compression of sample volume. Results of this calculation were used to compute the thermal diffusivity at high pressure. The method for estimating high pressure densities (Ref.2) from atmospheric data on ρ v.s. T , is based on the assumptions that isochors (constant volume lines) are straight, i.e. that $(dP/dT)_V$ is constant and that the $(dP/dT)_V$ v.s. ρ relationship is linear.

$$\left[\frac{P_2 - P_1}{T_2 - T_1}\right]_V = \left[\frac{dP}{dT}\right]_V = A\rho + B \qquad (1)$$

By using the few available data points (Ref.3)

PRESS. (ATM)	V_{rel}
1810	.885
2930	.853
4400	.824

where V_{rel} is the ratio of $V_P / V_{P=1at}$ and the density temperature relationship from the International Critical Tables ,

$$\rho(T) = .88448 - .9159 \times 10^{-3}\, T + .368 \times 10^{-6}\, T^2 \qquad (2)$$
$$(0 < T^{\circ} C < 110)$$

the density can be estimated over the relevant temperature and and prossure range (Fig. 1) .

The method was checked by calculating n-hexane densities and comparing with previously measured values (Ref.4); it was found to be within 1% up to 2000 atmospheres, deteriorating to about 5% around 6500 atmospheres, over the 0-100°C temperature range.

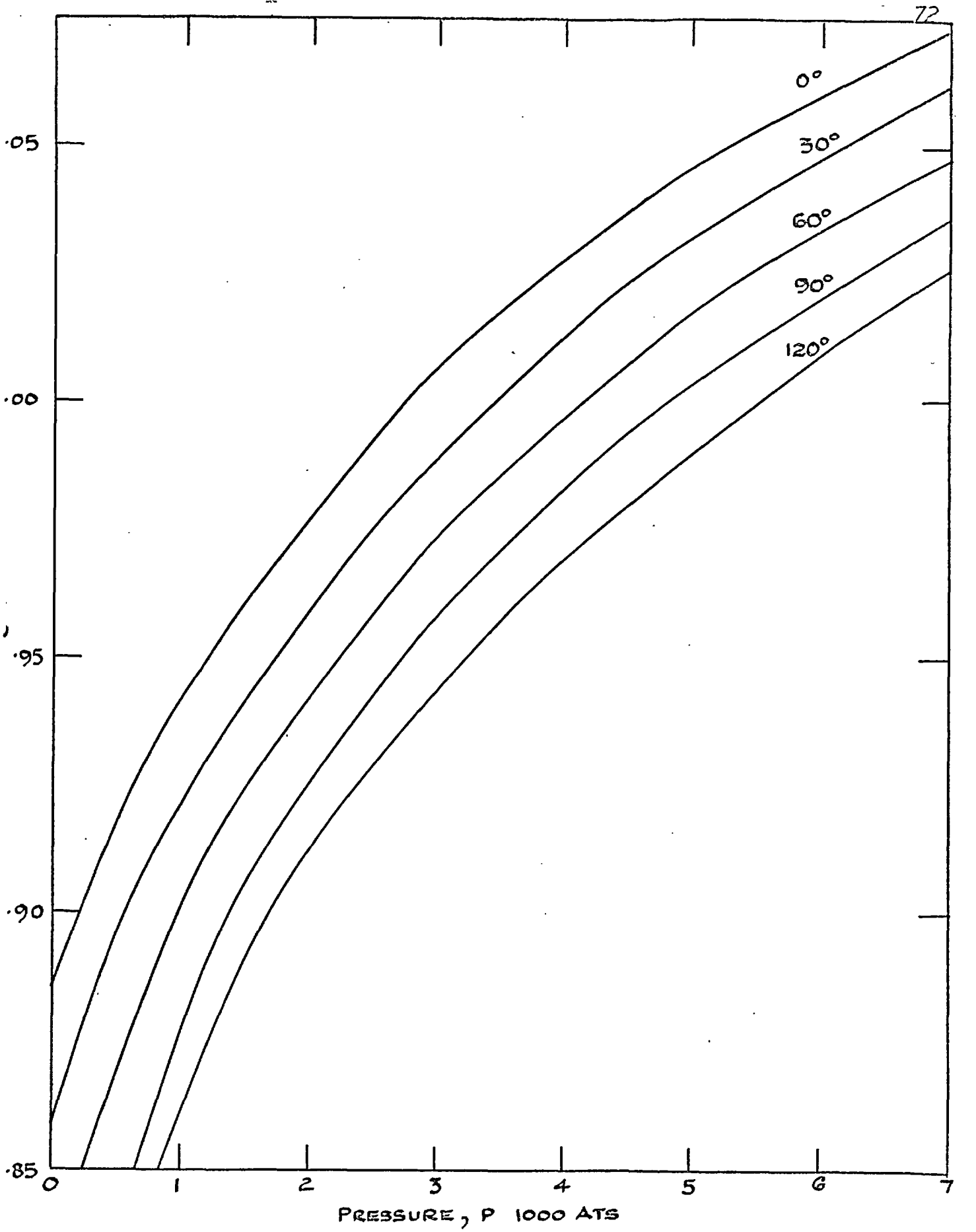

FIG. 1. TOLUENE DENSITIES AT HIGH PRESSURE (ESTIMATED)

3. The Wire

The length of the wire between the two potential taps was measured before the toluene runs. The cathetometer measurements, which were described in the previous chapter yielded

8.103

8.100

8.099 Mean : 8.100 cm.

The measurement was repeated after the conductivity determinations.

8.098

8.105

8.102 Mean : 8 .102 cm.

This change of less than .02% is within the accuracy of the measuring instruments, and in any case negligible.

The calculation of the temperature coefficient of wire resistance has been described in the last chapter. At each pressure, dR/dT was taken to be constant over the experimental temperature range, as the latter was rather small.

PRESS.(ATM)	dR/dT(ohm/°C)
1	.059875
1500	.059734
2250	.059663
3250	.059565
4850	.059407
6250	.059264

4. Toluene Thermal Conductivities.

Results obtained in the experiments are given below:

TABLE I

PRESSURE (ATM)	TEMP. (°C)	λ mw / cm-°C	λ(mean) mw/cm-°C	Av. % Deviation from the mean
1	28.2	1.297		
		1.300	1.298	0.1
		1.297		
	30.8	1.282		
		1.288	1.285	0.2
		1.286		
1500	30.8	1.633		
		1.631		
		1.630	1.633	0.12
		1.636		
	61.4	1.589		
		1.598	1.595	0.25
		1.598		
	91.5	1.537		
		1.543	1.538	0.5
		1.544		

TABLE I Cont..

PRESSURE (ATM)	TEMP. (°C)	λ mw / cm-°C	λ (mean) mw/cm-°C	Av. % Deviation from the mean
2250	30.8	1.824		
		1.814	1.815	.34
		1.808		
	61.4	1.822		
		1.776	1.793	1.1
		1.780		
	91.5	1.770		
		1.800	1.791	0.8
		1.803		
3250	30.8	1.917		
		1.911	1.914	0.1
	61.3	1.937		
		1.943	1.938	0.1
		1.935		
	91.6	1.940		
		1.935	1.938	0.1
		1.939		

TABLE I Cont..

PRESSURE (ATM)	TEMP. (°C)	λ mw/cm-°C	λ (mean) mw/cm-°C	Ave. % Deviation from the mean
4850	30.8	2.108		
		2.125	2.118	0.35
		2.123		
	61.3	2.170		
		2.183	2.173	0.3
		2.170		
	91.6	2.183		
		2.187	2.186	.1
		2.189		
6250	30.8	2.276		
		2.295	2.282	.4
		2.276		
	91.6	2.369		
		2.404	2.383	.6
		2.375		

These results are plotted in Fig. 2.

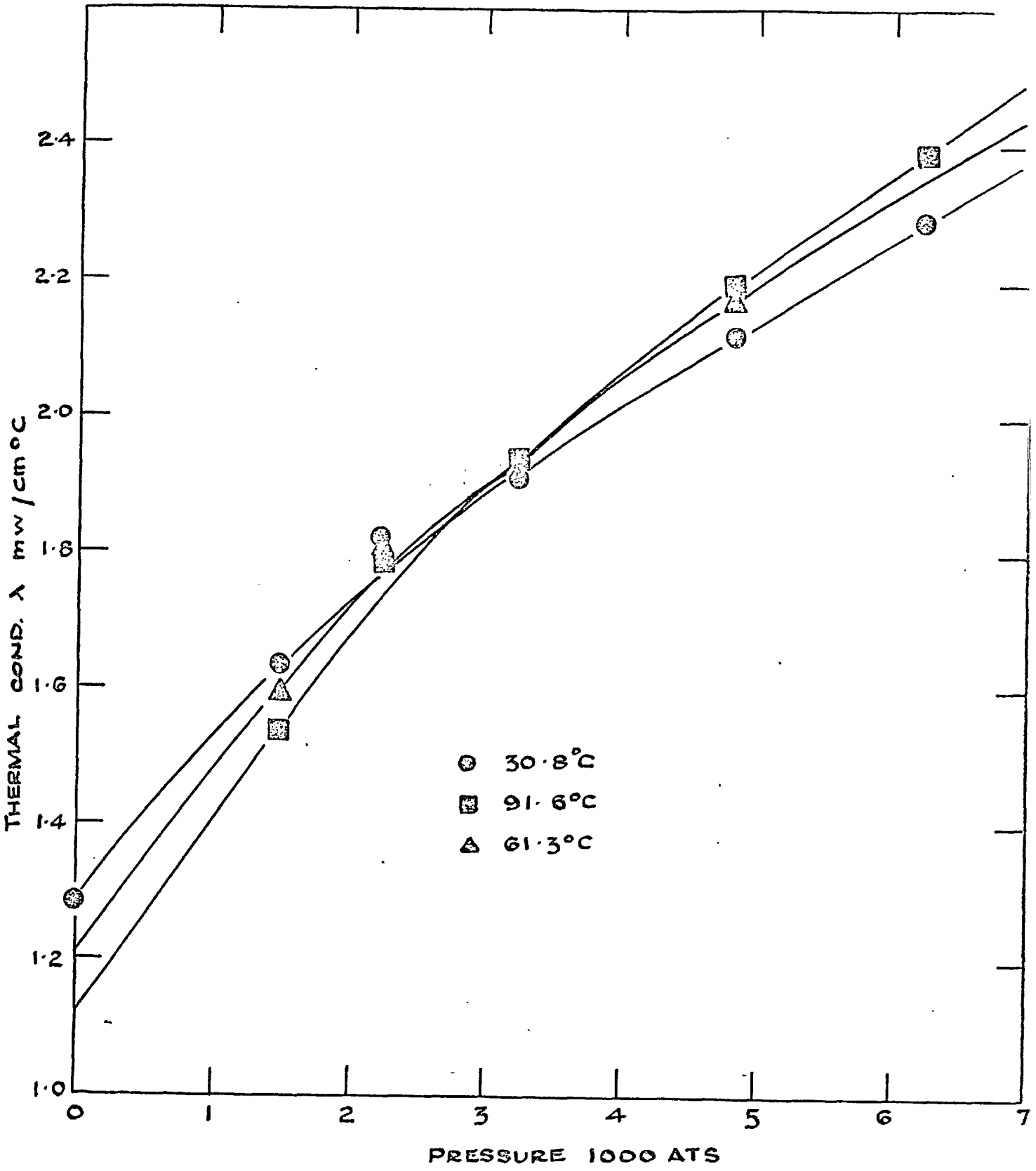

FIG. 2 THERMAL CONDUCTIVITY OF TOLUENE

5. Sample Calculation.

Run 23. Date: 1/8/196

Temperature = 30.8°C; Pressure = 4850 Ats.

Temperature Drift = .01 °C/hr

Measurements Before Run.

DC supply : 10V

Voltage Drop Across	Cell:	27.5970 mV
" " "	Ballast:	27.5971 mV
" " "	Standard Resistor:	9.8302 mV
" " "	Heating Section of Wire:	16.9312 mV

Back off Setting: 314.04 mV

DC Supply: 200 V.

Voltage Drop Across Standard Resistor: 196.494 mV

Summary from Computer Output.

Operating Current: 19.6478 milli Amp

Initial Resistance: 17.2250 ohms.

dR/dT (approx. value used): .058954 ohm/°C.

No. Pts Included	λ	Standard Deviation
15	$.21123 \times 10^{-2}$	$.64358 \times 10^{-6}$
33	$.21145 \times 10^{-2}$	$.60107 \times 10^{-6}$
51	$.21126 \times 10^{-2}$	$.75573 \times 10^{-6}$
69	$.21123 \times 10^{-2}$	$.76917 \times 10^{-6}$
87	$.21165 \times 10^{-2}$	$.74863 \times 10^{-6}$
105	$.21154 \times 10^{-2}$	$.81744 \times 10^{-6}$

Linear fit extrapolated to zero time gives

$$\lambda = 2.110 \text{ mw/cm.}^{\circ}\text{C}$$

Smoothed dR/dT = .59407 ohm/°C.

Corrected λ = 2.125 mw/cm.°C.

6. Sources of Error

During the experiments, temperature drifts in the cell were followed by measuring the cell resistance at short intervals. As each set of determinations was completed within the span of about two hours and the accepted drift rate was 0.03 °C/hr the measurements can be averaged with a maximum error of .1%, over the pressure range. On the other hand, as mentioned in the previous chapter, the experimental temperature is measured in the oil bath between a hollow cylinder surrounding the vessel, and the pressure vessel itself. While this arrangement somewhat shields the thermometer from temperature fluctuations in the oil bath ($\pm$ .1°C), the temperature seen by the thermometer is expected to be less stable than that in the cell, which is surrounded by the thermal mass of the pressure vessel. As the time lag between the exterior of the vessel and the cell is about 3 to 4 hours, the temperature difference (assuming continuous drift in one direction) could be as much as 0.3 to 0.4 degrees centigrade. This gives rise to two types of error.

1) The measured thermal conductivity, depending on the magnitude of $d\lambda/dT$ at the given pressure, would be in error, by 0.2 to 0.5%

2) In the evaluation of dR/dT, the cell resistance would be matched to a temperature different than that in the cell. The resistance value would be in error by about 0.2%. The error in dR/dT with an upper limit of about 0.5% due to this, might be expected to decrease through the double smoothing procedure of R v.s. T data outlined in the previous chapter. Furthermore, the shortness of the temperature range would be expected to affect the accuracy of the temperature coefficient. This error could be estimated to be in the range 1.0 to 3.0%. and closer to the larger value at the ends of the temperature range.

Errors in the thermal conductivity measurement due to convective effects are due to two types of mechanisms. The first is due to heating of the central part of the wire with the result that at the extremities vertical temperature gradients are set up. It has been assumed that the radial temperature field remains unchanged until the "cold front" approaches the bottom potential tap. To this must be added heat losses from the potential lead into the convecting fluid; this clearly ties in with and aggravates the problem of heat loss from the central wire by conduction into the potential leads, with the result that the radial temperature field is distorted. These errors, however, may be

minimised by extrapolating the data to zero time, provided that the fluid is assumed to be initially stagnant. This brings us to the second type: free convection at the start of the experiment due to vertical temperature gradients. The observed fall in apparent conductivity with time observed in many runs is consistent with hot fluid rising from below the heating wire in the cell. It is difficult to estimate the error arising from these initial vertical temperature gradients in the cell, since these would depend on the magnitude of the gradient. This effect is somewhat smaller at higher pressures, as would be expected, and the error arising from it would be estimated in the range 0.2 to 0.5% after extrapolation to zero time. This initial free convection would also imply that potential tap losses are not completely eliminated by extrapolation to zero time. The resulting error could be as high as 0.5%. Errors due to radiation losses may be ignored with little error when the data is extrapolated to zero time. Finally, as can be seen from percent deviations from the mean an error of 0.1 to 1.0% must be accepted from random factors, such as electrical noise, and scatter in the extraplated lines.

Summarizing, the error due to averaging the results of each run should give rise to 0.1%, uncertainty in the

temperature measurement to 0.4 to 1%, the initial convection effect to 0.2 to 0.5%, uncertainty in dR/dT to 1 to 3%, end effects to 0.1 to 0.5%, and random errors to 0.1 to 1%.

CHAPTER 5

THE HEAT TRANSFER EQUATION WITH VARIABLE PHYSICAL PROPERTIES

1. Introduction

In Chapter 2 a set of linearization transformations, proposed by Kudryashev and Zhemkov, were applied to a problem where the inversion procedure was rather straightforward due to ξ reducing to Kt without significant error. Here the evaluation of these transformations as a tool for solving certain types of partial differential equations will be attempted. For a chosen simple geometry, the solution obtained by this method will be compared with two other ways of solving the problem. It will be seen that while all three methods agree for small nonlinearities, the differences for large values of the temperature coefficient of the thermal conductivity are significant.

2. The Infinite Slab

For purposes of comparison, a problem solved with a variational technique (Ref.1) has been chosen.

An infinite slab of thickness 2L is held at uniform temperature T_s , and the boundaries -L and L subjected to $T(-L,t) = T(L,t) = 0$, for $t > 0$. The temperature profiles are symmetric with respect to the plane $x = 0$. The density and the heat capacity are assumed constant and the thermal conductivity is given by

$$\lambda(T) = \lambda_1 \left(1 + \lambda_2 T \right) \quad \text{where} \quad \lambda_2 = \frac{1}{\lambda_1} \frac{d\lambda}{dT} . \tag{1}$$

The problem can now be stated as

$$T(x,0) = T_s \quad ; \qquad -L \leq x \leq L$$

$$T(-L,t) = T(L,t) = 0 \quad ; \quad t > 0$$

with the partial differential equation

$$\rho C_p \frac{\partial T}{\partial t} = \frac{\partial}{\partial x} \left[\lambda(T) \frac{\partial T}{\partial t} \right] . \tag{2}$$

In order to simplify handling, the problem is put in dimensionless form. The new variables are defined as :

$$\beta = \frac{x}{L} ; \quad \tau = \frac{\lambda_2}{\rho C_p} \frac{t}{L^2} \quad ; \quad \theta = \frac{T}{T_s} \quad ; \quad \sigma = T_s \lambda_2 \tag{3}$$

and the problem can be re-stated in dimensinless form as follows:

$$\theta(\beta,0) = 1 \qquad ; \qquad -1 \leq \beta \leq 1 \tag{4}$$

$$\theta(-1,\tau) = \theta(1,\tau) = 0 \; ; \; \tau > 0 \tag{5}$$

$$\frac{\partial \theta}{\partial \tau} = \frac{\partial}{\partial \beta} \left[\left(1 + \sigma\theta \right) \frac{\partial \theta}{\partial \beta} \right] . \tag{6}$$

For this particular problem, the Kudryashev and Zhemkov transformations (ref. 2) can be re-cast as follows.

The enthalpy/mass, referred to the initial temperature is defined as

$$dh = d\theta \tag{7}$$

and the quantity ϕ as

$$\phi = \int_0^h \lambda \, dh' \quad . \tag{8}$$

Differentiating (8) and using (7)

$$d\phi = \lambda \, d\theta \tag{9}$$

which immediately leads to

$$\frac{d\phi}{dR} = \lambda \frac{d\theta}{dR} \quad \text{and} \quad , \quad \nabla^2\phi = \nabla\cdot(\lambda \nabla\theta) \, . \tag{10}$$

Furthermore, we define the quantity

$$\xi = \int_0^\tau \lambda \, d\tau' \quad ; \quad d\xi = \lambda \, d\tau \quad . \tag{11}$$

Using equations (9)-(11) we get

$$\nabla^2\phi = \frac{\partial\phi}{\partial\xi} \quad , \tag{12}$$

and by (7) and (8)

$$\phi(R,0) = 0 \, . \tag{13}$$

In order to obtain the boundary conditions,

$$h = \int_0^h dh' = \int_1^\theta d\theta' = \theta - 1$$

At $\theta = 0$, $h = -1$. Therefore

$$\phi(-L,\xi) = \phi(L,\xi) = \int_0^1 [1+\sigma(h'+1)] dh' = -(1+\frac{\sigma}{2}) . \quad (14)$$

The solution to the problem stated in equations(12)-(14) is well known (Ref. 3) .

$$\chi(x,\xi) = \frac{4\chi_o}{\pi} \sum_{n=o}^{\infty} \frac{(-1)^n}{(2n+1)} \exp[-\frac{(2n+1)^2\pi^2\xi}{4}] \cos \frac{(2n+1)\pi\beta}{2} \quad (15)$$

where $\chi = \phi + (1 + \frac{\sigma}{2})$, and $\chi_o = (1 + \frac{\sigma}{2})$.

The transformation must now be inverted in order to get $\theta(\beta,\tau)$. If equation (10) is integrated with respect to β

$$\int_L^\beta \frac{d\phi}{d\beta'} d\beta' = \int_L^\beta \lambda \frac{d\theta}{d\beta'} d\beta' . \quad (16)$$

By using (5) and(14)

$$\phi(\beta,\xi) + (1+\frac{\sigma}{2}) = \theta(\beta,\tau) + \frac{\sigma}{2} \theta^2(\beta,\tau) ,$$

from which it immediately follows that

$$\chi(\beta,\xi) = \theta(\beta,\tau) + \frac{\sigma}{2} \theta^2(\beta,\tau) . \quad (17)$$

This equation, coupled with eqn. (11)

$$\xi = \int_0^\tau (1+\sigma\theta) d\tau' \quad (18)$$

will be used to obtain $\theta(\beta,\tau)$.

3. Solution of Equations (15),(17) and (18).

In order to solve the system of equations (15),(17) and (18), it is necessary to resort to numerical procedures. ξ is taken to be the polynomial of the form

$$\xi = \tau + \sum_1 A_i \exp(-\gamma_i \tau) \qquad (19)$$

where each pair of constants A_i and γ_i are computed from successive approximations. For any given pair of β and τ, we first integrate under the curve $\theta(\beta,\tau)$ by setting $\xi=\tau$ Then

$$\xi = \tau + \sigma \int_0^\tau \theta \, d\tau' = \tau + A_1 \exp(-\gamma_1 \tau) \quad . \qquad (20)$$

Clearly, in the first approximation

$$A_1 \exp(-\gamma_1 \tau) = \sigma \int_0^\tau \theta \, d\tau' \quad . \qquad (21)$$

Taking the natural logarithm of both sides and differentiating with respect to τ, we get

$$\gamma_1 = - \frac{\theta_1(\tau)}{\int_0^\tau \theta \, d\tau'} \quad . \qquad (22)$$

Substituting this result in (21) and solving for A_1

$$A_1 = \sigma \, [\exp(\gamma_1 \tau)] \int_0^\tau \theta \, d\tau' \quad . \qquad (23)$$

The second pair is obtained similarly; ξ now is given by

$$\xi = \tau + A_1 \exp(-\gamma_1 \tau) \quad .$$

A new value for the integral $\int_0^\tau \theta \, d\tau'$ can now be calculated

$$A_i \exp(-\gamma_1 \tau) + A_2 \exp(-\gamma_2 \tau) = \sigma \int_0^\tau \theta \, d\tau' \quad ,$$

where A_1 and γ_1 are known. Proceeding as before

$$\gamma_2 = -\gamma_1 - \theta(\tau) \Big/ \int_0^\tau \theta \, d\tau' \quad \text{and}$$

$$A_2 = \left[-A_1 \exp(-\gamma_1 \tau) + \sigma \int_0^\tau \theta \, d\tau' \right] \exp(\gamma_2 \tau) \quad .$$

It can easily be shown that the n-th pair of coefficients is given by

$$\gamma_n = -\left[\sum_{k=1}^{n-1} \gamma_k + \frac{\theta(\tau)}{\int_0^\tau \theta \, d\tau'} \right] \tag{24}$$

and

$$A_n = \left[\sigma \int_0^\tau \theta \, d\tau' - \sum_{k=1}^{n-1} A_k \exp(-\gamma_k \tau) \right] \exp(\gamma_n \tau). \tag{25}$$

The iteration was stopped when the last two calculated values of $\theta(\tau)$ were less than 10^{-5} apart. The calculation was repeated for each given pair of β and τ. A 16 point Gauss-Legendre quadrature was used for performing the integrations.

4. The Finite Difference Approximation

For the purpose of comparison, the problem of equations (4) - (6) was solved using the finite difference technique (Ref.4); as only a general outline of the way to deal with the problem was found in the literature, the essentials of the solution will be given here.

If we divide the one-dimensional space-time plane into a grid where the space variable incrment is h, and time increment k, the first derivative of u [=u(x,t)] is approximated by

$$\delta u \doteq \frac{1}{h}\left[\, u(x+h/2) - u(x-h/2) \,\right] . \qquad (26)$$

Then

$$\delta(\lambda\ \delta u) \doteq \frac{1}{h}\left[\lambda(x+h/2)u'(x+h/2) - \lambda(x-h/2)u'(x-h/2)\right] \qquad (27)$$

where u'is given by (26). Denoting the central grid element by $u_{i,j}$ rather than u(x,t) we have

$$\nabla\cdot(\lambda \nabla u) \doteq \left[\lambda_{i+\frac{1}{2}}(u_{i+1}-u_i) - \lambda_{i-\frac{1}{2}}(u_i - u_{i-1})\right]\frac{1}{h^2} \qquad (28)$$

and the time derivative of u

$$\frac{\partial u}{\partial t} \doteq \frac{1}{k}\left(\, u_{i,j+1} - u_{i,j} \,\right) . \qquad (29)$$

By defining $r = \frac{k}{h^2}$, $\alpha_n = r\lambda_n$ and $\lambda = 1 + \sigma u$,

and using the Crank-Nicholson method (Ref.5),

$$u_{i,j+1} = \frac{-(2r+2) + \sqrt{A}}{2r\sigma} \qquad (30)$$

where

$$A=(2r+2)^2+4r\sigma\left[\frac{\sigma r}{2}\,u_{i+1}^2+ru_{i+1}+\frac{\sigma r}{2}\,u_{i-1}^2+ru_{i-1}+2b_i\right]. \qquad (31)$$

Here all u's are understood to denote the grid point j + 1.

In equation (31)

$$b_i=u_i+\tfrac{1}{2}\left[\alpha_{i+\frac{1}{2}}\,(u_{i+1}-u_i)-\alpha_{i-\frac{1}{2}}\,(u_i-u_{i-1})\right], \qquad (32)$$

where u's are understood to denote the grid point j.

Using Gauss-Seidel iterations (Ref.5), the n + 1'th approximation for $u_{i,j+1}$ is given by

$$u_i^{n+1}=\frac{-(2r+2)+\sqrt{A^{n+1}}}{2\sigma r} \qquad (33)$$

where

$$A^{n+1}=(2r+2)+4r\sigma\left[\frac{r\sigma}{2}\,u_{i+1,n}^2+ru_{i+1,n}+\frac{\sigma r}{2}\,u_{i-1,n+1}^2+ru_{i-1,n+1}+2b_i\right] \qquad (34)$$

where b_i is given by (32) with the u's denoting the n + 1'th approximation. For faster convergence the iterations were carried out with successive over relaxation (SOR).

Defining $\Delta=u_i^{n+1}-u_i^n$, in SOR

$$u_i^{n+1}=u_i^n+w_b\,\Delta$$

where the SOR coefficient w_b is defined by

$$w_b=2/(1+\sqrt{1-\mu^2}) \qquad \text{and} \qquad \mu=\frac{r}{1+r}\cos\frac{\pi}{N}.$$

(Ref.5).

5. Results and Conclusions

Temperature profiles were calculated by the two methods. Figure 1 shows that for $\sigma = .1$ agreement is quite good. On Figure 2 results of the solution of the problem by the variational technique (Ref.1) are plotted as well as the two previous methods for $\sigma = 1$. Assuming that the finite difference solution is the "correct" one, it will be seen that for $\sigma = 1$

a) the variational technique is inaccurate for small times, and gets progressivaly better for longer times, and that

b) the method resulting from the Kudryashev-Zhemkov transformations shows that better agreement for short times but rapidly deteriorates as τ gets large.

That the error should grow with time is probably indicative of instability in the integration procedure, as the set of equations (15), (17) and (18) is exact.

The results for $\sigma = .1$ can be taken as justification for the use of this method in the analysis of the experiment presented in earlier chapters, since the corresponding σ is less than .01. Thus in the present form this method is

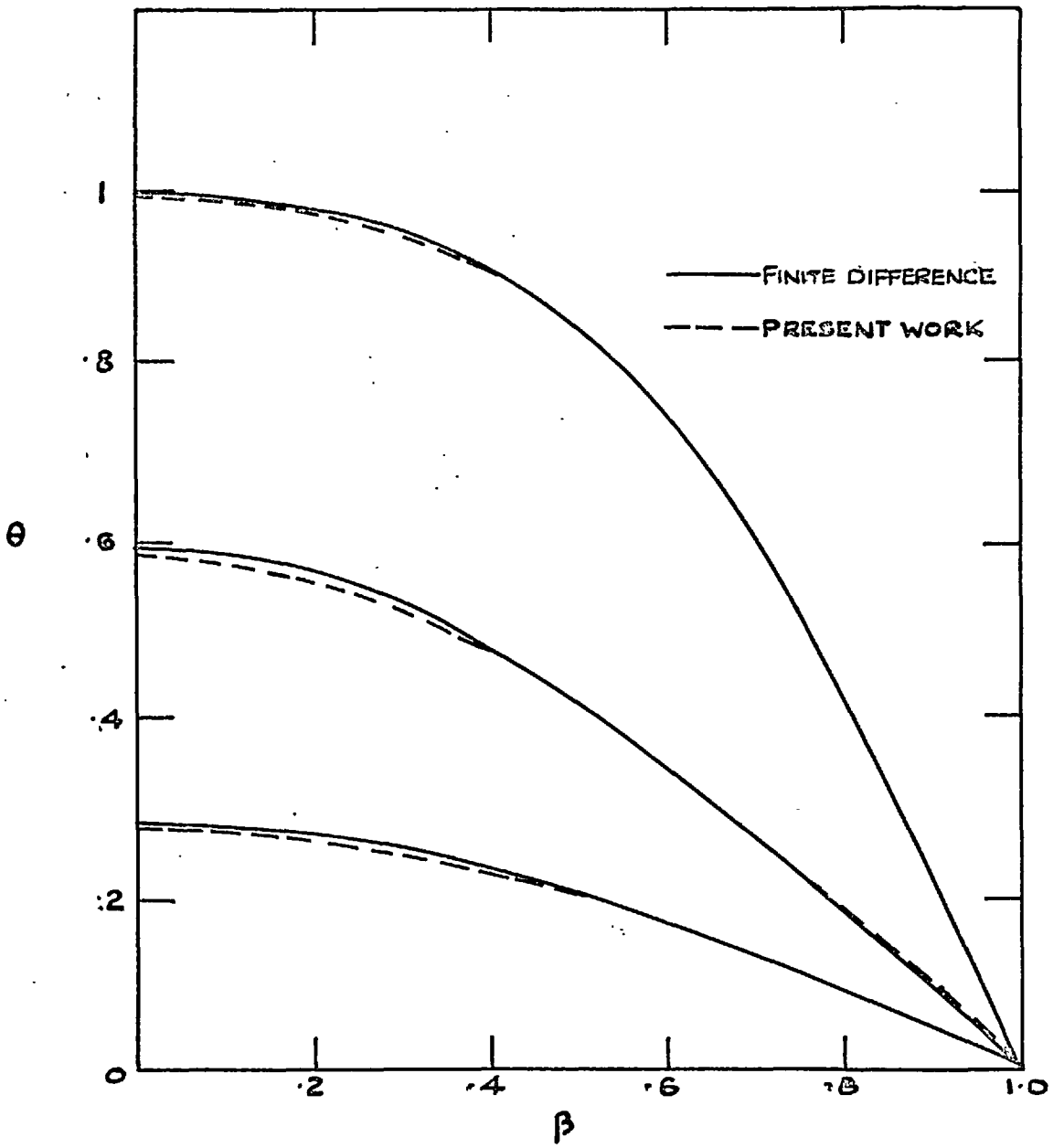

FIG.1. COMPARISON OF SOLUTIONS FOR $\sigma = \cdot 1$

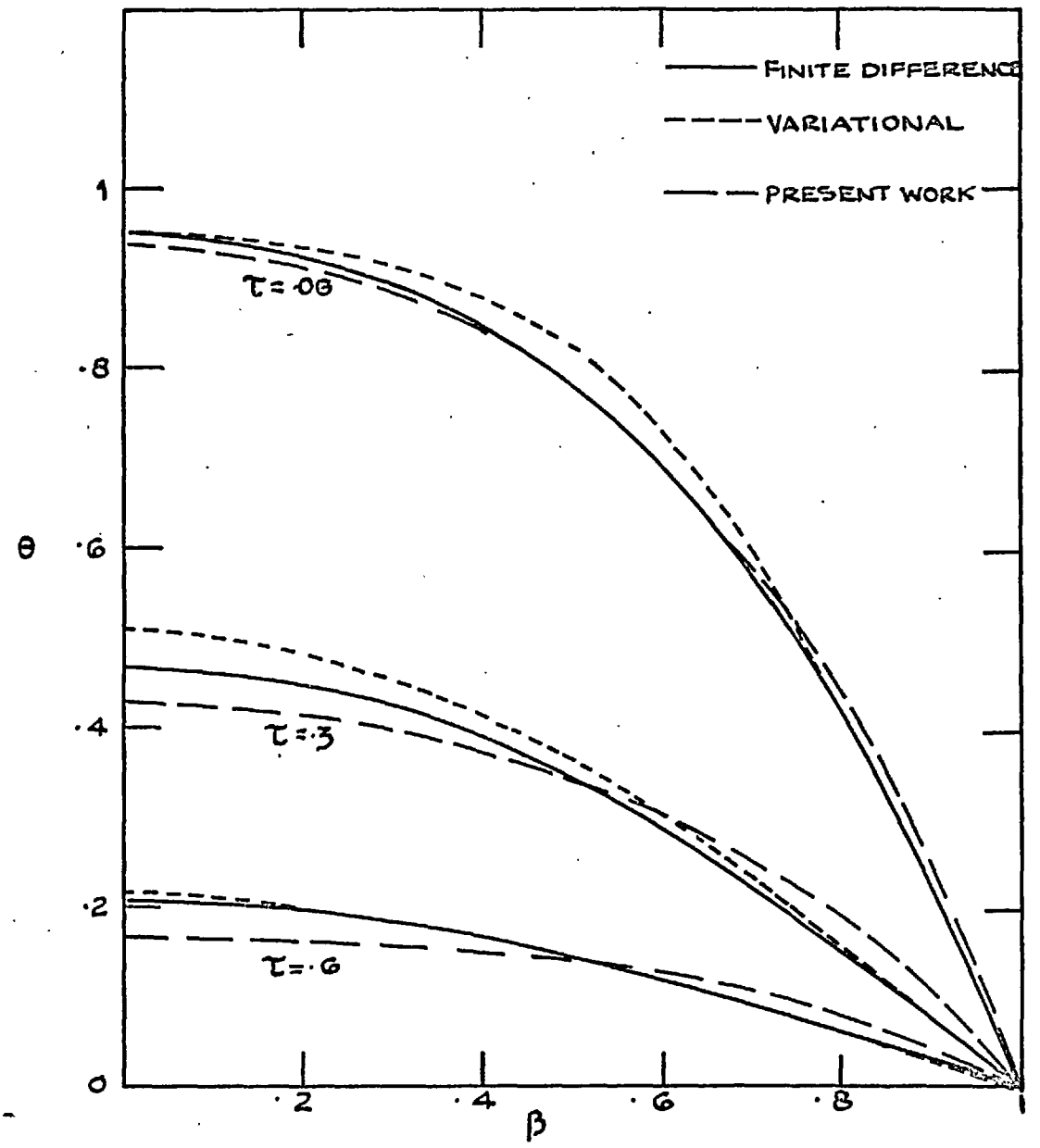

FIG 2 COMPARISON OF THE THREE METHODS.
$\sigma = 1$

applicable to a large number of problems. It also lends itself to a straightforward evaluation of the errors due to temperature dependence of the physical properties, by estimating the upper limit of the integral

$$\xi = \int_0^t \frac{\lambda}{\rho C_p} \, dt \quad ,$$

as illustrated in appendix 1.

Computer programs for the above calculations will be found in appendices 3C and 3D.

CHAPTER 6
The Harmonic Oscillator Model for Liquids of Spherical and Chain Molecules

A short account of the cell model for simple liquids, and its extension to the harmonic oscillator approximation will be given, followed by the application of these models to chain molecules. The assumptions involved in each case will be briefly discussed.

1. The Basic Equations

The Helmholtz free energy, A, of a system is defined by the equation

$$A = - kT \ln Z \qquad (1)$$

where k is the Boltzmann constant, T is the absolute temperature and Z is the partition function of the system, defined as the sum over all states of the Boltzmann factor. $\exp (- E_i/kT)$, E_i denoting the energy of state i.

In the classical approximation, the translational partition function can be expressed as an integral

$$Z = \frac{1}{N! h^{3N}} \int \cdots \int \exp \left[-H(\underline{P}_1, \ldots \underline{P}_N, \underline{r}_1, \ldots, \underline{r}_N) \right] d\underline{P}_1 \ldots d\underline{P}_N d\underline{r}_1 \ldots d\underline{r}_N$$

where H, the Hamiltonian is given by (2)

$$H = \sum_1^N \frac{\underline{P}i^2}{2m} + \phi (\underline{r}_1 \ldots\ldots\ldots \underline{r}_N). \qquad (3)$$

Here $\underline{P}_i = m \frac{d\underline{r}_i}{dt}$, and $\underline{r}_i$ is the position vector of molecule i, which has the mass m.

On the assumption that the $\underline{P}_i$ and $\underline{r}_i$ are independent of each other, the two sets of integrations, over the $\underline{P}_i$ and $\underline{r}_i$ can be performed separately and the partition function written as a product of the two. The set of integrations over the momenta yields:

$$\left[\frac{2\pi\, mkT}{h^2}\right]^{3N/2} .$$

The integral over the positions of the molecules is called the classical configurational integral defined as,

$$Q(N, T, V) = \frac{1}{N!} \int \cdots\cdots \int \exp(-U/kT)\, d\underline{r}_1 \cdots\cdots d\underline{r}_N \qquad (4)$$

where U is the total configurational energy, (potential energy) of the system. If one assumes this energy to be pairwise additive, then

$$U = \sum_{i>j} u(R_{ij}), \qquad (5)$$

where R_{ij}, denotes the intermolecular separation, and $u(R_{ij})$ the intermolecular potential. The translational partition function for the system is then written as,

$$Z = \left[\frac{2\pi mkT}{h^2}\right]^{3N/2} Q(N,T,V) \quad . \qquad (6)$$

2. The Equations of the Cell Lattice Model

For dense systems, composed of molecules with attractive forces, the potential energy is approximated by

$$U = U_0 + \sum_{i=1}^{N} [\epsilon(r_i) - \epsilon(0)] \qquad (7)$$

under the following assumptions:

a) That the volume of the system be subdivided into cells of equal volume,

b) that each of these cells contain one molecule, and

c) that each molecule move in its cell independently of molecules in neighbouring cells. Ref (1a).

In equation (7), U_o is the potential energy of the system when all molecules are positioned in the centers of their respective cells, r_i is the displacement of molecule i from the center of its cell and $\chi(r_i) - \chi(0)$ is the potential energy change involved in this displacement. Equation (4) then takes the form

$$Q(N,T,V) = \frac{1}{NI} \exp(-U_o/kT)\, \chi^N \qquad (8)$$

where

$$\chi = \int \exp\left[-\left[\phi(r) - \phi(0)\right]/kT\right] dv \qquad (9)$$

the integration being performed over the volume of each cell.

3. The Smearing Approximation

In order to calculate the mean displacement energy, given by equation (9), (Ref (2) and (3))we take a molecule, A, fixed while the second, B, is allowed to move about a sphere of radius r. The center of the sphere is a distance, α, from molecule A. The distance between molecule A and molecule molecule B is given by

$$d = [a^2 r^2 - 2ar\cos\theta]^{\frac{1}{2}}$$

where θ is the angle between "a" and "r". The average mutual potential over the surface of the sphere can be written as

$$\bar{\varepsilon}(r) = \frac{\int_0^{2\pi}\int_0^{\pi} \varepsilon(d)\sin\theta\, d\theta\, d\phi}{\int_0^{2\pi}\int_0^{\pi} \sin\theta\, d\theta\, d\phi} \qquad (10)$$

If $\varepsilon(r)$ is taken as the Lennard-Jones 12-6 potential

$$\varepsilon(r) = \left\{\left(\frac{r_o}{r}\right)^{12} - 2\left(\frac{r_o}{r}\right)^{6}\right\} \qquad (11)$$

where ε is the potential minimum, and r_o the intermolecular separation corresponding to that minimum, and if we donote the nearest number of neighbours by z, the average potential per cell is then given by:

$$\bar{\varepsilon}(r) = 4z\varepsilon\left\{\left[\frac{v^o}{v}\right]^4 [1(y)+1] - \left[\frac{v^o}{v}\right]^2 [m(y)+1]\right\} \qquad (12)$$

where

$$\frac{v^o}{v} = \frac{r_o^3}{a^3} \quad \text{and} \quad a = \frac{\sqrt{2V}}{N};\ y = \frac{r^2}{a^2},$$

$$1(y) = (1+12y+25.2\,y^2+12\,y^3+y^4)\,(1-y)^{-10} - 1, \qquad (13)$$

$$m(y) = (1+y)(1-y)^{-4} - 1. \qquad (14)$$

Using equation (12) to derive $\bar{\varepsilon}(0)$, we get

$$\bar{\varepsilon}(r) - \bar{\varepsilon}(0) = 4\varepsilon z\left\{\left[\frac{v^o}{v}\right]^4 1(y) - \left[\frac{v^o}{v}\right]^2 m(y)\right\}. \qquad (15)$$

4. The Harmonic Oscillator Approximation

By expanding equation (15) as a Taylor series about the center of the cell, in terms of y, we obtain an

expression for small oscillations of the molecule

$$\bar{\epsilon}(y)-\bar{\epsilon}(0)=y\bar{\epsilon}'(0)-y^2\bar{\epsilon}''(0)+ \cdots$$

by truncating the expansion after the first term, we obtain the harmonic approximation to the mean cell potential acting on a molecule which performs small oscillations about the center of its lattice cell. Ref. (4a).

$$\bar{\epsilon}(r)-\bar{\epsilon}(0)= z\varepsilon \left[22\left[\frac{v^o}{v}\right]^4 - 10 \left[\frac{v^o}{v}\right]^2 \right] \frac{r^2}{a^2} \qquad (16)$$

Thus, the configurational integral can be expressed in the harmonic oscillator approximation as in equation (8), with

$$\chi = \int_v \exp - \frac{z\varepsilon}{kT}\left[22 \left[\frac{v^o}{v}\right]^4 - 10\left[\frac{v^o}{v}\right]^2 \right] \left[\frac{r}{a}\right]^2 \quad dv . \qquad (17)$$

By making use of the expression for the restoring force constant for small vibrations, $k=4\pi^2\nu^2 m$, the mean frequency of oscillation can be given by

$$\nu = \frac{1}{2\pi\sqrt{m}} \left\{ \frac{2z\varepsilon}{a^2}\left[22 \left(\frac{v^o}{v}\right)^4 -10 \left(\frac{v^o}{v}\right)^2 \right]\right\}^{\frac{1}{2}} \qquad (18)$$

5. Discussion of the L-J-D Theory:

A. Kirkwood's Treatment . (Ref.5)

In an attempt to establish a firm theoretical basis for cell lattice theories, Kirkwood shows how the assumptions mentioned in paragraph two of this chapter, arise in the mathematical treatment. The classical configurational integral is written as

$$Q=\int_0^v \cdots \int_0^v \exp(-U/kT)\, dv_1 \cdots dv_N \qquad (19)$$

where v is the total volume. By assuming N lattices each of volume Δ, and expressing the integrals over V of each molecule as a sum of integrals over the individual cells, (assumption (a) in paragraph 2.) Q can be rewritten as

$$Q = \sum_{l_1=1}^{N} \cdots \sum_{l_N=1}^{N} \int_{\Delta l_1} \cdots \int_{\Delta l_N} \exp(-U/kT)\,dv_1 \cdots dv_N. \qquad (20)$$

The N^N integrals of equation (20) can also be written in terms of integrals $Z_N^{(m_1 \cdots m_N)}$ where the m_i are the number of molecules occupying each cell i:

$$Q = \sum_{\substack{m_1 \cdots m_N = 0 \\ \Sigma m_s = N}}^{N} \frac{N!}{\prod_{s=1}^{N} (m_s!)} \; Z_N^{(m_1 \cdots m_N)} \qquad (21)$$

Here there is one integral Z_N corresponding to the case of single occupancy of each cell, $Z^{(1,1, \cdots .1)}$. We can now define the parameter σ by the relation

$$\sigma^N = \sum_{\substack{m_1 \cdots m_N = 0 \\ \Sigma m_s = N}}^{N} \frac{1}{\prod_s (m_s!)} \; \frac{Z^{(m_1 \cdots m_N)}}{Z^{(1 \cdots 1)}} \qquad (22)$$

and

$$Q = \sigma^N \, Z^{(1,1 \cdots 1)} \, N! \qquad (23)$$

At high densities where the single occupancy assumption is reasonable, σ approaches unity, where as, as the density tends to zero σ will tend to the value e. The entropy calculated on the single occupancy assumption is low as σ is assumed to be equal to unity. The fact that more of the

total volume than just one cell is available to each molecule, and hence that σ lies between unity and one, gives rise to the concept of communal entropy.

Kirkwood continues his treatment by considering only the single occupancy integral. In order to write the free energy explicitly the third major assumption is introduced: the relative probability density in configuration space is written in the form of the product of probability densities of each cell, assumed to be independent of each other.

$$P_N = \prod_{s=1}^{N} \omega(r_s) \qquad (24)$$

where, r_s, the displacement of molecule s from the origin in its cell.

The subsequent minimisation of the free energy by Kirkwood, seems to yield lower energies than those of the L-J-D theory. However there is no theoretical justification for expecting the lowest calculated free energy to be closest to the real value. "It is much nearer to the truth to regard the variational theory as justified insofar as it approximates the L-J-D theory" (Ref. 1b)

B. Barker's Critique

i) The smearing approximation: For rigid spheres, free volumes calculated by using the smearing approximation are about thirty per cent lower than those calculated by detailed analysis

of the volume distribution. The pressures calculated by this approximation are not very different from those calculated from the "correct" free volumes, but the entropy is considerably lower. Similar behaviour is observed for potentials with attractive forces, the error passing through a maximum in the vicinity of the critical density. As the density approaches the triple point, and further increases to that of the solid, the error tends to zero. (Ref 1c).

ii) Correlation effects.

Calculations assuming that only first neighbour motion is significant has yielded good results about the critical density, and this result should be valid at higher densities as well. Most of the error due to assumption (c) of paragraph (2) can be accounted for by taking into account binary and ternary correlations. (Ref 1d).

iii) Multiple occupancy of cells: This remains as an essentially unsolved problem. Attempts have been made to modify the simgle occupancy configurational integral, in order to take multiple occupancy in to account, such as:

$$Q^{(m_1, \ldots, m_N)} = \left[\prod_s (\omega_{m_s}) \right] Q^{(1, \ldots, 1)} \qquad (25)$$

where $Q^{(1,\ldots,1)}$ is multiplied by a factor ω_i given by eqn.(25) for each cell that is occupied by i molecules; various ways to calculate the ω_i s have also been put forward, Refs. (6),(7),(8). These models however have so far failed to take into account

the altered correlations that arise from having multiple occupancy. (Ref 1e)

iv) The Harmonic Approximation. The approach is similar to the Einstein model of the solid and is a justifiable approximation only at high densities. The error arising from the assumption that the molecule vibrates in a cell where all neighbouring molecules are fixed, can be dealt with by taking into account short range correlations, as in paragraph (ii). A comprehensive treatment of these correlations will be found in Ref (1), Chapter 6.

The second major departure of this model from reality is the assumed constancy of the vibrational frequencies throughout the system. Clearly one expects to observe a whole spectrum of frequencies; the Debye model is relevant for the analogous problem in the solid.

6. The Cell Lattice Model for Pure Polymer Solutions. (Ref 4b)

This treatment consists of a cell model approach applied to long chain molecules, for the calculation of the configurational partition function in a manner that is essentially independent of chain length. The liquid is charachterised by three parameters, ϵ the attractive energy minimum, r^0 the intersegment separation corresponding to the energy minimum and the 3c, external degrees of freedom. The latter are independent of valency forces: intramolecular frequencies are at least one order of magnitude larger than the external frequencies, and the influence of external

factors on these frequencies (and there-by the internal degrees of freedom) need not be considered in the first approximation..

The 3c external degrees of freedom are determined empirically through a corresponding state treatment of a homologous series, in this case normal alkanes (Ref 4c). Here only odd numbered chains are considered since from x-ray data, the volume of a $CH_2 - CH_2$ segment is known to have about the same volume as the monomer of the series, CH_4. Thus the segment number R is defined by

$$R = \tfrac{1}{2}(n+1)$$

where n is the number of carbon atoms in the chain.

The major assumptions involved in the model are the following: The chain molecule is treated as a set of point centers, each of which moves in a spherically symmetric force field. The potential energy between two point centers of different r-mers (chains) is taken as a two parameter law

$$\epsilon(r) = \epsilon \ \varphi\left(\frac{r}{r_o}\right)$$

where r is the point center separation, and $\varphi\left(\frac{r}{r_o}\right)$ is most commonly taken as the Lennard-Jones 12-6 potential.

The criterion for the existence of lattice is that the mean distance between point centers be equal, whether the point centers belong to the same r-mer or not; i.e. that

$$a = d = r_o$$

where "a" is the mean distance between two neighbouring chain segments, belonging to two different chains, and d is the distance between two successive elements of the same chain. At absolute zero, $a = r_o$ and the r-mers are perfectly ordered on a regular

lattice. As the temperature is allowed to increase, the lattice will be distorted by the expansion of the liquid, and the model will progressively cease to represent the liquid structure. The treatment assumes that the distortions can be ignored if the volume expansion is less than a few per cent. Then the volume per segment is

$$v = \frac{V}{RN} = \gamma^{-1} a^3 \qquad (26a)$$

where for an f.c.c. lattice $\gamma = \sqrt{2}$, and the reduced volume per molecule is given by

$$v = \frac{v}{r^3} = \frac{1}{\gamma} \left[\frac{a}{r_o} \right]^3 \qquad (26b)$$

It then follows that, assuming the Lennard-Jones 12-6 potential between two point centers of different chains, in the smearing approximation yields an expression analogous to equation (15):

$$\bar{\varepsilon}(r) - \bar{\varepsilon}(0) = \frac{zq}{R} \left[\left(\frac{v^o}{v}\right)^4 I(y) - \left(\frac{v^o}{v}\right)^2 m(y) \right] \qquad (27)$$

where only the external number of contacts $\frac{zq}{R}$ is different from the analogous expression for the monomer. Here z is the coordination number of the f.c.c. lattice as before and (zq /R), defined as:

$$\frac{qz}{R} = z-2 +(2/R) \qquad (28)$$

is seen to be a weak function of chain length (Ref 4d).

In the harmonic approximation, the mean frequency of oscillation can be derived analogously:

$$\nu = \frac{1}{2\pi/m} \left[2\left(\frac{qz}{R}\right) \frac{\varepsilon}{a^2} \left[22\left(\frac{v^o}{v}\right)^4 - 10 \left(\frac{v^o}{v}\right)^2 \right] \right]^{\frac{1}{2}} \qquad (29)$$

7. The Heat Capacity

The partition function for this model can now be given by

$$Z = Z_{k.e.} \exp(-U_o/kT)\, \chi^{Nc/R} \qquad (30)$$

For spherical, harmonic oscillators, there exists three translational (kinetic energy) and three configurational (potential energy) degrees of freedom. The translational degrees of freedom remain unchanged for R-mer segments; however, the configurational degrees of freedom have to be modified to take into account the additional limitations imposed upon the segment by the intramolecular contacts. The surface around a segment is only partly free for intermolecular interactions, the remaining part being blocked by the adjacent segments in the same molecule (Ref. 9). Hence the number of configurational degrees of freedom per segment is $3c/R$; the coefficient 3 is absorbed into χ since the latter is a volume integration ; hence the exponent Nc/R in eqn. (29).

The derivation of the heat capacity at constant volume from eqn. (29) is straightforward and yields

$$C_v = \frac{3}{2} k \left(1 + c/R \right) . \qquad (31)$$

CHAPTER 7

The Harmonic Oscillator Model of Thermal Conductivity

In this chapter the theory of Horrocks and McLaughlin will be briefly discussed and then extended to pure liquids composed of R-mer molecules. Results of calculations will be presented and compared with experimental data for normal alkanes.

1. The Harmonic Oscillator Model of Thermal Conductivities of Simple Liquids (Ref 1a)

Heat transfer down a temperature gradient occurs by two molecular mechanisms: a) vibrational, b) convective.

a) Vibrational mechanism: The rate of heat flow can be written as

$$\frac{dQ}{dt} = -2nP\nu l \frac{dU}{dx} \qquad (1)$$

where n = number of molecules per unit area of the liquid quasi lattice.

ν = mean vibrational frequency of the molecule given by equation (18) of the previous chapter.

P = the probability that heat transfer occurs when two vibrating molecules collide.

$l \frac{du}{dx}$ = the energy difference between successive layers of the liquid quasi lattice.

The expression is multiplied by 2 since the molecule crosses a plane perpendicular to the temperature gradient twice for each complete vibration. Using

$$\frac{dU}{dx} = \frac{dU}{dT}\frac{dT}{dx} = C_v \frac{dT}{dx}$$

and the one dimensional Fourrier equation, we get

$$\lambda_{vib} = 2nP\nu l\, C_v \qquad (2)$$

where C_v is taken as $3k$. Assuming the virtual absence of holes $n \doteq 1/a^2$; also $l = \sqrt{2}\, a/2$ and $P \doteq 1$. Hence

$$\lambda_{vib} = \frac{\sqrt{2}}{a} C_v \nu \quad . \qquad (3)$$

b) Convective Contribution.- In the absence of a temperature gradient, the frequency of movement J of molecules from one adjacent layer in the liquid to the next is given by

$$J = \frac{n_h}{N} \left[\frac{kT}{2\pi m} \right]^{\frac{1}{2}} \frac{1}{v_f} \exp(-e_o / kT)$$

where v_f is the free volume of the liquid, e_o the energy barrier to be overcome for molecular convection, and n_h is the ratio of the number of holes to the total number of molecules. Then

$$\lambda_{conv.} = 2nJl \frac{dU}{dT} \quad . \qquad (4)$$

Without going into further detail it can be said that

$$\lambda = \lambda_{vib} + \lambda_{conv} \quad , \qquad (5)$$

and that for simple liquids, up to their boiling points, λ_{vib} is by far the dominant term in equation (5), and that the convective term can be dropped as a good approximation (Ref. 1b). Thus

$$\lambda = \frac{\sqrt{2}}{a} C_v \nu \qquad (6)$$

2. Application to Chain Molecules

As intercellular convection for individual chain segments is less likely than for spherical molecules, the assumption that

$$\lambda \stackrel{\circ}{=} \lambda_{vib}$$

is retained. Thus as before

$$\lambda = \frac{\sqrt{2}}{a} C_v \nu \tag{7}$$

where a is the length of a side of the cell, confining a chain segment, C_v is the vibrational specific heat of the same, and ν the mean vibrational frequency as defined by eqn. (29) of the previous chapter. Using equation (28), (29) and (31), the thermal conductivity of liquids composed of chain molecules can be written as

$$\lambda = \frac{3}{2}\frac{k}{a^2}\left(1 + \frac{c}{R}\right)\frac{1}{\pi/m}\left[\left(z - 2 + \frac{2}{R}\right) e\left[22\left(\frac{v^o}{v}\right)^4 - 10\left(\frac{v^o}{v}\right)^2\right]\right]^{\frac{1}{2}} \tag{8}$$

3. Comparison with Experiment

The above extension of the theory of Horrocks and McLaughlin to pure R-mers was compared with experimental data on normal alkanes. The values of r_o and ϵ used throughout the homologous series are those of the monomer, methane, (Ref. 2) as was indicated in paragraph 6 of the previous chapter. Density versus temperature data were obtained from Ref. 3, and the thermal conductivity data

for the same temperature intervals from Ref. 4 in the form of correlations of existing data. Calculations were executed on a computer; the relevant program for these calculations will be found in appendix 3.

A summary of the calculated results is given in Table 1 , along with the experimental data. It will be seen that the calculated and experimental slopes of the λ vs. T curves are in good agreement, certainly within experimental error, but that the absolute values differ by an amount which does not seem to change significantly over the homologous series.

Carbon Number	Temp Range °C	$\bar{A}$ mw/cm °K	SLOPE(DATA) mw/cm °K^2	SLOPE(DATA) mw/cm °K^2	%DIFF	$\Delta \bar{A}$
5	-80 to +40	.649	.0033	.0037	9.5	-
7	-120 to +20	.633	.0039	.0041	3.2	-.016
9	-40 to +120	.591	.0023	.0028	16.5	-.042
11	-30 to +130	.633	.0022	.0026	13	+.042
13	+40 to +200	.697	.0023	.0025	6.5	+.064
15	60 to 220	.734	.0022	.0023	3.9	+.037
17	60 to 220	.758	.0020	.0023	9.7	+.024
19	60 to 220	.771	.0020	.0022	8.2	+.013

TABLE I. $\bar{A}$ is the difference between λ_{exp} and $\lambda_{calc.}$ averaged over the temperature interval.

It has been shown by Harrocks and McLaughlin (Ref 5) that the principal factor controlling the temperature dependence of thermal conductivity is the coefficient of thermal expansion. This remains unchanged for chain molecules, where the equation

$$\lambda = \frac{\sqrt{2}}{a} C_v \nu$$

again leads to

$$\frac{1}{\lambda}\left[\frac{d\lambda}{dT}\right]_p = -\alpha\left[\frac{1}{3} - \frac{d \ln \nu}{d \ln v}\right] \qquad (9)$$

the expressions for v and ν being modified as in section 6 of the previous chapter. That this predicitin is a good one is reflected in table 1. The results indicate however that a second term, which would be additive and of the magnitude of about 0.65×10^{-3} mw/cm°K is missing. In the absence of further evidence two reasons may be put forward as contributing to this second term.

a) Heat transfer down the chain: Relative independence of chain length could be expected as the average length of chain parallel to the path of heat flow need not increase with the number of carbons in the chain.

b) Degrees of freedom associated with the hydrogen atoms attached to the carbons: As the average number of hydrogen atoms per segment can be taken as constant, this contribution would be independent of chain length. Further as the heat capacity arising from this vibrational contribution is expected to be insensitive to

the temperature changes, this term would be independent of temperature as well.

CHAPTER 8
Transport Coefficients of Pure Hard Sphere Fluids

1. Introduction

In this chapter the derivations leading up to the thermal conductivity and viscosity of pure hard sphere fluids for low pressures and dense gases will be summarised. These formulae will be used in the following chapter in the analysis of dense mixed fluid transport coefficients. As the latter have been derived only for the case of hard elastic spherical molecules, no other intermolecular interaction potential will be considered.

While the thermal conductivity coefficient is of primary concern here, the viscosity coefficient has also been considered, as the two derivations are very similar. Also, because thermal conductivity data for binary liquid mixtures of spherical molecules is lacking, corresponding viscosity data has been considered for comparing the model with experiment.

A word on notation should be added. Vector quantities in this and the next chapter will be written with a bar under the letter, and tensor quantitites with two bars. For the stress tensor, the Chapman and Cowling notation has been retained:

$$\underline{\underline{P}}^{0} \quad \frac{\partial}{\partial \underline{r}} \underline{c}_0 \ .$$

2. The Heat Flux Vector and the Pressure Tensor

It can be shown (Ref 1a) that if X is any molecular property which is a function of molecular velocity, the value of X averaged over all the molecules within a small volume element $d\underline{r}$, during a short time interval dt, is

$$\overline{X} = \frac{1}{n} \int X\, f(\underline{c}, \underline{r}, t)\, d\underline{c} \qquad (1)$$

where n is the number density in the defined region, $\underline{c}$ is the molecular velocity vector and $f(\underline{c}, \underline{r}, t)$ is the velocity distribution function; here $f(\underline{c}, \underline{r}, t)\, d\underline{c}\, d\underline{r}$ defines the probable number of molecules with velocity in the interval $\underline{c}$ to $\underline{c} + d\underline{c}$ in a region of space bounded by the volume element $d\underline{r}$. In equation (1), the integration is carried out over the whole of velocity space.

If, in particular, the relevant molecular property is heat, the heat flux vector can be written as (Ref 1b).

$$\underline{q} = \tfrac{1}{2} m \int C^2\, \underline{C}\, f\, d\underline{c}$$

here m = mass of the molecule

$\underline{C} = \underline{c} - \underline{c}_o$, $\underline{c}_o$ denoting the mean mass velocity of the gas which can be obtained from equation (1), and C = the magnitude of $\underline{C}$.

Clearly, if f is known, $\underline{q}$ can be derived explicitly and then combined with Fourrier's Law of heat conduction.

$$\underline{q} = -\lambda \frac{d\underline{T}}{d\underline{r}}$$

to yield the thermal conductivity.

For the case where X denotes molecular momentum $m\underline{c}$, the pressure

tensor can be written as

$$\underline{P} = \rho \int \underline{CC}\, f\, d\underline{c} \qquad (3)$$

where $\rho = n\,m$. The pressure tensor is the sum of the hydrostatic pressure and a second term composed of the stress tensor multiplied by the coefficient of viscosity, μ.

3. Thermal Conductivity and Viscosity at Low Pressures

Boltzmann's Equation for a non-uniform gas is

$$\frac{\partial f}{\partial t} + \underline{c} \cdot \frac{\partial f}{\partial \underline{r}} + \underline{F} \cdot \frac{\partial f}{\partial \underline{c}} = \left[\frac{\partial f}{\partial t}\right]_{coll} \qquad (4)$$

where in addition to previously defined quantities, $m\underline{F}$ is the external force acting on the particle, and $(\partial f/\partial t)_{coll}$ is the time rate of change of f due to collisions. Eqn. (4) can be written as

$$\beta(f) = 0 \qquad (5)$$

where β operates on f. It is assumed that

a) $f = f^o + f^1 + f^2 + \ldots$ where f^o turns out to be the Maxwellian velocity distribution function (i.e. that for a uniform gas) and f^i $(i>0)$ are successive correction terms, and that

b) the operator β can be broken down such that

$$\beta(f) = \beta^o(f^o) + \beta^1(f^1) + \beta^2(f^2) + \ldots \qquad (6)$$

where the $\beta^i(f^i)$ satisfy the separate equations

$$\beta^o(f^o) = 0\ ; \quad \beta^1(f^o, f^1) = 0\ ; \quad \beta^2(f^o, f^1, f^2) = 0\ , \text{etc.}$$

The quantities ϕ^r can now be defined (REf. 1c) as

$$f^r = f^o\, \phi^r \qquad (7)$$

such that the rth correction term to the average value of property X now becomes

$$\overline{X}^r = \frac{1}{n} \int X f^r \, d\underline{c} = \frac{1}{n} \int X f^o \, \phi^r \, d\underline{c} , \tag{8}$$

where the Maxwillian velocity distribution function f^o is explicitly given by:

$$f^o = n\left(\frac{m}{2\pi k T}\right)^{3/2} \exp(- mC^2/2kT) . \tag{9}$$

In this and the next chapter, we will work with only the first and second terms of equation (6) as, due to the increasing complexity of the successive approximations, the formulae for mixtures, with which we are ultimately concerned, have not been developed beyond ϕ^1. Thus, we will take

$$\overline{X} = \overline{X}^o + \overline{X}^1 = \frac{1}{n} \int X f^o d\underline{c} + \frac{1}{n} \int X f^o \phi^1 d\underline{c} \tag{10}$$

Since the first integral makes no contribution to the heat flux vector.

$$\underline{q} = \underline{q}^1 = \tfrac{1}{2} m \int C^2 \, \underline{C} f^o \, \phi^1 \, d\underline{c} \tag{11}$$

The solution of the Boltzmann equation, leads to an expression for $\underline{q}^1$, which can then be evaluated for hard spheres. The derived dilute gas thermal conductivity coefficient for a fluid of hard elastic spheres, λ_o , can then be written (Ref 1d) as:

$$\lambda_o = \frac{75}{64} \frac{1}{\sigma^2} \left(\frac{k^3 T}{\pi m}\right)^{\frac{1}{2}} \tag{12}$$

where k is the Boltzmann constant and σ the molecular diameter. The viscosity is obtained in a similar manner from the difference between the pressure tensor and the hydrostatic pressure:

$$\mu_o = \frac{5}{16} \frac{1}{\sigma^2} \left(\frac{k\,mT}{\pi}\right)^{\frac{1}{2}} \qquad (12)$$

4. Thermal Conductivity and Viscosity for Dense Gases.

In the above discussion, the transport coefficients have been derived by assuming that both momentum and energy transfer take place by the motion of molecules, between collisions, through the available volume. As the density is increased and the mean free path becomes comparable in magnitude to the molecular diameter, collisional transfer takes on increasing importance. The collision frequency is increased by a factor $g(\sigma)$, the contact radial distribution function. The details of $g(\sigma)$ are best considered outside the mainstream of the discussion of the transport coefficients; it will be used implicitly and defined in a later section.

It has been shown (Ref 1e) that the velocity distribution function for a non-uniform dense gas can be solved for, in a manner analogous to the dilute gas; f^o again turns out to be the Maxwellian distribution function, and makes no contribution to the heat flux vector. Three contributions to the latter arise (Ref 2), (Ref 1f):

1) from heat transfer by molecular motion between collisions, i.e. the kinetic contribution

$$\frac{1}{2}\rho\,\overline{C^2\,C} = -\frac{1}{g}\left(1 + \frac{12}{5}\,b^*\,g\right)$$

$$\lambda_k = \frac{\lambda_o}{g}\left(1 + \frac{12}{5}\,b^*\,g\right) \qquad (14)$$

where $b^* = (\pi/6)\, n\sigma^3$.

2) from that part of collisional transfer which can be looked at as taking place with a locally Maxwellian velocity distribution:

$$-C_v\, \bar{\omega}\, \frac{\partial T}{\partial r} = -\frac{512}{25\pi}\, b^*\, g\, \lambda_o\, \frac{dT}{dr}$$

$$\lambda_{Maxw} = \frac{512}{25\pi}\, b^{*2}\, g\, \lambda_o \qquad (15)$$

where $C_v = (3k/2m)$ and $\bar{\omega}$ is the bulk viscosity given by

$$\bar{\omega} = (4/9)\, g\, n^2\, \sigma^4\, (\pi m k T)^{\frac{1}{2}};$$

3) and finally from the distortion of the locally Maxwellian velocity distribution function.

$$\frac{6}{5}\, b^*\, g\rho\, \overline{C^2\, \underline{C}} = -\frac{12}{5}\, b^*\, \lambda_o\, (1 + \frac{12}{5}\, b^*\, g)\, \frac{dT}{dr}$$

$$\lambda_{Dist.} = \frac{12}{5}\, b^*\, \lambda_o\, (1+\frac{12}{5}\, b^*\, g).$$

In the first approximation then, the thermal conductivity of a dense fluid of hard spheres is given by

$$\lambda = 4\, \lambda_o\, b^* \left\{ \frac{1}{4b^*g} + \frac{6}{5} + 4\left(\frac{9}{25} + \frac{32}{25\pi}\right) b^*\, g \right\} \qquad (16)$$

Clearly, λ_o is the thermal conductivity of the dilute gas at the same temperature.

The viscosity of the dense gas is made up of contributions of the same origin (Ref 2):

1) The stress tensor arising from molecular motion between

collisions is

$$\rho \underline{C}\,\underline{C} = -\frac{\mu_o}{g}\left(1 + \frac{8}{5} b^* g\right) 2 \frac{\partial}{\partial \underline{r}} \overline{\overline{\overline{c_o}}}^{o}$$

which gives rise to

$$\mu_k = \frac{\mu_o}{g}\left(1 + \frac{8}{5} b^* g\right) . \tag{17}$$

2) The stress tensor arising from the locally Maxwellian velocity distribution function is

$$-\frac{2}{3} g n^2 \sigma^4 (\pi m k T)^{\frac{1}{2}} \frac{4}{5} \frac{\partial}{\partial \underline{r}} \overline{\overline{\overline{c_o}}}^{o}$$

which leads to

$$\mu_{Maxw} = \frac{768}{25\pi} g b^{*2} \mu_o . \tag{18}$$

3) Finally the stress tensor arising from the locally Maxwellian velocity distribution function

$$\frac{2}{5} b \rho^2 g \overline{\underline{C}\,\underline{C}}$$

gives rise to

$$\mu_{Dist.} = \frac{8}{5} b^* g \mu_k . \tag{19}$$

The first approximation to the viscosity the is:

$$\mu = 4 \mu_o b^* \left[\frac{1}{4 b^* g} + \frac{4}{5} + 4\left(\frac{4}{25} + \frac{48}{25\pi}\right) b^* g \right] \tag{20}$$

(Ref. 1g)

5 The Equations of Longuet-Higgins and Pople (Ref 3)

It has been shown that the purely collisional contribution to the transport coefficients can be derived via the assumptions: a) that the spatial pair distribution function depends only on the temperature and density and not on the temperature gradient or rate of strain, and b) that the velocity distribution function is Maxwellian with a mean equal to the local hydrodynamic velocity, and a spread determined by the local temperature. The resulting equations, in our notation can be written as

$$\lambda = \frac{512}{25\pi} \lambda_o b^{*2} g \qquad (21)$$

and

$$\mu = \frac{768}{25\pi} \mu_o b^{*2} g .$$

These equations are identical with the locally Maxwellian contributions to the expressions derived through the Chapman-Enskog theory, equations (15) and (18) respectively. (Ref 2).

As indicated by Dahler, the corrections to the collisional terms arising from the distortion of the velocity distribution function are not negligible; the contribution of the distortion term to the thermal conductivity is quoted at over 50% of the collisional term, and the corresponding correction to the viscosity is reported to be above 20% and increasing with density. (Ref 2).

6. The Contact Radial Distribution Function

The radial distribution function g(r) is defined as

$$g(r) = n^{(2)} (\underline{r}_1, \underline{r}_2) / n^2 \qquad (23)$$

where n is the number density and $n^{(2)} (\underline{r}_1, \underline{r}_2)\, d\underline{r}_1\, d\underline{r}_2$ is the probability that molecule 1 is in volume element $d\underline{r}_1$ about the point $\underline{r}_1$ and that molecule 2 is in the volume element $d\underline{r}_2$ at r_2 imultaneously. We now define the correlation function

$$h(r) = g(r) - 1 .$$

The limiting value of g(r) is exp[-u(r)/kT] where u(r) is the intermolecular potential. Hence as g(r) tends to the value unity for low densities, h(r) tends to zero. The latter is "a measure of the total influence of molecule 1 on another, molecule 2, at a distance r_{12}" (Ref 4).

h(r) can be split into two terms (Ref 5):

$$h(r_{12}) = C(r_{12}) + n \int C(r_{13})\, h(r_{23})\, d\underline{r}_3 \qquad (24)$$

where the first term on the right hand side is a direct correlation function representing short range interactions, and the second is the long range interactions propagated from molecule 1 to molecule 3, which in turn exerts its total influence on 2. Defining two further functions

$$F(r) = [\exp\ (-U(r)/kT)] - 1 \qquad (25)$$

and

$$y(r) = g(r) \exp\ [U(r)/kT] \qquad (26)$$

and making the Percus-Yevick approximation (Ref 6) that

$$C(r) = F(r)\, y(r), \qquad (27)$$

we can derive the equation ,

$$y_{12} = 1 + n \int F_{13}\, y_{13}\, h_{23}\, d\underline{r}_3 \qquad (28)$$

from equations (24) - (27).

This equation has been solved, (Ref 7), for the hard sphere potential, to obtain y_{12} at contact, i.e. when the intermolecular separation is σ, (the molecular diameter) where $g(\sigma) = y(\sigma)$. The result is:

$$g(\sigma) = \frac{2 + b^*}{2(1-b^*)^2} \quad . \qquad (29)$$

As before $b^* = \frac{\pi}{6} n\sigma^3$. This then is the expression for the contact radial distribution function for hard spheres, in the Percus-Yevick approximation, which can be used in the evaluation of the transport coefficients.

The equation of state of a dense fluid can be derived in two ways, leading to the pressure equation, through the virial theorem,

$$P = nkT - \frac{n^2}{6} \int r \frac{du(\underline{r})}{dr} g(r)\, d\underline{r} \qquad (30)$$

and the compressibility equation

$$kT \frac{\partial n}{\partial p} = 1 + n \int \left[g(r) - 1 \right] d\underline{r} \qquad (31)$$

derived from fluctuation theory. In the Percus-Yevick approximation, these two equations can be reduced, by using equation (29), to

$$P = nkT \left[(1 + 2b^* + 3b^{*2}) / (1-b^*)^2 \right] \qquad (32)$$

and

$$P = nkT \left[(1 + b^* + b^{*2}) / (1-b^*)^3 \right] \qquad (33)$$

respectively. (Ref 7).

CHAPTER 9

Transport Coefficients for Dense Binary Hard Sphere Mixtures

1. Introduction

In this chapter, the equations for the transport coefficients of dense hard sphere mixtures will be given, and combined with the corresponding radial distribution functions, (Ref 14) derived through the Percus-Yevick approximation. In order to compare with experiment these equations will be reduced to ratios: the mixture transport coefficient divided by that for pure species 1. The equations will also be factorized into the purely kinetic, distortional, and locally Maxwellian collisional terms, and the Enskog minimum will be shown to exist. Comparison will be made with experimental data.

2. Transport Coefficients for a Binary Dilute Gas Mixture (Ref 1a)

The method is analogous to that for pure systems. The Boltzmann's equation for the first gas is

$$\frac{\partial f_1}{\partial t} + \underline{c}_1 \cdot \frac{\partial f_1}{\partial \underline{r}} + \underline{F}_1 \cdot \frac{\partial f_1}{\partial \underline{c}_1} = \left[\frac{\partial_e f_1}{\partial t}\right]_{coll} \qquad (1)$$

and a similar equation can be written for the second gas, by changing the subscripts to 2. For the non-equilibrium case, the equations for f_1 and f_2 are solved, as before, by a method of successive approximations. Again the first approximation is a Maxwellian function, and again the f's can be written in the second approximation as

$$\begin{aligned} f_1 &= f_1^o \quad (1 + \phi_1^1) \\ f_2 &= f_2^o \quad (1 + \phi_2^1) \end{aligned} \qquad (2)$$

Here, however, the ϕ's contain cross terms of the properties and velocities of the two species.

The heat flux vector is now written as,

$$\underline{q} = \tfrac{1}{2} m_1 \int f_1 C_i^2 \underline{C}_1 \, d\underline{c}_1 + \tfrac{1}{2} m_2 \int f_2 C_2^2 \underline{C}_2 \, d\underline{c}_2 \qquad (3)$$

where all quantities have been defined in the previous chapter. The Maxwellian part of the distribution function makes no contribution to the heat flux vector. Of the terms arising from the integration over the $f_i^o \phi_i^1$, the one representing the heat flow due to the

temperature gradient is simply

$$\underline{q} = -\lambda_{mix,o} \frac{d\underline{T}}{d\underline{r}} \qquad (4)$$

where $\lambda_{mix,o}$ is the binary gas mixture thermal conductivity for low pressures. The expression is cumbersome and as it will not be made direct use of, will not be reproduced here (Ref 1b).

The coefficient of viscosity is derived along similar lines. (Ref 1c). We need only deal with the first correction term, as the Maxwellian part gives rise to a contribution to the pressure tensor that reduces to the hydrostatic pressure.

Then,

$$\underline{\underline{P}}^{(1)} = m_1 \int f_1^o \phi_1^1 \underline{C}_1 \underline{C}_1 d\underline{c}_1 + m_2 \int f_2^o \phi_2^1 \underline{C}_2 \underline{C}_2 \, d\underline{c}_2 \, . \qquad (5)$$

which is equivalent to

$$\underline{\underline{P}}^{(1)} = n_1 m_1 \overline{\underline{C}_1 \underline{C}_1} + n_2 m_2 \overline{\underline{C}_2 \underline{C}_2}$$

Solving the Boltzmann equations to obtain the rhs of equation (5) leads to the viscosity coefficient.

These methods for the derivation of the transport coefficients of mixed fluids have been extended by H. H. Thorne to the case of dense binary mixtures, (Ref 1d). In the first approximation, the thermal conductivity is found to be

$$\lambda_{mix} = \frac{75}{8} \frac{k^2 T}{g_{12}} \left(A_\lambda X_\lambda^2 + B_\lambda X_\lambda Y_\lambda + C_\lambda Y_\lambda^2 + D_\lambda \right) \qquad (6)$$

where

$$X_\lambda = 1 + 2\pi m_1 \sigma_1^3 g_1/5 + 8\pi M_1 M_2 n_2 \sigma_{12}^3 g_{12}/5 \qquad (7)$$

$$Y_\lambda = 1 + 2\pi n_2 \sigma_2^3 g_2/5 + 8\pi M_1 M_2 n_1 \sigma_{12}^3 g_{12}/5 \qquad (8)$$

$$M_1 = m_1/(m_1+m_2) \; ; \; M_2 = m_2/(m_1+m_2) \; ; \; m_o = m_1+m_2 \tag{9}$$

$$A_\lambda = \frac{a_{-1-1}}{m_1} \frac{x_1}{x_2} \left(a_{11}\, a_{-1-1} - a^2_{1-1}\right)^{-1} \tag{10}$$

$$B_\lambda = \frac{-2a_{-1-1}}{(m_1 m_2)^{\frac{1}{2}}} \left(a_{11}\, a_{-1-1} - a^2_{1-1}\right)^{-1} \tag{11}$$

$$C_\lambda = \frac{a_{11}}{m_2} \frac{x_2}{x_1} \left(a_{11}\, a_{-1-1} - a^2_{1-1}\right)^{-1} \tag{12}$$

$$D_\lambda = (2/3)\, n^2 (\pi k^3 T)^{\frac{1}{2}} \left\{ x_1^2 g_1 \sigma_1^4 m^{-\frac{1}{2}} + 2(8M_1M_2/\pi_o)^{\frac{1}{2}} x_1 x_2 g_{12} \sigma_{12}^4 + m_2^{-\frac{1}{2}} x_2^2 g_2 \sigma_2^4 \right\} \tag{13}$$

where x_1 and x_2 are mole fractions of species 1 and 2 respectively.

$$a_{11} = a'_{11} + \frac{x_1}{x_2} \frac{g_1}{g_{12}} a''_{11} \tag{14}$$

$$a'_{11} = 5kT \left[\tfrac{1}{4}(6M_1^2+5M_2^2) - \frac{3}{5} M_2^2 + \frac{4}{5} M_1 M_2 \right] / M_1 E \tag{15}$$

$$E = \left(\frac{2kT\pi_o}{\pi M_1 M_2}\right)^{\frac{1}{2}} 8\sigma_{12}^2 \; ; \quad \sigma_{12} = \tfrac{1}{2}(\sigma_1+\sigma_2) \tag{16}$$

$$a''_{11} = 5kT/2\mu_{10} \tag{17}$$

where μ_{10} is the dilute gas viscosity coefficient for species 1.

$$a_{-1-1} = a'_{-1-1} + \frac{x_2}{x_1} \frac{g_2}{g_{12}} a''_{-1-1} \tag{18}$$

where a'_{-1-1} corresponds to equation (15) with species numbers

interchanged and a^{n}_{-1-1} to equation (17) with μ_{10} replaced by μ_{20} Finally

$$a_{1-1} = -27\ kT\ (M_1M_2)^{\frac{1}{2}}/4E. \tag{19}$$

and the radial distribution functions g_{12}, g_1 and g_2 will be defined in the next section.

The first Approximation to the viscosity of a mixed dense hard sphere fluid is given by (Ref 1d)

$$\mu_{mix} = \frac{5kT}{2g_{12}} \left[A_\mu X_\mu^2 + B_\mu X_\mu Y_\mu + C_\mu Y_\mu^2 + D_\mu \right] \tag{20}$$

where

$$X_\mu = 1 + 4\pi\, n_1\sigma_1^3 g_1/15 + 8\pi\, M_2 n_2 \sigma_{12}^3 g_{12}/15 \tag{21}$$

$$Y_\mu = 1 + 4\pi\, n_2\sigma_2^3 g_2/15 + 8\pi\, M_1 n_1 \sigma_{12}^3 g_{12}/15 \tag{22}$$

$$A_\mu = b_{-1-1} \frac{x_1}{x_2} \left(b_{-1-1}\, b_{11} - b_{1-1}^2\right)^{-1} \tag{23}$$

$$B_\mu = -2\, b_{1-1} \left(b_{-1-1}\, b_{11} - b_{1-1}^2\right)^{-1} \tag{24}$$

$$C_\mu = b_{11} \frac{x_2}{x_1} \left(b_{-1-1}\, b_{11} - b_{1-1}^2\right)^{-1} \tag{25}$$

$$D_\mu = (4/15)\, n^2 (\pi kT)^{\frac{1}{2}} \left[m_1^{\frac{1}{2}} x_1^2 g_1 \sigma_1^4 + 2(2m_0 M_1 M_2)^{\frac{1}{2}} x_1 x_2 g_{12} \sigma_{12}^4 + m_2^{\frac{1}{2}} x_2^2 g_2 \sigma_2^4 \right] \tag{26}$$

and

$$b_{11} = b'_{11} + \frac{x_1}{x_2}\frac{g_1}{g_{12}} b''_{11} \qquad (27)$$

with $b'_{11} = 5kT(\frac{2}{3} + \frac{2M_2}{5M_1})/E$

and $b''_{11} = a''_{11}$. Further,

$$b_{-1-1} = b'_{-1-1} + \frac{x_2}{x_1}\frac{g_2}{g_{12}} b''_{-1-1} \qquad (28)$$

where

$$b'_{-1-1} = 5kT\ (\frac{2}{3} + \frac{2M_1}{5M_2})/E \qquad (29)$$

and $b''_{-1-1} = a''_{-1-1}$. Finally

$$b_{1-1} = -4kT/3E. \qquad (30)$$

The radial distribution functions g_{12}, g_1 and g_2 will now be defined.

3 Equilibrium Properties of Dense Hard Sphere Fluids. (Ref 3)

The methods for the treatment of pure and mixed dense hard sphere fluids are analogous. The compressibility equation assumes the form

$$1 - \sum_i n_i \int C_{ij}(\underline{r})\, d\underline{r} = \frac{1}{kT}\frac{\partial P}{\partial n_i} \qquad (31)$$

and the direct correlation functions C_{ij} for an m component liquid can be written as

$$[g_{ij}(\underline{r})-1] = C_{ij}(\underline{r}) + \sum_{l=1}^{m} n_l \int [g_{ij}(\underline{r}-y)-1]C_{ij}(y)dy \qquad (32)$$

where g_{ij} is the radial distribution function. In order to obtain the g_{ij}'s we need another equation relating the two sets of functions:

$$g_{ij}(r) \quad \exp[-u_{ij}(r)/kT] - 1 \quad = \exp[-u_{ij}(r)/kT]c_{ij}(r) \qquad (33)$$

This is the Percus-Yevick approximation for mixed dense fluids. The essential implication, as before, is that the direct correlation function is of the same range as the intermolecular interaction potential. Thus, assuming a binary mixture and the hard sphere potential, it can be shown that

$$g_{12} = (\sigma_2 g_1 + \sigma_1 g_2)/2\sigma_{12} \qquad (34)$$

where

$$g_1 = \left[1 + \frac{\xi}{2} + \frac{3}{2}\frac{\pi}{6} n\sigma_2^2(\sigma_1-\sigma_2)\right] (1-\xi)^{-2}$$

and (35)

$$g_2 = \left[1 + \frac{\xi}{2} + \frac{3}{2}\frac{\pi}{6} n\sigma_1^2(\sigma_2-\sigma_1)\right] (1-\xi)^{2}$$

Here,

$$\xi = \frac{\pi}{6}(n_1\sigma_1^3 + n_2\sigma_2^3) = \frac{v_1}{v}(x_1 + x_2 r^3) \qquad (36)$$

$$v_1^* = \pi\sigma_1^3/6 \; ; \; r = \sigma_2/\sigma_1 \; ; \; v = 1/n \qquad (37)$$

where n is the number density. Using the expression for the radial distribution function, the compressibility equation for a binary mixture can be written as (Ref 5)

$$\frac{pv}{kT}^* = \frac{\xi(1+\xi+\xi^2)}{(1-\xi)^3(x_1+x_2r^3)} - \frac{3x_1x_2(1-r)^2\xi^2}{(x_1+x_2r^3)^2} \cdot \qquad (38)$$

$$\frac{(1+r)+r\xi\left(\frac{x_1+x_2r^2}{x_1+x_2r^3}\right)}{(1-\xi)^3} \cdot$$

The pressure equation, the pure analogue of which was given in

equation (30) of the previous chapter, can be treated in the same manner and should yield identical results with equation (38) if the distribution function were exact. Though this clearly is not so, results from both expressions are sufficiently close (Ref 5) for us to work with only one of these expressions. The information obtained through the compressibility equation will not be substantially different from that of the pressure equation.

4 Reduction of Equations (6) and (20)

Equations (6) and (20) have been derived for mixtures of hard sphere fluids. One expects the error due to this simplification to be reduced if the ratios λ_{mix}/λ_1 and μ_{mix}/μ, are considered rather than the absolute values.

The denominators λ, and μ, denote the transport coefficients of pure dense species 1. Thus by (6) and equation (16) of the previous chapter.

$$\frac{\lambda_{mix}}{\lambda_1} = \frac{1}{f_\lambda}\left[A_\lambda^* X_\lambda^2 + B_\lambda^* X_\lambda Y_\lambda + C_\lambda^* Y_\lambda^2 + D_\lambda^* \right] \qquad (39)$$

where

$$X_\lambda = 1 + 12 g_1 x_1 \omega/5 + 6 M_1 M_2 g_{12}\, {}_2(1+r)^3 \varphi/5 \; ; \; \omega = \frac{v_1^*}{v} \; , \qquad (40)$$

$$Y_\lambda = 1 + 12\, g_{2} r^2 \varphi/5 + 6 M_1 M_2 g_{12} X_1 (1+r)^3 \omega/5, \qquad (41)$$

$$f_\lambda = 4\varphi_p \left[\frac{1}{4 g \varphi_p} + \frac{6}{5} + 4\left(\frac{9}{25} + \frac{32}{25\pi}\right) g\, \varphi_p \right] , \qquad (42)$$

and

$$A^{\circ}_{\lambda} = \frac{8}{g_{12}} k \left(\frac{M_1}{M_2}\right)^{\frac{1}{2}} \left[\frac{2}{r+1}\right]^2 \frac{x_1}{x_2} q_{1-1}/(q_{-1-1}q_{11}-q_{1-1}^2) \tag{43}$$

$$B^{\circ}_{\lambda} = -\frac{16}{g_{12}} \left(\frac{\varepsilon}{r+1}\right)^2 \left(\frac{1}{M_2}\right)^{\frac{1}{2}} q_{1-1}/(q_{-1-1}q_{11}-q_{1-1}^2) \tag{44}$$

$$C^{\circ}_{\lambda} = \frac{x_2}{x_1} \frac{\varepsilon}{g_{12}} k \left(\frac{M_1}{M_2}\right)^{\frac{1}{2}} \left(\frac{2}{r+1}\right)^2 \left(\frac{1}{M_2}\right)^{\frac{1}{2}} q_{11}/(q_{-1-1}q_{11}-q_{1-1}^2) \tag{45}$$

$$D^{\circ}_{\lambda} = \frac{512}{25\pi} \varphi^2 \left[x_1^2 g_1 + \left(\frac{M_1 M_2}{8}\right)^{\frac{1}{2}} x_1 x_2 g_{12} (1+r)^4 + \left(\frac{M_1}{M_2}\right)^{\frac{1}{2}} x_2^2 r^4 g_2 \right] \tag{46}$$

and

$$q_{-1-1} = \rho_{\lambda} + \frac{8x_1}{x_2} \frac{g_2}{g_{12}} \left(\frac{2r}{1+r}\right)^2 \left(\frac{1}{M_2}\right)^{\frac{1}{2}} \tag{47}$$

where (48)

$$\rho_{\lambda} = \frac{40}{M_2} \left(\frac{M_1 M_2}{2}\right)^{\frac{1}{2}} \left[\frac{1}{4} (6M_2^2 + 5M_1^2) - \frac{3}{5} M_1^2 + \frac{4}{5} M_1 M_2 \right].$$

q_{11} can be obtained by interchanging subscripts 1 and 2 in equations (47) and (48). Finally $q_{1-1} = -(54/\sqrt{2}) M_1 M_2$

Likewise, the μ_{mix}/μ, can be obtained by equation (20) and equation (20) of the previous chapter.

$$\frac{\mu_{mix}}{\mu_1} = \frac{1}{f_{\mu}} \left[A^{\circ}_{\mu} Y_{\mu}^2 + B^{\circ}_{\mu} X_{\mu} Y_{\mu} + C^{\circ} Y_{\mu}^2 + D^{\circ}_{\mu} \right] \tag{49}$$

where

$$X_\mu = 1 + 8\varphi x_1 g_1/5 + 2\varphi M_2 g_{12} x_2 (1+r)^3/5 \qquad (50)$$

$$Y_\mu = 1 + 8\varphi x_2 r^3 g_2 + 2\varphi M_1 g_{12} x_1 (1+r)^3/5 \qquad (51)$$

$$A^*_\mu = 8\frac{x_1}{x_2}\left(\frac{2}{r+1}\right)^2 \left(\frac{1}{M_1}\right)^{\frac{1}{2}} P_{-1-1}/(P_{-1-1}P_{11} - P_{1-1}^2) \qquad (52)$$

$$B^*_\mu = -16\left(\frac{1}{M_1}\right)^{\frac{1}{2}} \left(\frac{2}{r+1}\right)^2 P_{1-1}/(P_{-1-1}P_{11} - P_{1-1}^2) \qquad (53)$$

$$C^*_\mu = 8\frac{x_2}{x_1}\left(\frac{1}{M_1}\right)^{\frac{1}{2}} \left(\frac{2}{r+1}\right)^2 P_{11}/(P_{-1-1}P_{11} - P_{1-1}^2) \qquad (54)$$

$$D^*_\mu = \frac{768}{25\pi}\varphi^2 \left[x_1^2 g_1 + \left(\frac{2M_2}{8}\right)^{\frac{1}{2}} g_{12} x_1 x_2 (1+r)^4 + \left(\frac{M_2}{M_1}\right)^{\frac{1}{2}} g_2 r^4 x_2^2 \right] , \qquad (55)$$

and

$$P_{-1-1} = \beta_\mu + 8\frac{x_2}{x_1}\frac{g_2}{g_{12}}\left(\frac{1}{M_2}\right)^{\frac{1}{2}}\left(\frac{2r}{1+r}\right)^2 \qquad (56)$$

where

$$\beta_\mu = 40\left(\frac{2}{3} + \frac{2}{5}\frac{M_1}{M_2}\right)\left(\frac{M_1 M_2}{2}\right)^{\frac{1}{2}} \qquad (57)$$

P_{11} can be obtained by interchanging subscripts 1 and 2 in equations (56) and (57). Finally $q_{1-1} = -(32/3)\left(\frac{M_1 M_2}{2}\right)^{\frac{1}{2}}$, and

$$f_\mu = 4\varphi_p \left[\frac{1}{4g\varphi_p} + \frac{4}{5} + 4\left(\frac{4}{25} + \frac{48}{25\pi}\right)\varphi_p g \right] . \qquad (58)$$

In both equations (42) and (58) φ_p is the value of v_1^*/v for pure species 1. This value has been computed from equation (38) by setting $x_1 = 1$.

In order to evaluate the ratios of equations (39) and (48), the φ's corresponding to each pressure, composition and diameter ratio must be known. This was done by solving equation (38), by fixing $(P v_1^*/kT)$, r, and x. The solution of (38) for φ at $x = 1$ was used to evaluate the contact radial distribution function and the transport coefficients of pure species 1, in the compressed state. Calculations of v_1^*/v and the λ_{mix}/λ_1 and μ_{mix}/μ_1 were made for the following sets of values:

$(Pv_1^*/T) = 1, 2, 4, 8, 20, 30$; $r = \frac{1}{2}, \frac{2}{3}, 1, \frac{3}{2}$ and $R\ (= M_2/M_1) = \frac{1}{2}, 1, 2$, over the full composition range. Three Fortran IV programmes were written for the execution of these computations, the texts of which will be found in the appendixes 3F, 3G, and 3H for (v_1^*/v), λ_{mix}/λ_1 and μ_{mix}/μ_1 respectively. A sample set of curves, from those computed have been presented in Fig. 1. for the case $R = \frac{1}{2}$, $(Pv_1^*/KT) = 4$ over the composition range, for four values of r. Results for both λ_{mix}/λ_1 (greater than 1) and μ_{mix}/μ_1 (less than 1) reproduce the quadratic type dependence on composition that is observed in simple liquid mixtures.

At this stage it would be desirable to split equations (39) and (48) into their respective kinetic and collisional terms. In connection with this, it is relevant, first, to look at a purely collisional model of the thermal conductivity of mixtures.

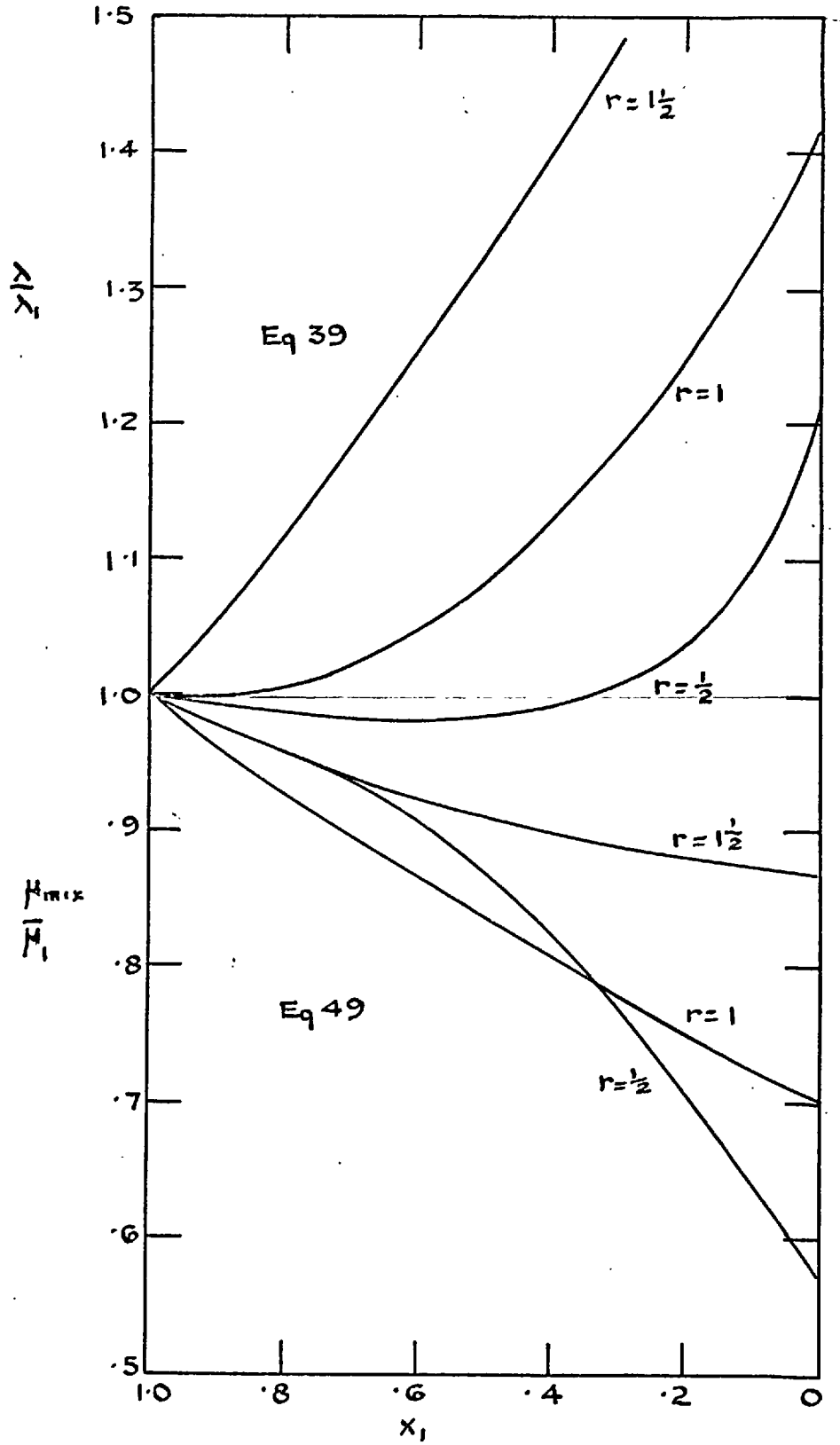

FIG. 1. COMPOSITION DEPENDENCE OF λ/λ_1 AND η/η_1 FOR A DENSE HARD SPHERE FLUID MIXTURE $R=\frac{1}{2}$ $pV_1^*/KT=4$

5 The Collisional Approximation to Thermal Conductivity of Dense Mixtures (Ref 2a)

By assuming that the two particle density function can be taken as that of the fluid in equilibrium and that the velocity distribution function for each species can be taken as a Maxwellian function, the heat flow vector due to the temperature gradient can be written for the case of equal diameters, for the two species as (Ref 2b)

$$\underline{J}_o = -\frac{2\pi k y \nabla T}{n} \sum_A \sum_B \frac{n_A n_B}{m_A + m_B} \left(\frac{2S_{AB} kT}{\pi}\right)^{\frac{1}{2}}$$

and hence the thermal conductivity of the binary mixture as

$$\lambda_{mix} = \frac{2\pi k y}{n} \sum_A \sum_B \frac{n_A n_B}{m_A + m_B} \left(\frac{2S_{AB} kT}{\pi}\right)^{\frac{1}{2}} \qquad (59)$$

where $y = \frac{P}{nkT} = 1$ and $S_{AB} = m_A m_B/(m_A + m_B)$

λ_{mix} in this approximation is purely collisional since the kinetic term vanishes for a Maxwellian velocity distribution, and clearly there is no distortion term involved. Equation (57) can be written as

$$\lambda_{mix}/\lambda_{10} = x_1^2 + 2x_1x_2 \left(\frac{8R}{(1+R)3}\right)^{\frac{1}{2}} + x_2^2 R^{-\frac{1}{2}} \qquad (60)$$

where λ_{10} is the thermal conductivity of pure component 1, for low pressures.

6. The Collisional and Kinetic Contributions in Equations (39) and (49).

It can easily be shown that if D_λ, given in equation (13), is divided by λ_{Maxw}, given in equation (15) of the previous chapter, and $\sigma_1 = \sigma_2$, one obtains equation (60). The origin of the term suggests that equation (13) arises from collisional heat transfer due to the locally Maxwellian velocity distribution. The obvious step then is to write the locally Maxwellian collisional term for $\sigma_1 \neq \sigma_2$.

$$\lambda_{mix}/\lambda_1 = (\tfrac{v_1^\circ}{v})^2 \tfrac{1}{g}\left[x_1^2 g_1 + \left[\tfrac{R}{8(1+R)^3} \right]^{\frac{1}{2}} x_1 x_2 g_{12} (1+r)^4 + R^{-\frac{1}{2}} x_2^2 g_2 r^4 \right] \qquad (61)$$

where v_1° is the molar volume of pure species 1, v is that of the mixture, and g is given by eqn. (29) of the previous chapter. Though Longuet-Higgins, Pople and Valleau did not extend their treatment to the viscosity coefficient, analogous expressions can be written for the viscosity, using (26) of this chapter and eqn. (18) of the previous chapter.

$$\mu_{mix}/\mu_1 = (\tfrac{v_1^\circ}{v})^2 \tfrac{1}{g}\left(x_1^2 g_1 + \tfrac{1}{8} x_1 x_2 g_{12} (1+r)^4 (\tfrac{2R}{1+R})^{\frac{1}{2}} + R^{\frac{1}{2}} x_2^2 r^4 g_2 \right) \qquad (62)$$

and for $\sigma_1 = \sigma_2$

$$\mu_{mix}/\mu_1 = x_1^2 + (\tfrac{2R}{1+R})^{\frac{1}{2}} 2 x_1 x_2 + x_2^2 R^{\frac{1}{2}} . \qquad (63)$$

This analysis can be extended to the three initial terms of equation (6). The kinetic contribution to the heat flux vector for dense fluid mixtures is defined similarly to that of mixtures at low pressures, i.e. eqn. (3) which immediately leads, by definition, to

$$\underline{q} = \tfrac{1}{2}\ \rho_1\ \overline{C_1^2\ \underline{C}_1}\ + \tfrac{1}{2}\ \rho_2\ \overline{C_2^2\ \underline{C}_2}\ .$$

The total flow of heat (Ref 1e) is given by

$$\underline{q} = \tfrac{1}{2}\rho_1 C_1^2 \underline{C}_1 + (X_\lambda - 1)\ \tfrac{1}{2}\rho_1\ \overline{C_1^2\ \underline{C}_1} + \tfrac{1}{2}\rho_2\ \overline{C_2^2 \underline{C}_2} + (Y_\lambda - 1)\ \tfrac{1}{2}\rho_2\ \overline{C_2^2 \underline{C}_2} - D_\lambda \frac{\partial T}{\partial T} \tag{64}$$

where X_λ, Y_λ and D_λ are given by equations (7), (8) and (13) respectively. While a rigorous factorization to separate the kinetic contribution from the distortional one (i.e, the term arising from the distortion of the locally Maxwellian velocity distribution) is called for, it would be extremely laborious. Hence the following method has been used:

Consider the first three terms of equation (6), and assume the existence of two unknown kinetic contribution terms, U, and U_2, such that, by dropping the subscripts,

$$AX^2 + BXY + CY^2 = XU_1 + YU_2 \tag{65}$$

where $U_1 + U_2 = \lambda_k$

and λ_k is defined as the purely kinetic contribution to the thermal conductivity of the mixed dense fluid. The form of equation

(65) necessitates

$$U_1 = AX + GY$$
$$U_2 = CY + FX \qquad (66)$$

where A and C are those of equation (65) and G and F are as yet unknown. Hence

$$U_1X + U_2Y = AX^2 + (G + F)\,XY + CY^2 \qquad (67)$$

Clearly $B = G+F$. The symmetry of equation (64) suggests that it would be reasonable to assume $G = F = B/2$. This assumption has been checked by calculating the kinetic, distortional and locally Maxwellian collisional contributions separately and comparing the sum against the unfactored equation, over the full range given in paragraph 4.

The identical argument applies to the viscosity and for both transport coefficients the kinetic part, in the brackets of either one of equations (6) and (20), has the form

$$AX + (B/2)\,(X + Y) + CY \qquad (68)$$

and the distortion term

$$(X-1)\,[AX+(B/2)Y] + (Y-1)\,[CY + (B/2)\,X]. \qquad (69)$$

Computations, of the various contributions, have been carried out and the sums $(\lambda_v/\lambda_{10}\,v_1^*)$ and $(\mu_v/\mu_{10}\,v_1^*)$ plotted against the dimentionless pressure $y = (P/nkT) - 1$.

Figs (2) and (3) show a set of representative results for the thermal conductivity and viscosity respectively. These have been calculated for constant composition $X_1 = .5$, and $r = 1.5$, $R = 2$. On both of these graphs curve 1 gives the kinetic contribution, curve 2 the sum of the distortional and locally Maxwellian collisional, and curve 3 gives the sum of the two curves. These results are similar to those obtained for a pure substance (Ref 6). As the density is increased, at the same temperature and constant composition, the influence of heat transfer through molecular flux decreases (as molecular convection decreases for increasing density) and heat transfer through collisions increases. Also both graphs show that the transport coefficients of mixed fluids also go through the Enskog minimum as the pressure is increased and the collisional contribution takes over linearly.

In these calculations, $(\lambda v / \lambda_{10} v_1^*)$ and $(\mu v / \mu_{10} v_1^*)$ have been obtained from programs identical to those of paragraph 4. of this chapter simply by letting $f = v_1^*/v$ in equations (42) and (58). The splitting of the collisional and kinetic contributions introduces minor differences, and hence these programs will not be reproduced here.

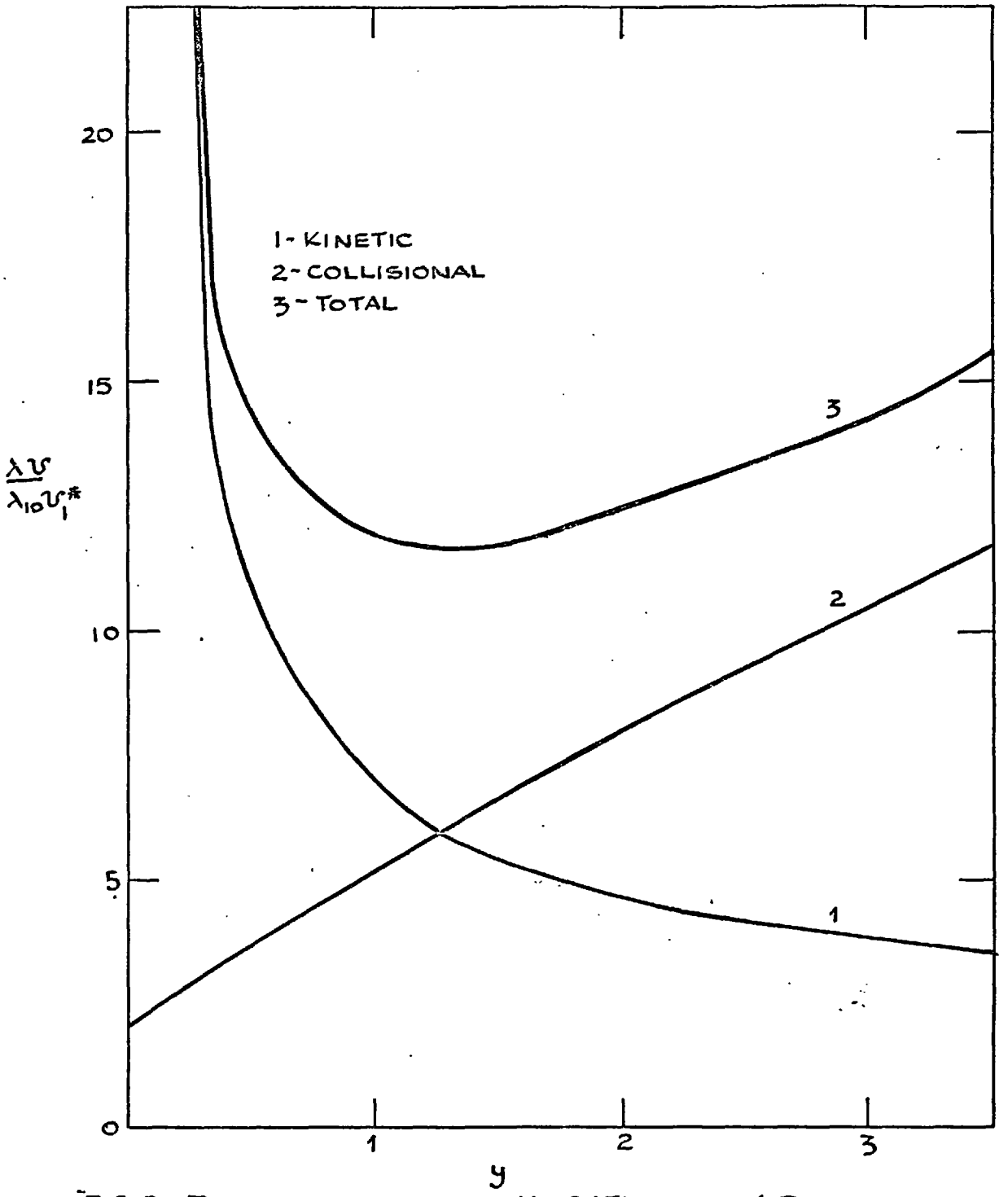

FIG. 2. THERMAL CONDUCTIVITY RATIO V.S. y; RELATIVE CONTRIBUTIONS OF THE KINETIC AND COLLISIONAL MECHANISMS

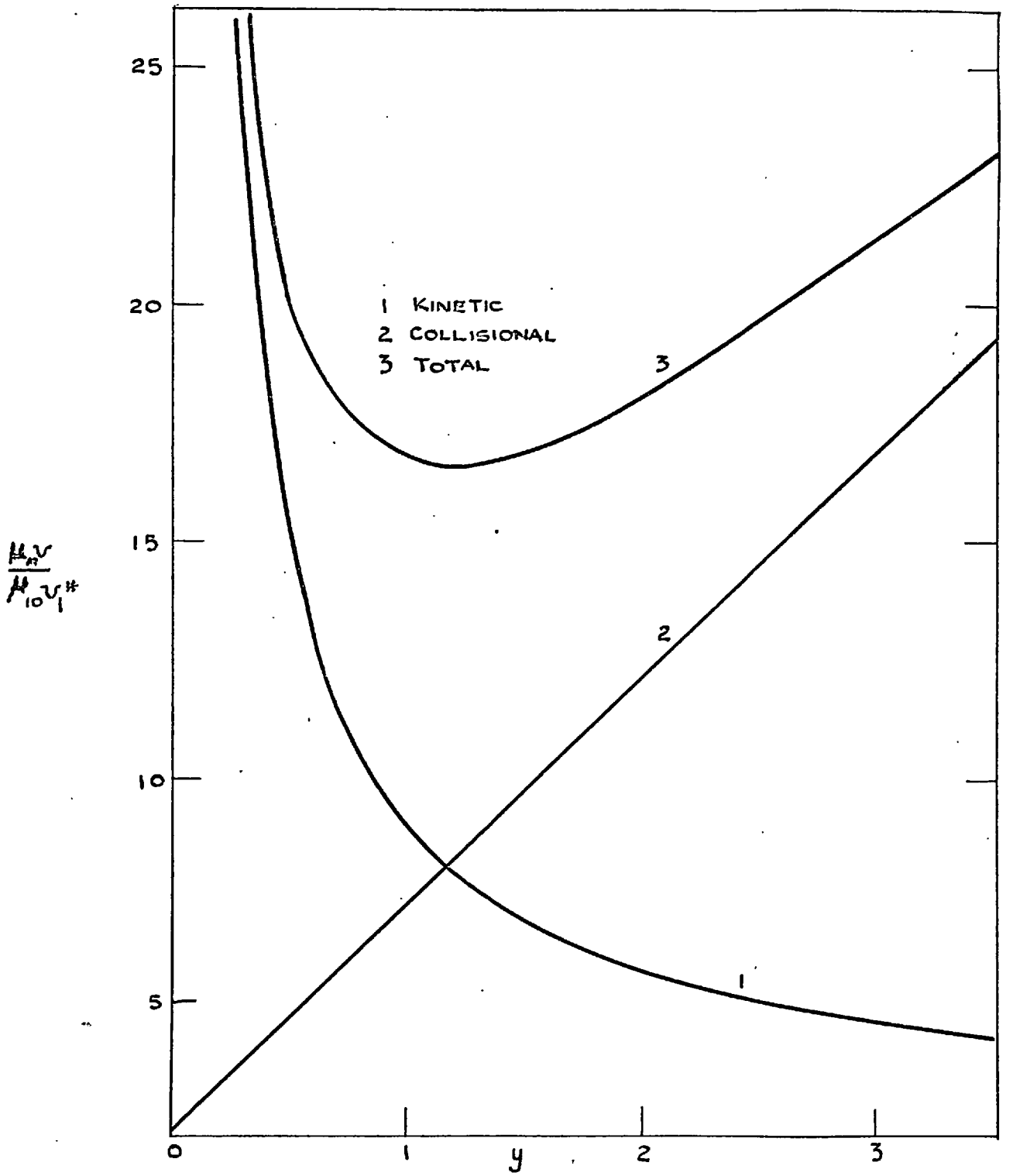

FIG3 VISCOSITY RATIO V·S y; RELATIVE CONTRIBUTIONS OF KINETIC AND COLLISIONAL MECHANISMS

7 Comparison with Experiment

Equations (6) and (20) have been derived for hard sphere fluids, and while one could obtain values of the transport coefficients, directly, by combining these equations with (34) and (35), one would not expect good agreement with experimental data. The effect of intermolecular forces should be reduced however if ratios of the transport coefficients were taken as in equations (39) and (49). Clearly the most suitable systems for comparison are mixtures of simple liquified gases. No data on the thermal conductivities of the latter were found and hence data on the system carbon tetrachloride + benzene (Ref 7) was used for comparison with theoretical calculations of both ratios, while data on the viscosity of the system argon + methane (Ref 8) was used for comparison with theory.

i) The system carbon tetrachloride + benzene. Density data on the system (Ref 9) at 30°C and the molar volume of carbon tetrachloride at absolute zero (Ref 10) were used for the calculation of (v_1^*/v) over the composition range.

$N_A v_1^* = 55.24$ cc/mole

$N_A v = (v_1 w_1 + v_2 w_2)/\bar{\rho}_{mix}$

where x denotes the mole fraction, ρ_{mix} density of the mixture and N_A Avogadro's constant. r was taken as

$$r = \left(\frac{v_2^o}{v_1^o} \right)^{\frac{1}{3}}$$

where v_i^o denotes the molar volume of pure species i at the given temperature, and R = .5077 from the molecular weights. The values of the ratios of eqn.s (39) and (49) were computed using this information. Also, similar calculations were executed on equations (60) through (63) and the results plotted in fig. 4, along with experimental data.

For the thermal conductivity, all three theoretical curves conform to the general behaviour of the experimental data. Agreement between calculated and experimental values is within 10%, and gets even better for equation (39). A similar situation is observed for the viscosity ratios. Equations (62) and (49) give practically identical results.

ii) The system argon + methane.

Calculated results were compared with data (Ref 8) taken at 90.91°K. Density data for the pure components (Ref 11) and excess volume data (Ref 12) were used to compute the molar volumes over the composition range, r was taken as

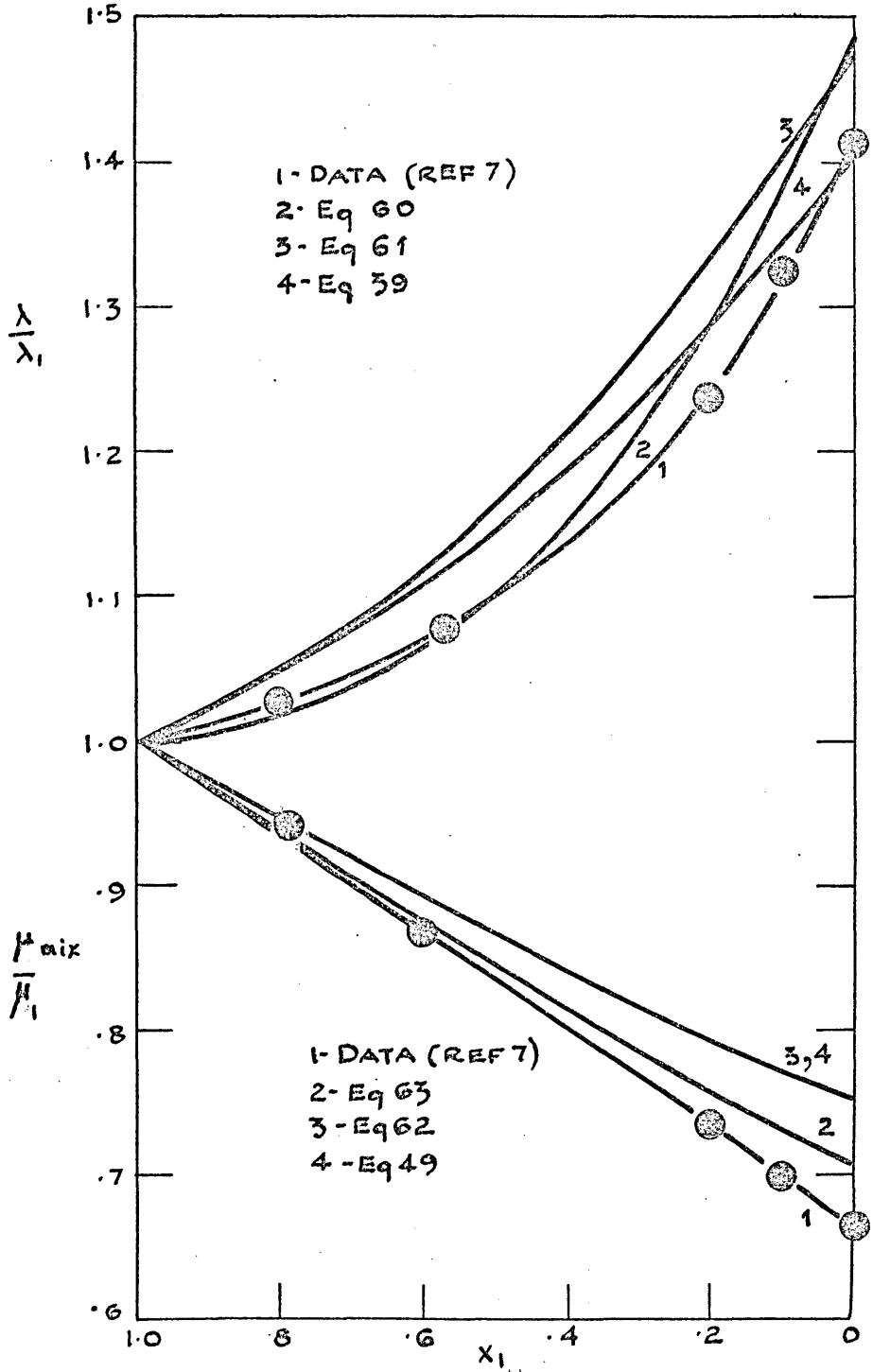

FIG. 4. CALCULATED AND EXPERIMETAL VISCOSITIES AND THERMAL CONDUCTIVITIES FOR THE SYSTEM CARBON TETRACHLORIDE(1) + BENZENE(2) AT 303°K

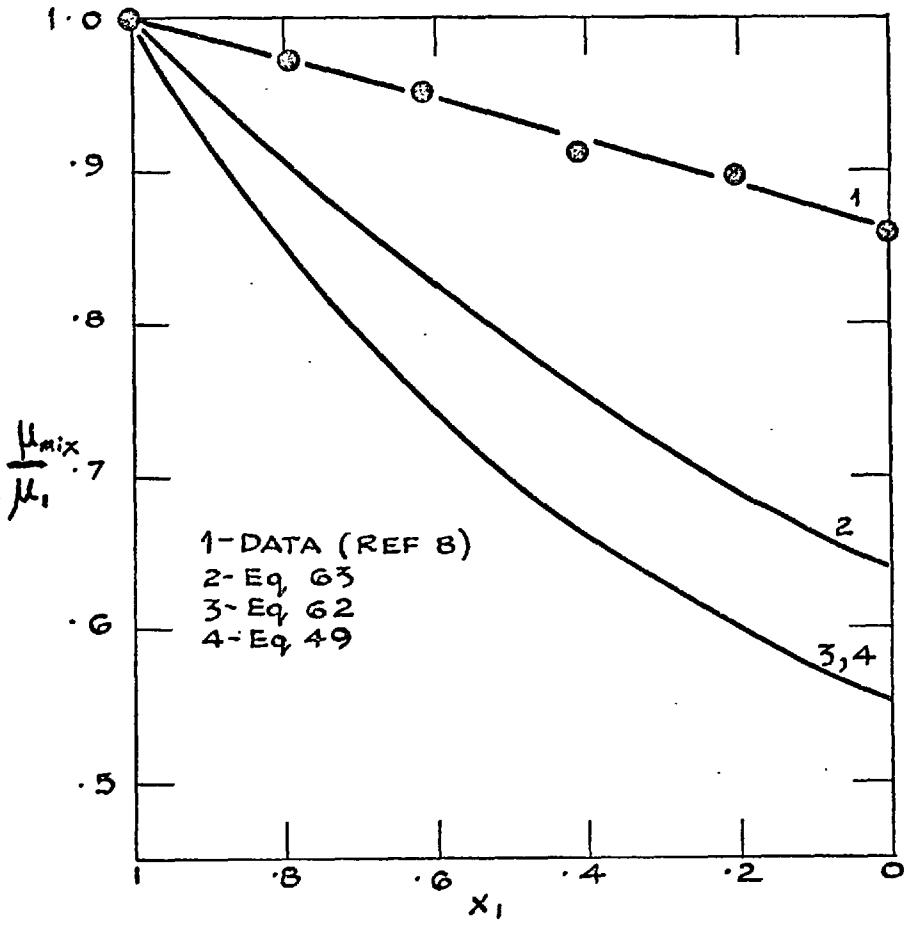

FIG. 5. CALCULATED AND EXPERIMENTAL VISCOSITIES FOR THE SYSTEM ARGON(1) + METHANE (2) AT 90·91°K

$$\left(\frac{v_2^o}{v_1^o}\right)^{\frac{1}{3}} = 1.067$$

and v_1^* from the molar volume of solid argon (Ref 13) at 0^oK. Fig. (5) shows that agreement of experiment with any of the three theoretical curves is not as good as that of the previous system.

Thermal Diffusion in Dense Hard Sphere Fluids

1. Introduction

A treatment similar to that of the previous two chapters, has been applied to thermal diffusion. Using the Lebowitz radial distribution functions, theoretical calculations have been executed with both the Chapman-Enskog and the Longuet-Higgins, Pople and Valleau theories. Results from these two theories were compared with experimental thermal diffusion ratios as a function of composition and pressure.

2. The Theoretical Expressions

Diffusion of one component relative to the other takes place if the mean velocities of the two sets of molecules in a binary mixture are not the same. Then in a small volume about $\underline{r}$, between time t and $t + \Delta t$.

$$\bar{\underline{c}}_1 - \bar{\underline{c}}_2 = \frac{1}{n_1}\int f_1 \underline{c}_1 \, d\underline{c}_1 - \frac{1}{n_2}\int f_2 \underline{c}_2 \, d\,\underline{c}_2 \neq 0 \qquad (1)$$

where the second approximation to f_1 and f_2 are taken as

$$f_1 = f_1^{\,o}\,[\,1 + \phi_1^{(1)}\,]\;;\; f_2 = f_2^{\,o}\,[\,1 + \phi_2^{(1)}\,], \qquad (2)$$

and the quantities ϕ have been defined previously (Ref.1a).

Substituting for $\phi^{(1)}$ in eqn. (1) explicitly leads to an expression which indicates that diffusion takes place

a) in the direction tending to reduce inhomogeneity in the mixture,

b) when accelerative effects of forces acting on molecules of the two gases are non-uniform,

c) when pressure is non-uniform;

d) the velocity of diffusion posesses a component in the direction of the temperature gradient. This thermal diffusion produces a non-uniform steady state in a gas parts of which are maintained at different steady temperatures. (Ref. 1a).

If the absence of external forces and pressure gradients is assumed

$$\bar{C}_1 - \bar{C}_2 = - \frac{n^2}{n_1 n_2} \left\{ \frac{D_{12}}{n} \frac{\partial n_1}{\partial r} + D_T \frac{\partial \ln T}{\partial r} \right\} \quad (3)$$

where n is the number density of the mixture

$n_1 = x_1 n$

D_{12} = mutual diffusion coefficient.

D_T = thermal diffusion coefficient.

Equation (3) can be rewritten as

$$\bar{C}_1 - \bar{C}_2 = - \frac{n^2}{n_1 n_2} D_{12} \left\{ \frac{1}{n} \frac{\partial n_1}{\partial r} + k \frac{\partial \ln T}{\partial r} \right\} \quad (4)$$

where k_T ($= D_T/D_{12}$) is called the thermal diffusion ratio, or using $n_i = x_i n$

$$\underline{C}_1 - \underline{C}_2 = - D_{12} \left\{ \frac{1}{x_1 x_2} \frac{\partial x_1}{\partial r} + \alpha \frac{\partial \ln T}{\partial r} \right\}$$

where α ($= kT/x_1 x_2$) is called the thermal diffusion factor. (Ref. 1b)

The Chapman-Enskog derivation of k_T for dilute gas mixtures has been extended by Thorne to dense fluid mixtures. In the first approximation, the thermal diffusion ratio of dense hard sphere fluid mixtures is given by (Ref.1c)

$$k_T = (AX + BY)/C \tag{5}$$

where

$$A = -10 x_1 \left[\left(\frac{M_2^3}{2M_1} \right)^{\frac{1}{2}} F + \frac{M_1}{\sqrt{2}} \gamma \right] \tag{6}$$

$$B = 10 x_2 \left[\left(\frac{M_1^3}{2M_2} \right)^{\frac{1}{2}} G + \gamma \right] / \sqrt{2} \tag{7}$$

$$C = g_{12} \left[G F - \gamma^2 \right] \tag{8}$$

$$G = 3 + 8 \frac{x_2}{x_1} \frac{g_2}{g_{12}} \left(\frac{2r}{1+r} \right)^2 \left(\frac{1}{M_2} \right)^{\frac{1}{2}} \tag{9}$$

$$F = \alpha + 8 \frac{x_1}{x_2} \frac{g_1}{g} \left(\frac{2r}{1+r} \right)^2 \left(\frac{1}{M_1} \right)^{\frac{1}{2}} \tag{10}$$

$$X = 1 + \frac{12}{5} g_1 x_1 \omega + \frac{6}{5} M_1 M_2 g_{12} x_2 (1+r)^3 \omega. \tag{11}$$

Y can be obtained by interchanging subscripts in equation (11). Finally α, β and γ have been given in the previous chapter, and the quantities g_1, g_2 and g_{12}, as before are

the radial distribution functions arising in the Percus-Yevick approximation (Ref. 2 and 3).

With the assumption that the velocity distribution function is locally Maxwellian, and that the pair distribution function is that at local equilibrium, Longuet-Higgins, Pople and Valleau (Ref. 4) have derived an expression for k_T, for an isotopic binary mixture. In the absence of pressure gradients and external forces

$$k_T = x_1 x_2 (M_2 - M_1) \frac{v_1^*}{v} g, \qquad (12)$$

where all quantities have been defined in the two previous chapters.

Fig. 1 compares values calculated from the Longuet-Higgins, Pople and Valleau theory (HPV) and from Thorne's extension of the Chapman-Euskog theory (CE). It can be seen that for both low and high values of the reduced pressure p^* ($= pv_1^*/kT$), results of HPV rise more sharply than those of CE, towards the middle of the composition range. It is also seen, though not very clearly on the graph, that while HPV predicts symmetric behaviour of k_T about $x_1 = .5$, this is not the case for CE. For $m_2/m_1 = 0.5$, $\sigma_2/\sigma_1 = 1$, and $p^* = 1$

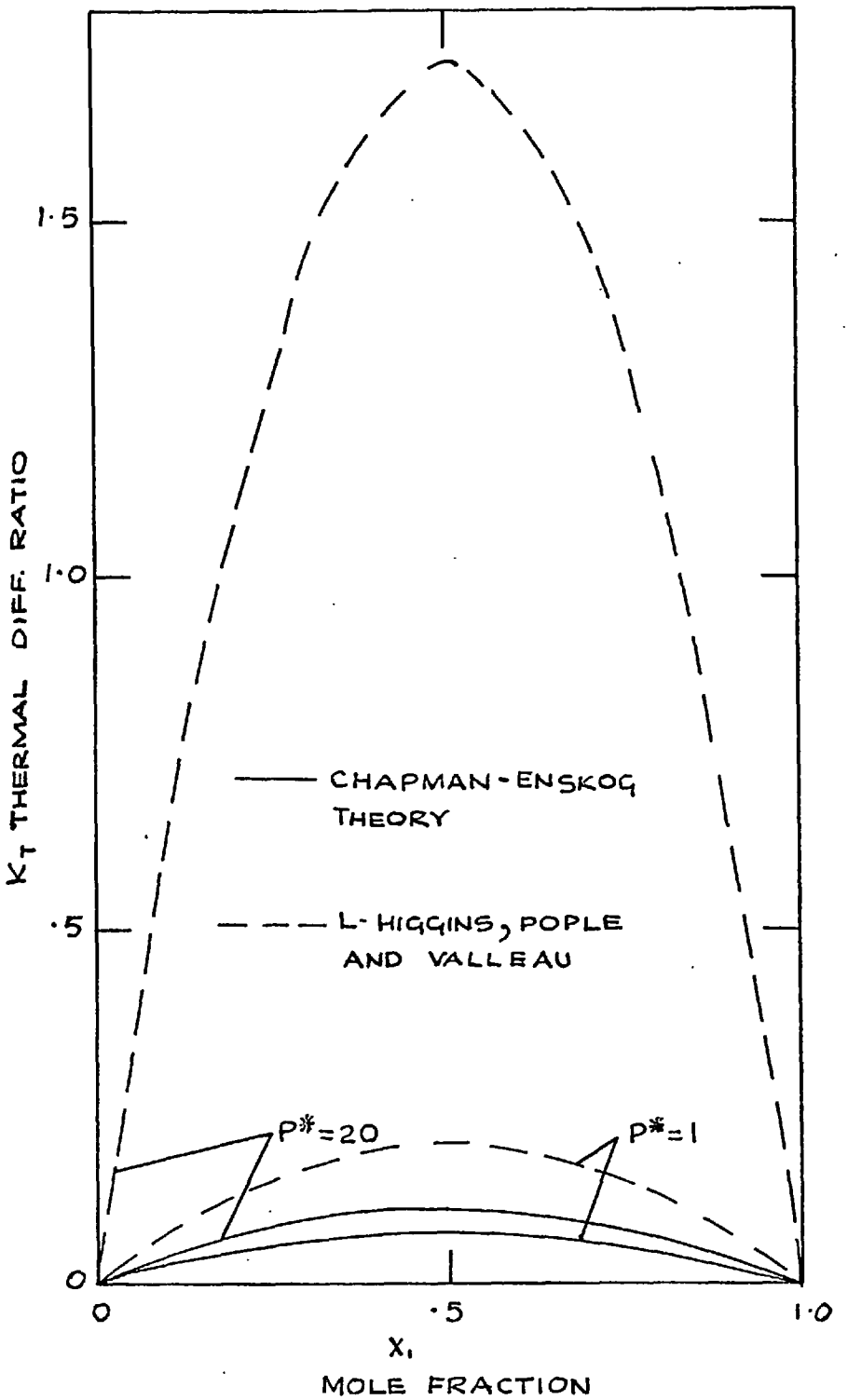

FIG.1 COMPARISON OF K_T FROM THE CHAPMAN-ENSKOG THEORY WITH THAT OF L-HIGGINS ET. AL.

r_1	k_T (CE)	k_T (HPV)
0.1	0.030917	0.072832
0.2	0.052982	0.12948
0.3	0.067168	0.16994
0.4	0.074298	0.19422
0.5	0.075064	0.20231
0.6	0.070040	0.19422
0.7	0.059696	0.16994
0.8	0.044403	0.12948
0.9	0.024442	0.072832

Fig. 2 shows the density dependence on these two theories. It is seen that for r = .5 α falls monotonically, that for r = 1, α goes through a shallow minimum

p^*	α(CE)
.04	.27454
.07	.27433
.1	.27455
.2	.27676

and that for r = 2, α rises slowly. In contrast HPV (r = 1) predicts the rather sharp rise of α with density.

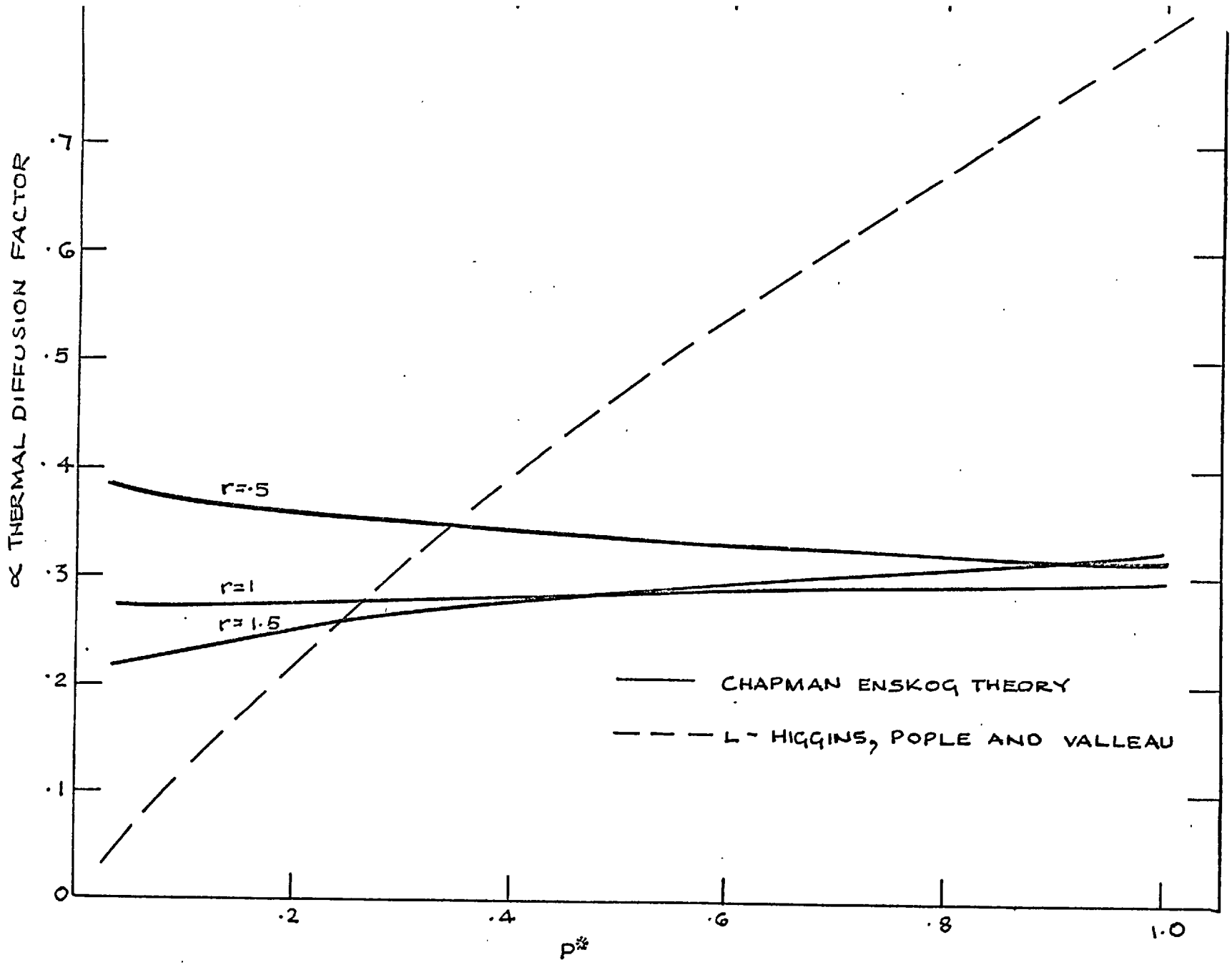

FIG. 2. α V.S. PRESSURE $m_2/m_1 = \cdot 5$; $K = \cdot 5$

3. Comparison with Experiment

Results obtained from the CE and HPV theories were compared with experimental data. The composition dependences of the calculated α's were compared with data for the system CCl_4-Cyclohexane (Ref.6) and the pressure dependence with the system Xe - CH_4 (Ref. 5). Calculations were similar to those of the previous chapter. The Fortran IV program written for this purpose will not be presented in the appendix as it is very similar to the thermal conductivity program.

a) The system CCl_4(1) + Cyclohexane (2). As can be seen from fig. 3, there are considerable differences regarding values of α, between measurements of different experimenters. While results of Horne and Bearman (Ref. 6) go through a minimum around $x_1 = .5$ those of Thomaes (Ref. 7) exhibit quasi linear behaviour over the composition range. Furthermore agreement of both theories with experiment is poor. Theα calculated from HPV rises with the mole fraction of CCl_4; all values are about 100% higher than the measured ones. α calculated from CE, on the other hand seems relatively insensitive to composition changes.

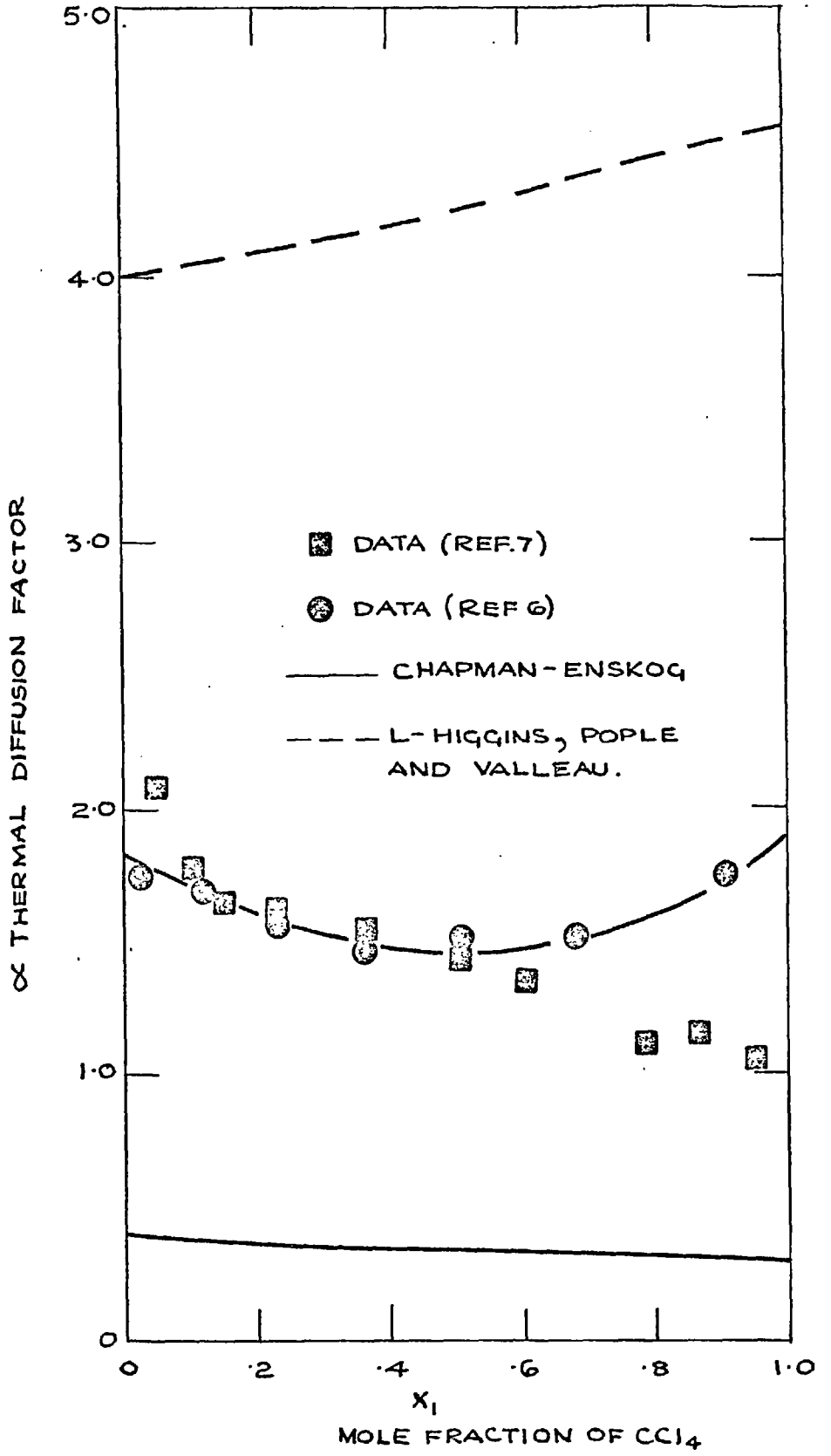

FIG 3. COMPOSITION DEPENDENCE OF ∝ FOR MIXTURES OF CCl_4 (1) + CYCLOHEXANE (2) AT 25°C

Density data used in these calculations were taken from Wood and Gray (Ref. 8) and the N v_1^* from Klitz and Sapper (Ref. 9)

b) The system Xe (1) + CH_4 (2). α has been measured for x_1 = .0015, at 25°C, as a function of pressure, the latter going up to about 100 atmospheres. Two different ways (Ref. 10 and 11) of analyzing the same set of data give widely differing results. Those resulting from the method of Drickamer, Tung and Mellow seem internally more consistent as seen in fig. 4. There, it can also be seen that HPV theory is very sensitive to pressure changes and rises rapidly to values much higher than the ones likely to be the correct values. This behaviour could be expected from results plotted on fig. 2.

Although not apparent on Fig 4, the CE results go through a shallow minimum around ρ = .01

ρ	α'
.002	.74471
.006	.74455
.008	.74454
.01	.74458
.015	.74488

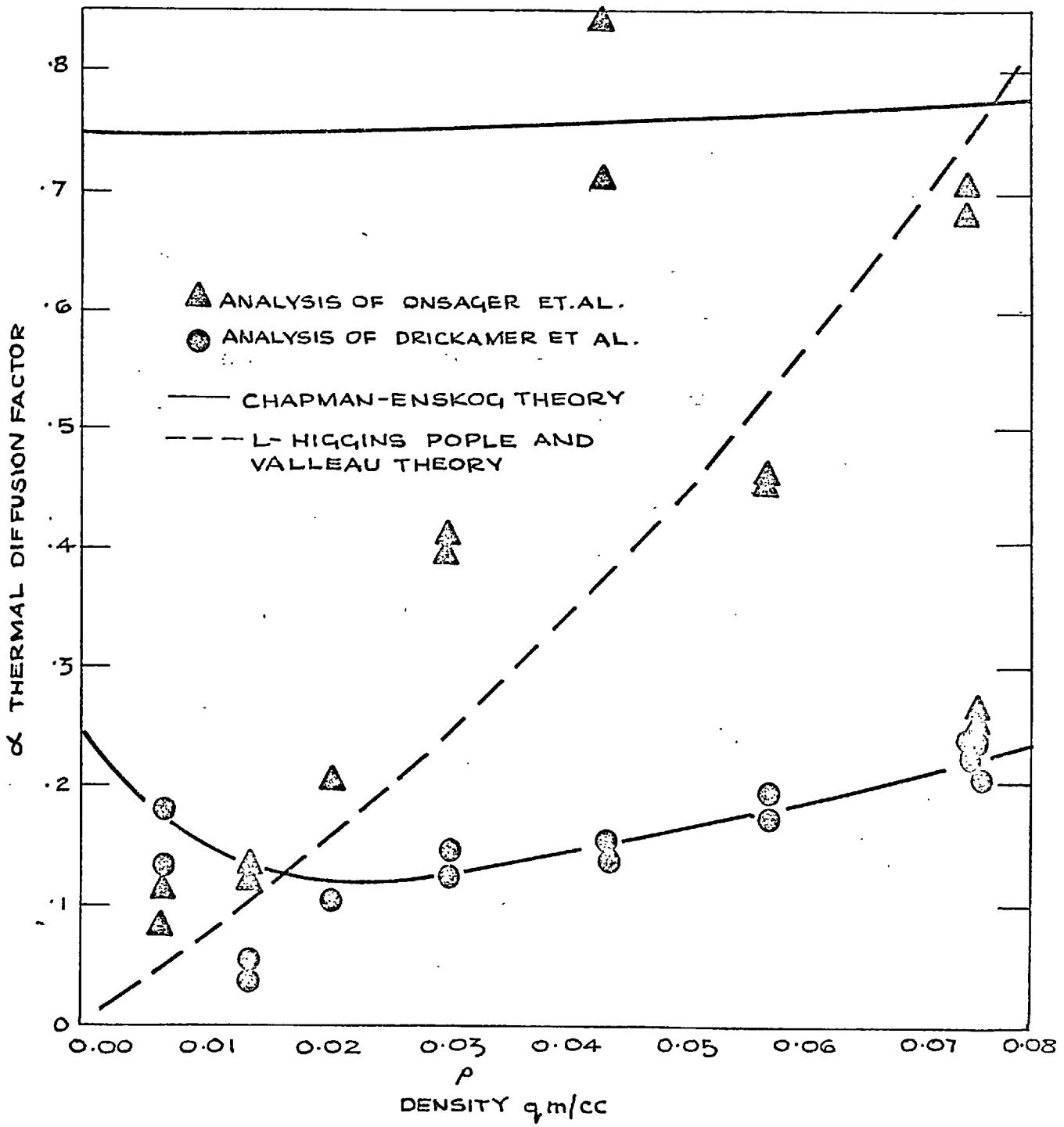

FIG. 4 PRESSURE DEPENDENCE OF α FOR THE SYSTEM Xe(1) + CH_4(2) AT 25°C, x_1 = ·0015

If the Drickamer et. al. treatment of the data is accepted, CE does qualitatively predict the behaviour of α as a function of pressure.

Here density data for the calculations was obtained from Ref. 5, and Nv_1^* from Ref. 12.

A P P E N D I X 1

A. Evaluation of $T \alpha DP/Dt$

For the case of axial motion only, DP/Dt reduces to

$$\frac{DP}{Dt} = \frac{\partial P}{\partial t} + v_z \frac{\partial P}{\partial z} \quad . \tag{A1}$$

The pressure at the bottom of the cell is given by

$$P = P_E + \rho g h \tag{A2}$$

where

P_E is the equilibrium vapor pressure of the liquid at the given temperature

ρ is the density

g is the acceleration of gravity, and

h is the height of the cell.

(A2) then becomes

$$\frac{DP}{Dt} = \frac{\partial P_E}{\partial t} + v_z \rho g \quad . \tag{A3}$$

Here has been assumed constant. Also

$$\frac{\partial P_E}{\partial t} = \frac{\partial P_E}{dT} \frac{\partial T}{\partial t} \quad ; \tag{A4}$$

hence

$$\frac{DP}{Dt} = \frac{\partial P_E}{\partial T} \frac{\partial T}{\partial t} + v_z \rho g \quad . \tag{A5}$$

For toluene at 90° C

$$\frac{dP_E}{dT} \doteq 1.3 \times 10^4 \quad \text{gm / cm-sec}^2 - {}^\circ\text{C} ,$$

$$\frac{\partial T}{\partial t} \doteq 10^{-3} \quad {}^\circ\text{C / sec} \qquad \text{at} \quad t=10 \text{ sec}$$

assuming the uniform distribution of temperature; also

$$v_z \rho g \doteq 98 \quad \text{gm/cm-sec}^3 .$$

Therefore

$$\frac{DP}{Dt} \doteq 110 \quad \text{gm/cm-sec}^3$$

and

$$T \alpha \frac{DP}{Dt} \doteq 40 \quad \text{ergs/cm}^3 - \text{sec}$$

which is much smaller than

$$\rho C_p \frac{\partial T}{\partial t} \doteq 10^4 \quad \text{ergs/cm}^3 - \text{sec} .$$

B. Comparison of ξ vs. Kt

We assume at 90 °C, a temperature rise of .5 °C in 15 seconds. Choosing the maximum ξ as K(90.5 °C)t, we insure that the calculation overestimates the error.

$$K(90\ ^{\circ}C) = .76498 \times 10^{-3}$$
$$K(90.5\ ^{\circ}C) = .76376 \times 10^{-3}$$

Using

$$\lambda_1 T(a,t) + \frac{\lambda 2}{2} T^2(a,t) = \frac{Q}{4\pi} \left[\ln \frac{4\xi}{Ca^2} + \frac{a^2}{2\xi} + \frac{\alpha-2}{2\alpha\xi} a^2 \ln \frac{4\xi}{Ca^2} + \ldots \right]$$

and comparing values of λ_1 obtained from the calculations with K(90 °C) and K(90.5 °C), the error is .015%. For t=1 sec. the error is less than .01%.

APPENDIX 2

Derivation of Equation 37 of Chapter 2.

A. Solution of Fourrier's Equation in Cylindrical Coordinates with Time Dependent Heat Input and Temperature Dependent Physical Properties.

Fourrier's equation can be written as

$$\rho C_p \frac{\partial T}{\partial t} = \frac{1}{r} \frac{\partial}{\partial r} \left[r\lambda \frac{\partial T}{\partial r} \right] \tag{1}$$

where

$$\lambda = \lambda_1 + \lambda_2 T$$

$$\rho = \rho_1 + \rho_2 T$$

$$C_p = C_{p1} + C_{p2} T$$

are the thermal conductivity, density and heat capacity respectively, of the medium surrounding the central cylinder. The initial and boundary conditions are:

$$T(r,0) = 0 \tag{2}$$

$$\frac{dT}{dr}(r,0) = 0 \tag{3}$$

$$T(a,t) = f(t) \tag{4}$$

where $f(t)$ is obtained in digital form as the data. Further,

$$2\pi a\lambda \frac{\partial T(a,t)}{\partial r} + (q_1 + q_2 t + q_3 t^2) = \pi a^2 \rho C_p \frac{\partial T(a,t)}{\partial t} \tag{5}$$

$$\lim_{r \to \infty} T(r,t) = 0 \tag{6}$$

Equations (1)-(6) are linearized by making use of the transformations listed in chapter 2.

$$\nabla^2 \phi = \frac{\partial \phi}{\partial \xi} \tag{7}$$

$$\phi(r,0) = 0 \quad ; \quad r>a \tag{8}$$

$$\lim_{r\to\infty} \phi(r,\xi) = 0 \tag{9}$$

$$2\pi a \frac{d\phi}{dr} + Q_1 + Q_2\xi + Q_3\xi^2 = \frac{2\pi a^2}{\alpha} \frac{d\phi}{d\xi} \quad ; \quad r=a \tag{10}$$

where $Q_i = q_i/K^i$, and K is the thermal diffusivity. Transformation of

$$q = q_1 + q_2 t + q_3 t^2$$

to

$$q = Q_1 + Q_2 \xi + Q_3 \xi^2$$

is straightforward because $\xi = Kt$ as in chapter 2.

Using the initial condition, the Laplace transform of the boundary value problem is taken:

$$\frac{\partial^2 \bar{\phi}(r,s)}{\partial r^2} + \frac{1}{r} \frac{\partial \bar{\phi}(r;s)}{\partial r} = s\, \bar{\phi}(r,s) \tag{11}$$

$$2\pi a \frac{\partial \bar{\phi}}{\partial r} + \frac{Q_1}{s} + \frac{Q_2}{s^2} + \frac{Q_3}{s^3} = \frac{2\pi a}{\alpha} s\, \bar{\phi} \quad ; \quad r=a \tag{12}$$

$$\lim_{r\to\infty} \bar{\phi}(r,s) = 0$$

where $\bar{\phi}$ is the Laplace transform of ϕ and s is the complex variable of the transformation.

Here $=2\rho C_p'/\rho C_p$ where ρ and C_p are the density and specific heat of the fluid medium respectively and ρ' and C_p' are the corresponding properties of the central cylinder. As mentioned in Chapter 2, α is assumed constant; the justification of this assumption is given below.

The solution of the heat transfer equation where in addition to the assumptions listed in Chapter 2, the physical properties are accepted to be temperature independent, and the power input constant is

$$T(r,t) = \frac{Q_1}{4\pi\lambda}\left[\ln\frac{4\tau}{C} + \frac{1}{2\tau} + \frac{\alpha-2}{\alpha}\frac{1}{2\tau}\ln\frac{4\tau}{C} + \dots\right] \qquad (13)$$

where $\tau = \frac{Kt}{r^2}$, $C = \exp(\gamma)$ and γ is Euler's constant. For times longer than .5 sec in the thermal conductivity experiment, both the second and the third terms become negligible i.e. ($<.1\%$) in comparison to the first. Hence the dependence $T(a,t)$ on α is confined to the early part of the curve, which in the experiment is discarded. While it does not seem possible at this stage to show rigorously that the temperature dependence of does not sensibly (i.e. $>.1\%$) alter the solution of equations (7) to (10) of this section it is reasonable to assume $\alpha =$ is constant as the term containing α, itself is rather small.

Equation (11) is now an ordinary differential equation, the general solution of which is well known:

$$\bar{\phi}(r,s) = C_1 I_o(\beta r) + C_2 K_o(\beta r) \tag{14}$$

where C_1 and C_2 are arbitrary constants, $\beta = \sqrt{s}$ and I_o and K_o are modified. Bessel functions, of zero order, of the first and second kinds respectively.

As I_o increases with r, using equation (13) $C_1 = 0$. Then

$$\bar{\phi}(r,s) = C_2 K_1(\beta r) \quad , \frac{d\bar{\phi}(r,s)}{dr} = -C_2 \beta K_1(\beta r); \tag{15}$$

clearly

$$\frac{d\bar{\phi}(a,s)}{dr} = -C_2 \beta K_1(\beta a) \tag{16}$$

and using equations (12) and (16)

$$\frac{\partial\bar{\phi}(a,s)}{\partial r} = \frac{-q}{2\pi as} + \frac{as}{\alpha} C_2 K_o(\beta a) = -C_2 \beta K_1(\beta a) \; . \tag{17}$$

Solving (17) for C_2 and substituting in (15)

$$\bar{\phi}(r,s) = \frac{1}{2\pi as}\frac{Q_1}{s} + \frac{Q_2}{s^2} + \frac{2Q_3}{s^3}\frac{K_o(\beta r)}{\left[\beta K_1(\beta a) + \frac{as}{\alpha} K_o(\beta a)\right]} \tag{18}$$

We will now use two identities which will be drived in the last paragraph of this Appendix.

$$K_o(\beta r) = -\left[\ln(\tfrac{1}{2}C\beta r) + \tfrac{1}{4}\beta^2 r^2\left[\ln(\tfrac{1}{2}C\beta r) - 1\right] + \ldots\right] \tag{19}$$

and

$$\beta K_1(\beta a) = \frac{1}{a}\left[1 + \tfrac{1}{2}\beta^2 a^2\left[\ln(\tfrac{1}{2}C\beta a) - \tfrac{1}{2}\right] + \ldots\right] \tag{20}$$

and by long division

$$\begin{aligned}\bar{\phi}(r,s) = -\left[\frac{Q_1}{2\pi s} + \frac{Q_2}{2\pi s^2} + \frac{Q_3}{\pi s^3}\right]\Bigg\{ & \ln(\tfrac{1}{2}C\beta r) + \tfrac{1}{2}\beta^2 r^2 \ln(\tfrac{1}{2}C\beta r) \\ & - \tfrac{1}{2}\beta^2 a^2\left[\ln(\tfrac{1}{2}C\beta r)\right]^2 - \frac{\beta^2 a^2}{2}\ln(\tfrac{1}{2}C\beta r)\left[\ln\frac{a}{r} - \tfrac{1}{2}\right] \\ & + \frac{a^2 s}{\alpha}\left[\ln(\tfrac{1}{2}C\beta r)\right]^2 + \frac{a^2 s}{\alpha}\ln(\tfrac{1}{2}C\beta r)\cdot\ln\frac{a}{r} - \tfrac{1}{4}\beta^2 r^2 \\ & + \frac{a^4 s^2}{4\alpha}\left[\ln(\tfrac{1}{2}C\beta r)\right]^2 + \frac{a^4 s^2}{4\alpha}\ln(\tfrac{1}{2}C\beta r)\left[\ln\frac{a}{r} - 1\right] + \ldots\Bigg\}\end{aligned} \tag{21}$$

All that remains to be done now is to invert equation (21) from the complex to the real plane. In doing so, we will make use of the theorem that,* in the class of problem under consideration

$$\phi(t)=\frac{1}{2\pi i}\int_{\gamma-i\infty}^{\gamma+i\infty} e^{st}\,\phi(s)\,ds=\frac{1}{2\pi i}\int_{-\infty}^{0+} e^{st}\,\phi(s)ds \qquad (22)$$

when γ is real, and $i=\sqrt{-1}$. Hence we can make use of **

$$L^{-1}\,[\ln(ks)] = -1/t \qquad (23)$$

and

$$L^{-1}\,[s^n \ln(ks)] = (-1)^{n+1}\,(n\,!)\,/\,(t^{n+1}) \qquad (24)$$

where k is any constant,

and L^{-1} is denotes the inverse Laplace transform operator,

$$L^{-1}[\,\bar{\phi}(s)] = \frac{1}{2\pi i}\int e^{st}\cdot\bar{\phi}(s)\,ds = \phi(t) \qquad (25)$$

We also need the following inverse transformations***:

---

* Carslaw, H.S. and Jaqer, J.C., "Conduction of Heat in Solids", p 370 . Oxford University Press, 1959.

** ibid, p.341

*** Erdelyi, A., Editor, "Tables of Integral Transforms", McGraw-Hill Book Company, New York, 1954, p.251

$$L^{-1}[s^{-1} (\ln ks)^2] = [\ln \frac{Ct}{k}]^2 - \frac{\pi^2}{6} \tag{26}$$

$$L^{-1} [s^{-2} (\ln ks)^2] = t[(1-\ln \frac{Ct}{k})^2 + 1 - \frac{\pi^2}{6}] \tag{27}$$

and

$$L^{-1}[s^{-n-1} \ln ks] = [1+\frac{1}{2}+\frac{1}{3}+\ldots+\frac{1}{n}- \ln \frac{Ct}{k}] \frac{t^n}{n!} \tag{28}$$

The inversion of equation (21) follows directly from (22) - (28). By dropping terms containing $1/t^2$ or higher powers of $(1/t)$ we obtain

$$\phi(a,\xi)= \frac{Q_1}{4\pi}\left[\ln \frac{4\xi}{Ca^2} + \frac{a^2}{2\xi} + \frac{\alpha-2}{\alpha} \frac{a^2}{2\xi} \ln \frac{4\xi}{Ca^2} + \ldots \right] \tag{29}$$

$$+\frac{Q_2}{4\pi}\left[-\xi+\ln \frac{4\xi}{Ca^2} (\xi+\frac{a^2}{2}) + (\frac{a}{2}\ln \frac{4\xi}{Ca^2})^2 \frac{\alpha-2}{\alpha} + \frac{a^2}{2} - \frac{a^2\pi^2}{24} \frac{\alpha-2}{\alpha} + \ldots \right]$$

$$+\frac{Q_3}{2\pi}\left[-\frac{3\xi^2}{4} + \frac{\xi a^2}{2}\frac{\alpha-2}{\alpha} (1-\frac{\pi^2}{12}) + \xi\ln \frac{4\xi}{Ca^2} (\frac{\xi}{2} + \frac{a^2}{\alpha}) + \xi[\ln \frac{4\xi}{Ca^2}]^2 \frac{a^4}{4}\frac{\alpha-2}{\alpha} + \ldots\right]$$

where $\xi = Kt$. The time dependence of power is weak and the sum of the second and third brackets of equation (29) is less than 1% of the first. Thus, without introducing any sensible error into the analysis of the experimental data, terms that contribute less than 1% of their respective brackets in the second and third brackets can be ignored. For the second bracket taking toluene at 90°C,

$$K = 7.6 \times 10^{-4} \text{ cm}^2/\text{sec}, \quad a = 1.27 \times 10^{-3} \text{cm}, \quad \alpha \simeq 3.67$$

<u>at 1 sec.</u>

$$\frac{a^2}{2} \ln \frac{4Kt}{Ca^2} = 5.3 \times 10^{-3}$$

$$Kt = 7.6 \times 10^{-4}$$

$$Kt \ln\left(\frac{4Kt}{Ca^2}\right) = 5.3 \times 10^{-3}$$

$$\frac{\alpha-2}{\alpha} \frac{a}{4} \left[\ln \frac{4Kt}{Ca^2}\right]^2 \simeq 10^{-5}$$

$$\frac{a^2}{2} = 8 \times 10^{-7}$$

$$\frac{a^2\pi^2}{24} \frac{\alpha-2}{\alpha} = 5 \times 10^{-7}$$

<u>at 10 sec</u>

$$Kt = 7.6 \times 10^{-3}$$

$$Kt \ln \frac{4Kt}{Ca^2} = .07$$

$$\frac{a^2}{2} \ln \frac{4Kt}{Ca^2} = 7 \times 10^{-6}$$

$$\left[\ln \frac{4Kt}{Ca^2}\right]^2 \frac{\alpha-2}{\alpha} \frac{a^2}{4} = 3 \times 10^{-5}$$

So the major terms in the second bracket of equation (29) are

$$-Kt + Kt \ln\left(\frac{4Kt}{Ca^2}\right) . \qquad (30)$$

The same comparison of the relative magnitudes of terms can be carried out for the third bracket of equation (29).

<u>After 1 sec.</u>

$$\frac{3}{4}(Kt)^2 = 4.4 \times 10^{-7}$$

$$Kt \frac{a^2}{2} \frac{\alpha-2}{\alpha} \left[1 - \frac{\pi^2}{12}\right] = 1.3 \times 10^{-10}$$

$$\frac{(Kt)^2}{2} \ln \frac{4Kt}{Ca^2} = 2.04 \times 10^{-6}$$

$$Kt \frac{a^2}{\alpha} \ln \frac{4Kt}{Ca^2} = 8 \times 10^{-9}$$

$$Kt \left[\ln \frac{4Kt}{Ca^2}\right]^2 \frac{\alpha-2}{\alpha} \frac{a^2}{4} = 2.5 \times 10^{-8}$$

After 10 sec.

$$\frac{3}{4}(Kt)^2 = 4.3 \times 10^{-4}$$

$$Kt\,\frac{a^2}{2}\frac{\alpha-2}{\alpha}\left(1-\frac{\pi^2}{12}\right) = 1.33 \times 10^{-9}$$

$$\frac{(Kt)^2}{2}\ln\frac{4Kt}{Ca^2} = 2.7 \times 10^{-4}$$

$$Kt\,\frac{a^2}{\alpha}\ln\frac{4Kt}{Ca^2} = 1.2 \times 10^{-7}$$

$$Kt\ln\frac{4Kt}{Ca^2}\,\frac{\alpha-2}{\alpha}\,\frac{a^2}{4} = 2.2 \times 10^{-7}\ .$$

The terms that are large in the third bracket then are

$$-\frac{3}{4}(Kt)^2 + \frac{K^2t^2}{2}\ln\frac{4Kt}{Ca^2}\ . \tag{31}$$

Combining equations (29), (30) and (31), with $i = Q_1/K^i$, we get

$$\begin{aligned}\phi(a,t) = {} & \frac{q_1}{4\pi}\left[\ln\frac{4Kt}{Ca^2} + \frac{a^2}{2Kt} + \frac{\alpha-2}{\alpha}\frac{a^2}{2Kt}\ln\frac{4Kt}{Ca^2} + \cdots\right] \\ & + \frac{q_2}{4\pi}\left[t\left(\ln\frac{4Kt}{Ca^2} - 1\right) + \cdots\right] \\ & + \frac{q_3}{4\pi}\left[t^2\left(\ln\frac{4Kt}{Ca^2} - \frac{3}{2}\right) + \cdots\right]\ ,\end{aligned} \tag{32}$$

where ϕ is now related to T by equation (39) of Chapter 2.

$$\phi(a,t) = \lambda_1\, T(a,t) + \lambda_2\, T(a,t)\ .$$

B. Derivation of Equations (19) and (20)*

The modified Bessel equation

$$\frac{d^2y}{dz^2} + \frac{1}{z}\frac{dy}{dz} - \left[1 + \frac{\nu^2}{z^2}\right] y = 0$$

where z is the independent variable, $y = y(z)$ and ν any specified constant, is satisfied by

$$I_\nu(z) = \sum_{r=0}^{\infty} \frac{(\frac{1}{2}z)^{\nu+2r}}{r!\,\Gamma(\nu+r+1)}$$

where for ν an integer

$\Gamma(n) = (n-1)!$

Clearly for $\nu = 0$, and $z = \beta r$

$$I_o(\beta r) = 1 + (\tfrac{1}{2}\beta r)^2 + \frac{(\frac{1}{2}\beta r)^4}{(2!)^2} + \cdots . \qquad (34)$$

$K_\nu(\beta r)$ is now defined as

$$K_\nu(\beta r) = \frac{\pi}{2}\,\frac{I_{-\nu}(\beta r) - I_\nu(\beta r)}{\sin \nu\pi} \quad ; \qquad (35)$$

then

$$K_o(\beta r) = -\left[\ln \frac{\beta r}{2} + \gamma\right] I_o(\beta r) + \left(\frac{\beta r}{2}\right)^2 + \cdots \text{, and}$$

$$K_o(\beta r) = -\left[\ln(\tfrac{1}{2}C\beta r) + \frac{1}{4}\beta^2 r^2(\ln \tfrac{1}{2}C\beta r - 1) + \cdots\right] . \qquad (36)$$

Also by making use of the expression

$$zK_\nu'(z) - \nu K_\nu(z) = -zK_{\nu+1}(z)$$

for $\nu = 0$, we have

$$K_o'(\beta r) = -K_1(\beta r) . \qquad (37)$$

---

* Carslaw, H.S. and Jaeger, J.C., "Conduction of heat in Solids," p. 448, Oxford University Press, London, 1959. (2nd Ed.)

Hence

$$\beta K_1(\beta a) = -\beta \frac{d}{d(\beta a)} \left[K_o(\beta a) \right] \quad \text{leads to}$$

$$\beta K_1(\beta a) = \frac{1}{a} \left[1 + \tfrac{1}{2}\beta^2 a^2 \left(\ln \tfrac{1}{2}C\beta a - \tfrac{1}{2} \right) + \ldots \right]$$

APPENDIX IIIA

PROGRAM WRITTEN FOR PROCESSING THERMAL CONDUCTIVITY DATA

SUBROUTINE POLYFT FROM IMPERIAL COLLEGE PROGRAM LIBRARY
ROUTINE FOR CODE TRANSLATION IN MACHINE CODE IS OMITTED

```
$JOB  100013063   R. KANDIYOTI MAP      3.0   3000      CRQ
$*    NAME CARD
$*     PLEASE LOAD TAPE A0146 ON A5 FILE PROTECT
$PAUSE
$EXECUTE         IBJOB
$IBJOB           FIOCS,MAP
$IBFTC DECK1
      DIMENSION B(250),DRT(10)
      DIMENSION ADJTIM(250),POWER(250),CURREN(250)
      DIMENSION BOVOLT(10),CP(10),CPPT(10),CVAR(250),CUR(250)
      DIMENSION CON(250),CONSD(250),CRR3(250),CRR4(250)
      DIMENSION CRR12(250),DV(250),FLINE(250),FITRES(250),NRUN(10)
      DIMENSION NTR(250),PEXP(10),POWRES(250),RO(10),ROPT(10)
      DIMENSION RIVT(10),SV1(10),SV2(10),STANDV(250),SMOOTH(250)
      DIMENSION TEXP(10),TIM(250),THCOND(250),TCONO(40),V(6,500)
      DIMENSION VOLT(250),VO(2),V1(2),V2(2),V3(2),V4(2),W(250)
      DIMENSION Z(250),P(250),DCUR(250),STDIV(250)
      DIMENSION XX(250),YY(250),NMAX(100),A(400)
      DIMENSION ID(500),FLINRS(250),CURRES(250),C(200)
      DIMENSION SMOTH1(250),SMOTH2(250),SMOTH3(250),SMOTH4(250)
C
C
      MMM=0
      COMMON/IMAGES/NMX(100),NX
      CALL ATLAS7
      STANR=10.0008
      PIE=2.*1.570796326795
      PER=.10
      WIREL=8.100
      READ(5,100)NBATCH
  100 FORMAT(I2)
      NOBAT=1
  999 READ(5,101)NOTAPE
  101 FORMAT(I1)
      IMAX=NOTAPE-1
C     TAPE INPUT SECTION
 1800 DO 800 I=1,NOTAPE
      MMM=MMM+1
      MM=NMX(MMM)
      NMAX(I)=5*(MM-1)
      K1=1
      K5=5
 1801 DO 801 N=1,MM
      READ(14,103) (ID(J),J=K1,K5)
```

```
  103 FORMAT(5(I7,1X))
 1802 DO 802 J=K1,K5
  802 V(I,J)= .00000I*FLOAT(ID(J))
      K1=K1+5
      K5=K5+5
  801 CONTINUE
  800 CONTINUE
C
C
      READ(5,105)TD,DLAMDA
  105 FORMAT(2E13.6)
 1304 DO 304 I=1,IMAX
      READ(5,106)RO(I),CP(I),ROPT(I),CPPT(I)
  106 FORMAT(4E13.6)
      READ(5,107)TEXP(I),RIVT(I),BOVOLT(I),PEXP(I)
C     TEXP IN DEG C
  107 FORMAT(4E13.6)
C     NRUN IS RUN NUMBER
      READ(5,108)NRUN(I),SV1(I),SV2(I),DRT(I)
  108 FORMAT(I4,E13.6,E13.6,E13.6)
  304 CONTINUE
C
C     CHOOSING JMAX
      JMAX=NMAX(1)
      DO 399 I=2,NOTAPE
      IF(NMAX(I)-JMAX)398,399,399
  398 JMAX=NMAX(I)
  399 CONTINUE
      IF(JMAX .LT. 250) GO TO 402
      JMAX=250
  402 JNN=JMAX-5
C
C
      WRITE(6,24)JMAX
   24 FORMAT(3X,9H****JMAX=,I4)
C
C     CALCULATING TIMES
 1400 DO 400 J=5,JMAX
      TIM(J)=TD+(.125*(FLOAT(J-1)))
      ADJTIM(J-4)=TIM(J)
  400 FLINE(J)=(TIM(J)/PER)*(ALOG(1.+(PER/TIM(J))))+ALOG(TIM(J)+PER)
C     CALCULATING CURRENT VARIATION
C
      I=NOTAPE
      DO 303 J=5,JMAX
      CVAR(J)=V(I,J)/STANR
      CURREN(J-4)=CVAR(J)
  303 CONTINUE
      NJ=JMAX-5+1
      KOR=2
      NOUT=-1
      CALL POLYFT(ADJTIM,CURREN,NJ,KOR,C,CO,A,NOUT,STDV,SMOTH1,CURRES)
      CVR1=C(1)
C
C     FORMING I-LOOP
C
```

```
      CVR2=C(2)
 1451 DO 451 I=1,IMAX
      SETCUR=SV2(I)/STANR
 1401 DO 401 J=5,JMAX
      CUR(J)=SETCUR+(CVR1*TIM(J))+(CVR2*((TIM(J))**2))
      P(J)=(CUR(J)*(V(I,J)+BOVOLT(I)))/WIREL
      POWER(J-4)=P(J)
  401 CONTINUE
      NJ=JMAX-5+1
      KOR=2
      NOUT=-1
      CALL POLYFT(ADJTIM,POWER,NJ,KOR,C,CO,A,NOUT,STDV,SMOTH2,POWRES)
      Q1=C(1)
      Q2=C(2)
      PSDIV=STDV
      CELLR=(RIVT(I)/SV1(I))*STANR
C
C     CALCULATING AVERAGE POWER
      QO=(SETCUR**2)*(CELLR/WIREL)
      N=JMAX
      TMAX=TIM(N)
      POWAV= QO+(Q1*TMAX)/2.+ (Q2*(TMAX**2))/3.
      DRDT=DRT(I)
C
C
C     MAIN CALCULATIONS
      JJ=10
      JJJ=10
 1699 GO TO 699
  697 JJJ=JJ+3
  698 JJ=JJ+3
  699 JF=5
      JL=(2*JJ)-5
      J=JF
      NN=JL-4
      L=1
  700 XX(L)=FLINE(J)
      YY(L)=V(I,J)
      J=J+1
      L=L+1
      IF(L .LE. NN) GO TO 700
      NOUT=-1
      KOR=2
      N=NN
C
      CALL POLYFT(XX,YY,N,KOR,C,CO,A,NOUT,STDV,SMOTH3,FLINRS)
      STANDV(JJ)=STDV
      DV(JJ)=C(1)*(XX(NN)-XX(1))+C(2)*((XX(NN)**2)-(XX(1)**2))
      VOLT(JJ)=BOVOLT(I)+V(I,JJ)
      DFLINE=XX(NN)-XX(1)
      SLPLIN=DV(JJ)/DFLINE
      DCUR(JJ)=CUR(JL)-CUR(JF)
      BRALIN=(SLPLIN/CUR(JJ))- (VOLT(JJ)/(CUR(JJ)**2))*(DCUR(JJ)/DFLINE)
      M=1
      CON(M)=((POWAV/(4.*PIE))*DRDT)/BRALIN
      IF(CON(M))530,530,531
```

```
530 K=((JJ-JJJ)/3)+1
    CONSD(K)=1.0
    CRR12(K)=1.0
    CRR3(K)=1.0
    CRR4(K)=1.0
    NTR(K)=1.0
    Z(K)=1.0
    W(K)=1.0
    GO TO 535
C
C     GOING INTO MAIN SOLN TRIALS
531 B0=Q0/(4.*PIE)
    THCOND(K)=1.0
    B1=Q1/(8.*PIE)
    B2=Q2/(12.*PIE)
    B3=((Q0/(4.*PIE))**2)*(DLAMDA/(2.*PER))
    B4=R0(I)*CP(I)
    ALFA=(2.*B4)/(ROPT(I)*CPPT(I))
    ALRAT=(ALFA-2.)/ALFA
C
C     LAMDA ITERATIONS
508 DIFF=CON(M)/B4
    AOK=(1.6129*.000001)/DIFF
    TAU=TIM(JF)
    CALL BRA1(TAU,DIFF,AOK,ALRAT,FZERO,RAT,FONE,FTWO,FTHRI)
    IF(ABS(RAT) .GT. 100.) GO TO 697
    V0(1)=B0*FZERO
    V1(1)=B1*FONE
    V2(1)=B2*FTWO
    V3(1)=B3*FTHRI/(CON(M)**2)
    V4(1)=RAT*V0(1)
    FUN1=V0(1)+V1(1)+V2(1)+V3(1)
    TAU=TIM(JL)
    CALL BRA1(TAU,DIFF,AOK,ALRAT,FZERO,RAT,FONE,FTWO,FTHRI)
    V0(2)=B0*FZERO
    V1(2)=B1*FONE
    V2(2)=B2*FTWO
    V3(2)=B3*FTHRI/(CON(M)**2)
    V4(2)=V0(2)*RAT
    FUN2=V0(2)+V1(2)+V2(2)+V3(2)
    DFUN=FUN2-FUN1
    M=M+1
    SLPFUN=DV(JJ)/DFUN
    BRAFUN=(SLPFUN/CUR(JJ))-(VOLT(JJ)/(CUR(JJ)**2))*(DCUR(JJ)/DFUN)
    CON(M)=DRDT/BRAFUN
    CHANGE=(ABS(CON(M)-CON(M-1)))/CON(M)
    IF(CHANGE .GT. .0001) GO TO 508
    K=((JJ-JJJ)/3)+1
    THCOND(K)=CON(M)
    CONSD(K)=STANDV(JJ)
    SUB0=ABS(V0(2)-V0(1))
    SUB1=ABS(V1(2)-V1(1))
    SUB2=ABS(V2(2)-V2(1))
    SUB3=ABS(V3(2)-V3(1))
    SUB4=ABS(V4(2)-V4(1))
```

```
      CRR12(K)=(SUB1+SUB2)/SUB0
      CRR3(K)=SUB3/SUB0
      Z(K)=FLOAT(JJ)
      B(K)=FLOAT(JL)
  535 IF(JL .LT. JNN) GO TO 698
      JJFIN=JJ
      CRR4(K)=SUB4/SUB0
      NTR(K)=M
C
C     THCOND FIT BEGINS
C
      L=0
      LMAX=3
  519 L=L+1
      KOR=L
      NOUT=-1
      N=((JJFIN-JJJ)/3)+1
      CALL POLYFT(Z,THCOND,N,KOR,C,CO,A,NOUT,STDV,SMOTH4,FITRES)
      STDIV(L)=STDV
      TCOND(L)=CO
 1519 IF(L .LT. LMAX)GO TO 519
C
C     OUTPUT SECTION
C
      WRITE(6,200)NRUN(I)
  200 FORMAT(1H1,35X,7HRUN NO ,I4)
      WRITE(6,201)TEXP(I),PEXP(I)
  201 FORMAT(//6X,17HEXPERIMENT TEMP= ,E13.6,6H DEG C,20X,18HEXPERIMENT
     1PRESS= ,E13.6,4H ATM)
      WRITE(6,202)SETCUR,CELLR,BOVOLT(I)
  202 FORMAT(1H0,6X,17HCURRENT (AMP) =  ,E13.6,12H  ****  RO= ,E13.6,18H
     10HM **** BACKOFF= ,E13.6,6H VOLTS)
      WRITE(6,203)QQ,Q1,Q2,PSDIV
  203 FORMAT(6X,17HPOWER(J/CM/SEC)= ,E13.6,11H+ T(SEC) * ,E13.6,19H  +
     1(T(SEC)**2)  ,E13.6,13H  **** STDV= ,E13.6)
      WRITE(6,204)DRDT
  204 FORMAT(6X,17HDR/DT (OHM/DEG)= ,E13.6)
      WRITE(6,205)RO(I),CP(I),DLAMDA
  205 FORMAT(1H0,6X,17HLIQUID       RO = ,E13.6,12H  **** CP = ,E13.6,19H
     1 J/G/D**** DLAMDA= ,E13.6,17H  J/CM/SEC/DEG**2)
      WRITE(6,206)ROPT(I),CPPT(I),ALFA
  206 FORMAT(6X,17HWIRE        ROPT= ,E13.6,12H **** CPPT= ,E13.6,19H J/G
     1/D **** ALFA = ,E13.6)
      WRITE(6,207)JJJ,JJFIN
  207 FORMAT(1H0,6X,5HJMIN=,I4,13H  ****  JMAX=,I4)
      WRITE(6,208)
  208 FORMAT(1H ,6X,36HTHERMAL CONDUCTIVITY POLYNOMIAL FITS)
      WRITE(6,209)
  209 FORMAT(7X,5HORDER,6X,5HLAM 0,13X,6HST DIV)
 1601 DO 601 L=1,LMAX
      WRITE(6,210)L,TCOND(L),STDIV(L)
  210 FORMAT(8X,I2,5X,E13.6,5X,E13.6)
  601 CONTINUE
      WRITE(6,211)LMAX
  211 FORMAT(1H0,6X,16HPOLYNOM ORDER = ,I4)
```

```
      WRITE(6,212)CO
  212 FORMAT(6X,6HLAMO= ,E13.6)
      DO 602 K=1,LMAX
      WRITE(6,213)K,C(K)
  213 FORMAT(6X,3HLAM,I1,2H= ,E13.6)
  602 CONTINUE
      WRITE(6,214)
  214 FORMAT(1H0,6X,2HNO,4X,3HNTR,6X,6HTHCOND,7X,6HSTANDV,12X,3HRGB,9X,6
     1HPOW CR,8X,7HDLAM CR)
      LAST=((JJFIN-JJJ)/3)+1
 1603 DO 603 K=1,LAST
      WRITE(6,215)B(K),NTR(K),THCOND(K),CONSD(K),CRR4(K),CRR12(K),CRR3(K
     1)
  215 FORMAT(3X,F6.1,2X,I3,2X,E13.6,2X,E13.6,2X,E13.6,2X,E13.6,2X,E13.6)
  603 CONTINUE
  451 CONTINUE
      NOBAT=NOBAT+1
      IF(NOBAT-NBATCH)999,999,1000
 1000 STOP
      END
```

```
$IBFTC DECK2
      SUBROUTINE BRAI(SEC,DIFF,AOK,ALRAT,FZERO,RAT,FONE,FTWO,FTHRI)
C     LOG((T+DT)/AOK)   CALLED  RLTDT
C     LOG(T/AOK)        CALLED  RLTIM
C     LOG(1.+PER/T)     CALLED  RLD
C     BETA IS LINE SOURCE PART OF FZERO
C     GAMMA IS SECOND PART OF FZERO
      PER=.1
      EULER=EXP(.5772156649)
      RLTDT=ALOG((4.*(SEC+PER))/(AOK*EULER))
      RLTIM=ALOG((4.*SEC)/(AOK*EULER))
      RLD=ALOG(1.+(PER/SEC))
      BETA=(SEC/PER)*RLD+(ALOG(SEC+PER))
      GAMMA=((AOK/(2.*PER))*RLD)+ALRAT*(AOK/(4.*PER))*((RLTDT**2)-(RLTIM
     1**2))
      RAT=GAMMA/BETA
      FZERO=BETA+GAMMA
      FONE=((SEC**2)*(RLD/PER))+(2.*SEC*RLTDT)-(3.*SEC)
      FTWO=((SEC**3)*(RLD/PER))+(3.*(SEC**2)*RLTDT)-5.5*(SEC**2)
      FTHRI=((SEC+PER)*(RLTDT**2))-(SEC*(RLTIM**2))-(2.*SEC*RLD)-(2.*PER
     1*RLTDT)+2.*PER
      RETURN
      END

$IBFTC DECK3
      SUBROUTINE POLYFT(X,Y,N,KOR,C,CO,A,NOUT,STDV,SMOOTH,RES)
C
C     DIMENSION FOR ARGUMENTS
      DIMENSION X(250),Y(250),A(400),C(200),SMOOTH(250),RES(250)
C
C     DIMENSION FOR SELF-GENERATED VALUES
      DIMENSION SUMX(200),SMYX(100),AMEANX(100)
      PTS= N
      NT = NOUT
      KTOR= 2*KOR
C
C     INITIALIZATION
      DO  1  I=1,KOR
      SMYX(I)= 0.0
    1 AMEANX(I)= 0.0
      DO  2  I=1,KTOR
    2 SUMX(I)= 0.0
      SUMY= 0.0
C
C     NORMALIZATION WITH RESPECT TO XMAX
      XMAX= X(1)
      DO  100  I=2,N
      IF( X(I) -XMAX) 100,101,101
  101 XMAX= X(I)
  100 CONTINUE
      DO  102  I=1,N
  102 X(I)= X(I)/XMAX
C
C
C     FORMULATION OF NORMAL EQUATIONS
      DO  3 J=1,KTOR
      DO  3 I=1,N
    3 SUMX(J)= SUMX(J) +X(I)**J
```

```
      DO  4  I=1,N
    4 SUMY= SUMY+ Y(I)
      AMEANY= SUMY/PTS
      DO  6 J=1,KOR
      AMEANX(J)= SUMX (J)/PTS
      DO  6 I=1,N
    6 SMYX(J)= SMYX(J) +Y(I)*X(I)**J
      DO  8 I=1,KOR
      C(I)= SMYX(I) -PTS*AMEANX(I)*AMEANY
      DO  8 J=1,KOR
      K= I+J
      IJ =(J-1)*KOR +I
    8 A(IJ) =SUMX(K) -PTS* AMEANX(I)*AMEANX(J)
C
C     CROUT'S  REDUCTION  METHOD
      DO  11 I=2,KOR
      III=(I-1)*KOR + 1
   11 A(III) = A(III)/ A(1)
      DO  12 J=2,KOR
      KM= J-1




      DO 14 I=J,KOR
      AP1= 0.0
      DO114 K=1,KM
      IK =(K-1)* KOR+ I
      KJ =(J-1)* KOR+ K
  114 AP1 = AP1 + A(IK) *A(KJ)
      IJ =(J-1)* KOR+ I
   14 A(IJ) = A(IJ) -AP1
      JP= J+1
      IF (JP- KOR) 444, 444, 445
  444 DO 16 I=JP,KOR
      AP1= 0.0
      DO116 K=1,KM
      JK =(K-1)* KOR + J
      KI =(I-1)* KOR + K
  116 AP1=AP1+A(JK)*A(KI)
      JI =(I-1)* KOR  + J
      JJ =(J-1)* KOR + J
   16 A(JI) = (A(JI) -AP1)/A(JJ)
  445 DUMMY= 0.0
   12 CONTINUE
      C(1) =C(1)/A(1)
      DO  18 I=2,KOR
      AP1= 0.0
      IM=I-1
      DO 118 K=1,IM
      IK =(K-1)* KOR + I
  118 AP1=AP1 +A(IK) *C(K)
      II =(I-1)* KOR + I
   18 C(I) =(C(I)- AP1) / A(II)
      KORM= KOR-1
      IF (KORM) 122, 123,122
  122 DO  21 I=1,KORM
      AP1= 0.0
      M= KOR-I
```

```
      MP= M+1
      DO 121 K=MP,KOR
      MK =(K-1)* KOR +M
  121 AP1 =AP1 + A(MK)* C(K)
   21 C(M) =C(M) -AP1
  123 AP1= 0.0
      DO 24  I=1,KOR
   24 AP1 =AP1 +AMEANX(I) *C(I)
      CO  = AMEANY -AP1
C
C     END OF POLYFT
      SRES=0.0
      DO 77 I=1,N
      SMOOTH(I)=CO
      DO 27 J=1,KOR
   27 SMOOTH(I)=SMOOTH(I)+C(J)*X(I)**J
      RES(I)=Y(I)-SMOOTH(I)
      SRES=SRES+RES(I)**2
C
C     DENORMALIZATION WITH RESPECT TO XMAX
      X(I)=X(I)*XMAX



   77 CONTINUE
      STDV=SQRT(SRES/PTS)
      DO 28 I=1,KOR
   28 C(I)=C(I)/(XMAX**I)
      RETURN
      END
```

APPENDIX IIIB
PROGRAM WRITTEN FOR SMOOTHING DR/DT DATA

THE POLYNOMIAL FITTING ROUTINE IS THE SAME ONE THAT WAS USED IN THE PROGRAM FOR PROCESSING VOLTAGE VS TIME DATA AND WILL NOT BE REPRODUCED AGAIN.

```
      DIMENSION X(50),Y(50),A(400),C(50),PRESS(10),NC(20),THERMR(10,20)
      DIMENSION CELVT(10,20),SVOLT(10,20),T(10),TEMP(10,20),CELLR(10,20)
      DIMENSION CC(20),TT(20),P0(10),PP(10,5),R(10),R0(10),R1(10),R2(10)
      DIMENSION TCRCRS(10),RR(20)
      NORMAX=3
      R0=24.3978
      ALFA=0.00392669
      BETA=0.1093
      DELTA=1.4936
      STANR=10.0008
  555 READ(5,100)NP
  100 FORMAT(I3)
 1300 DO 300 I=1,NP
      READ(5,101)PRESS(I)
  101 FORMAT(F9.2)
      READ(5,102)NC(I)
```

```
 102 FORMAT(I3)
     NNC=NC(I)
1301 DO 301 J=1,NNC
     READ(5,103)THERMR(I,J),CELVT(I,J),SVOLT(I,J)
 103 FORMAT(3E12.5)
     K=1
     T(K)=(THERMR(I,J)-R0)/(ALFA*R0)
 400 T(K+1)=(THERMR(I,J)-R0)/(ALFA*R0)+DELTA*((T(K)/100.)-1.)*(T(K)/100
    1.)+BETA*((T(K)/100.)-1.)*((T(K)/100.)**3)
     STEP=ABS(T(K+1)-T(K))
     K=K+1
1401 IF(STEP .GE. .000001)GO TO 400
     TEMP(I,J)=T(K)
     CELLR(I,J)=(CELVT(I,J)*STANR)/SVOLT(I,J)
 301 CONTINUE
 300 CONTINUE
     TCROSS=30.
     IIMAX=7
1302 DO 302 LL=1,NORMAX
1304 DO 304 I=1,NP
     NNC=NC(I)
1305 DO 305 J=1,NNC
     CC(J)=CELLR(I,J)
     TT(J)=TEMP(I,J)
 305 CONTINUE
     N=NNC
     KOR=1
     NOUT=-1
     CALL POLYFT(TT,CC,N,KOR,C,CO,A,NOUT)




     PO(I)=CO
1306 DO 306 K=1,LL
     PP(I,K)=C(K)
 306 CONTINUE
 304 CONTINUE
1320 DO 320 II=1,IIMAX
1321 DO 321 I=1,NP
     R(I)=PO(I)
1307 DO 307 K=1,LL
     R(I)=R(I)+(PP(I,K)*(TCROSS**K))
 307 CONTINUE
 321 CONTINUE
     N=NP
     KOR=2
     NOUT=-1
     CALL POLYFT(PRESS,R,N,KOR,C,CO,A,NOUT)
     RO(II)=CO
     R1(II)=C(1)
     R2(II)=C(2)
     TCROSS=TCROSS+10.
 320 CONTINUE
1308 DO 308 I=1,NP
     TCRCRS(1)=30.
1309 DO 309 II=1,IIMAX
     RR(II)= RO(II)+R1(II)*PRESS(I)+R2(II)*(PRESS(I)**2)
     TCRCRS(II+1)=TCRCRS(II)+10.
```

```
  309 CONTINUE
      N=IIMAX
      KOR=LL
      NOUT=6
      CALL POLYFT(TCRCRS,RR,N,KOR,C,CO,A,NOUT)
      WRITE(6,200)PRESS(I),LL
  200 FORMAT(//////8X,13HDRDT CALC FOR,2X,F9.2,3X,11HATMOSPHERE5,10X,13H
     1POLYNOM ORDER,2X,I2)
      WRITE(6,201)
  201 FORMAT(//12X,4HTEMP,11X,4HDRDT,11X,6HCELL R)
      NNC=NC(I)
      NCC=NNC+3
      MA=NCC-2
      MB=NCC-1
      MC=NCC
 1310 DO 310 J=1,NCC
      TEMP(I,MA)=30.
      TEMP(I,MB)=60.
      TEMP(I,MC)=90.
      RESFIT=CO
 1311 DO 311 K=1,LL
      RESFIT=RESFIT+C(K)*(TEMP(I,J)**K)
  311 CONTINUE
      DRDT=C(1)
      IF(LL .LE. 1)GO TO 401
 1312 DO 312 K=2,LL
      KK=K-1
      DRDT=DRDT+(FLOAT(K))*C(K)*(TEMP(I,J)**KK)
  312 CONTINUE
  401 WRITE(6,202)TEMP(I,J),DRDT,RESFIT



  202 FORMAT(8X,3(E13.6,2X))
  310 CONTINUE
  308 CONTINUE
  302 CONTINUE
      GO TO 555
      END
```

APPENDIX IIIC

PROGRAM WRITTEN FOR CALCULATING TEMPERATURE PROFILES IN INFINITE SLAB.

THE CRANK -NICHOLSON METHOD HAS BEEN USED WITH SUCCESSIVE OVER RELAXATION.

```
      DIMENSION U(100,50),T(100),BJ(100)
      DIMENSION TIME(5)
C**** NONLINEAR SLAB FDS
      S=.1
      S5=S/2.
      BB=1.1
      NTT=0
      JJ=0
      TIME(1)=.06
```

```
      TIME(2)=.3
      TIME(3)=.6
      PIE=3.14159265358
      NMAX=50
      NK=500
      NH=40
      NH1=NH+1
      NH2=NH**2
      R=FLOAT(NH2)/FLOAT(NK)
      R5=R/2.
      RP1=R+1.
      RR= R/(2.*RP1)
      S=2.*R+2.
      RMU=(R/RP1)*(COS(PIE/(FLOAT(NH1))))
      W=2./(1.+SQRT(1.-(RMU**2)))
 1300 DO 300 N=1,NMAX
      U(1,N)=0.0
  300 CONTINUE
      NN=NH/10
 1301 DO 301 I=1,NH1
      T(I)=1.0
  301 CONTINUE
  555 N=1
      NTT=NTT+1
      T(NH1+1)=T(NH1-1)
 1302 DO 302 I=2,NH1
      AP5J=R*(1.+(S5*(T(I+1)+T(I))))
      AM5J=R*(1.+(S5*(T(I-1)+T(I))))
      BRA=AP5J*(T(I+1)-T(I))-AM5J*(T(I)-T(I-1))
      BJ(I)=T(I)+(.5)*BRA
      U(I,1)=T(I)
  302 CONTINUE
  420 NLOOP=1
 1303 DO 303 I=2,NH
      BRA2=(R*S5)*(U(I+1,N)**2)+R*U(I+1,N)
      BRA3=(R*S5)*(U(I-1,N+1)**2)+R*U(I-1,N+1)+2.*BJ(I)
      BRA23=4.*S*R*(BRA2+BRA3)
      ROOT=SQRT((B**2)+BRA23)
      DELTA=((ROOT-B)/(2.*S*R))-U(I,N)



      DD=W*DELTA
      U(I,N+1)=U(I,N)+DD
      Q=ABS(DD/U(I,N+1))
      IF(Q .LE. .0001)GO TO 303
      NLOOP=2
  303 CONTINUE
      I=NH1
      U(NH1+1,N)=U(NH1-1,N+1)
      BRA2=(R*S5)*(U(I+1,N)**2)+R*U(I+1,N)
      BRA3=(R*S5)*(U(I-1,N+1)**2)+R*U(I-1,N+1)+2.*BJ(I)
      BRA23=4.*S*R*(BRA2+BRA3)
      ROOT=SQRT((B**2)+BRA23)
      DELTA=((ROOT-B)/(2.*S*R))-U(I,N)
      DD=W*DELTA
      U(I,N+1)=U(I,N)+DD
      Q=ABS(DD/U(I,N+1))
```

```
      IF(U .LE. .0001)GO TO 501
      NLOOP=2
  501 CONTINUE
      IF(NLOOP .LT. 2)GO TO 1304
  400 N=N+1
      GO TO 420
 1304 DO 304 I=1,NH1
      T(I)=U(I,N+1)
  304 CONTINUE
      IF(NTT-30)555,198,402
  402 IF(NTT-150)555,198,403
  403 IF(NTT-300)555,198,198
  198 JJ=JJ+1
      WRITE(6,200)TIME(JJ)
  200 FORMAT(1H1,7X,4HTAU=,F9.2)
      WRITE(6,201)
  201 FORMAT(///4X,4HBETA,7X,5HTHETA,10X,3HNTR)
 1306 DO 306 I=1,NH1,NN
      BB=BB-.1
      WRITE(6,202)BB,T(I),N
  202 FORMAT(2X,F9.2,2X,E15.8,3X,I3)
  306 CONTINUE
      BB=1.1
      IF(NTT .LT. 300)GO TO 555
      STOP
      END
```

APPENDIX IIID

PROGRAM RWITTEN FOR CALCULATING TEMPERATURE PROFILES IN AN INFINITE SLAB, USING THE KUDRYASHEV-ZHEMKOV TRANSFORMATIO

```
      DIMENSION TAU(10),B(20),V(50),XSI(10)
      COMMON /F1/BB,SIGMA
      COMMON /F2/K,G(50),A(50)
      SIGMA=.1
      XSI(1)=0.0
      TAU(1)=0.0
      TAU(2)=.06
      TAU(3)=.3
      TAU(4)=.6
      B(1)=0.0
      B(2)=.2
      B(3)=.3
      B(4)=.4
      B(5)=.5
      B(6)=.6
      B(7)=.7
      B(8)=.8
      B(9)=.9
      B(10)=.95
 1300 DO 300 I=1,10
      BB=B(I)
 1301 DO 301 J=2,4
      K=2
```

```
      T=TAU(J)-TAU(J-1)+XSI(J-1)
      V(1)=TEMP(T)
      Z=TAU(J)
      ZM=TAU(J-1)
  400 CALL BIGSUM(Z,ZM,S)
      TIN=TAU(J)+(SIGMA*S)-TAU(J-1)+XSI(J-1)
      V(K)=TEMP(TIN)
      WRITE(6,205)K,V(K)
  205 FORMAT(1H0,3X,2HK=,I3,5X,2HV=,E15.8)
      DV=ABS(V(K)-V(K-1))
      IF(DV .LT. .00001)GO TO 401
      K=K+1
      NP=88
      IF(K .GT. 30)GO TO 401
      NP=1
      DUMG=-V(K)/S
      DUMA=(SIGMA*S)
      IF(K .LT. 3)GO TO 399
      LL=K-1
 1302 DO 302 L=2,LL
      DUMG=DUMG-G(L)
      DUMA=DUMA-(A(L)*(EXP(-G(L)*TAU(J))))
  302 CONTINUE
  399 G(K)=DUMG
      A(K)=DUMA*(EXP(G(K)*TAU(J)))



      GO TO 400
  401 CONTINUE
      XSI(J)=TIN
      WRITE(6,201)BB
  201 FORMAT(/1X,5HBETA=,F9.5)
      WRITE(6,202)TAU(J)
  202 FORMAT(2X,4HTAU=,F9.5)
      IF(NP .GT. 2)GO TO 402
      WRITE(6,203)K,V(K),TIN
  203 FORMAT(7X,I2,7HTH APRX,2(E15.8,3X))
      GO TO 403
  402 WRITE(6,204)K,V(K),TIN
  204 FORMAT(7X,I2,7HTH APRX,2(E15.8,3X),3X,3H***)
  403 CONTINUE
  301 CONTINUE
  300 CONTINUE
      STOP
      END
      SUBROUTINE BIGSUM(T,TM,S)
      DIMENSION U(16),TT(16),R(16)
      COMMON /F2/K,G(50),A(50)
      U(1) =-.98940093
      U(2) =-.94457502
      U(3) =-.86563120
      U(4) =-.75540441
      U(5) =-.61787624
      U(6) =-.45801678
      U(7) =-.28160355
      U(8) =-.09501251
      U(9) =-U(8)
```

```
      U(10)=-U(7)
      U(11)=-U(6)
      U(12)=-U(5)
      U(13)=-U(4)
      U(14)=-U(3)
      U(15)=-U(2)
      U(16)=-U(1)
      R(1) = .02715246
      R(2) = .06225352
      R(3)= .09515851
      R(4) = .12462897
      R(5) = .14959599
      R(6) = .16915652
      R(7) = .18260341
      R(8) = .18945061
      R(9) = R(8)
      R(10) = R(7)
      R(11)= R(6)
      R(12)= R(5)
      R(13)=R(4)
      R(14)= R(3)
      R(15)= R(2)
      R(16)= R(1)


      DUMMY=0.0
      D=(T-TM)/2.
 1300 DO 300 L=1,16
      Q=D*U(L)+TM+D
      XSI=Q
 1301 DO 301 M=2,K
      XSI=A(M)*(EXP(-G(M)*Q))+XSI
  301 CONTINUE
      TT(L)=TEMP(XSI)
      DUMMY=DUMMY+(R(L)*TT(L))
  300 CONTINUE
      S=D*DUMMY
      RETURN
      END
      FUNCTION TEMP(T)
      DIMENSION A(20),B(20),C(20)
      COMMON /F1/BB,SIGMA
      PIE=3.14159265358
      A0=2.46740110
      B0=PIE/2.
      A(1)= 22.20660990
      A(2)= 61.68502751
      A(3)=120.90265391
      A(4)=199.85948912
      A(5)=298.55553313
      A(6)=416.99078594
      A(7)=555.16524755
      A(8)=713.07891797
      A(9)=890.73179719
      B(1)=  4.712388980
      B(2)=  7.853981634
      B(3)= 10.995574288
```

```
      B(4)= 14.137166941
      B(5)= 17.278759595
      B(6)= 20.420352248
      B(7)= 23.561944902
      B(8)= 26.703537555
      B(9)= 29.845130209
      C(1)=-.333333333
      C(2)=+.200
      C(3)=-.142857143
      C(4)=+.111111111
      C(5)=-.090909091
      C(6)=+.076923077
      C(7)=-.066666666
      C(8)=+.058823524
      C(9)=-.052631579
      SUM=(EXP(-(A0*T)))*(COS(B0*BB))
 1701 DO 701 K=1,9
      SUM=SUM+(C(K))*(EXP(-(A(K)*T)))*(COS(B(K)*BB))
  701 CONTINUE
      S=(4./PIE)*SUM*(1.+(SIGMA/2.))
      IF(SIGMA .GT. 0.0)GO TO 600
      TEMP=S
      GO TO 601
  600 TEMP=(-1.+SQRT(1.+(2.*SIGMA*S)))/SIGMA
  601 RETURN
      END
```

APPENDIX IIIE

PROGRAM WRITTEN FOR CALCULATING THERMAL CONDUCTIVITIES OF CHAIN MOLECULES FROM THE CELL MODEL FOR PURE POLYMERS

```
      INTEGER PRESS
      DIMENSION KIND(10),RO(10,15,15),EPS(10),W(10),N(10),MJ(10)
      DIMENSION TEMP(10,15,15)
      DIMENSION VSTAR(10),TCOND(10,15,15),NK(10,15),PRESS(10,15)
      NI=5
C
C     NK  DEPENDS ON PRESSURE
C     RO IN  CC/MOLE IN SFERIK  ***   GM/CC IN CHAIN
C     CV IN   J/(DEGK * MOLE)
C     I=SUBSTANE, J=PRESS., K=TEMP.
C     INPUTS 100,OUTPUTS 200 , DOS 300, IFS 600, ARIT 700
C       NI ETC NO OF SUBSTANCES, TEMP, PRESS
C
      DO 301 I=1,NI
      READ(5,102)EPS(I),W(I),KIND(I),VSTAR(I),MJ(I)
  102 FORMAT(E12.5,E12.5,I1,E12.5,I2)
  600 READ(5,104)N(I)
  104 FORMAT(I2)
      NJ=MJ(I)
      DO 301 J=1,NJ
      READ(5,110) NK(I,J),PRESS(I,J)
  110 FORMAT(I2,I5)
      MK=NK(I,J)
      DO 301 K=1,MK
```

```
      READ(5,103)RO(I,J,K),TEMP(I,J,K)
  103 FORMAT(E12.5,E12.5)
  301 CONTINUE
      DO 304 I=1,NI
      ENE=EPS(I)
      WMOL=W(I)
      NOSEG=N(I)
C           * DE=RO * ENE=EPS * WMOL=W * NOSEG=N * VOLUM=VSTAR
      NJ=MJ(I)
      DO 302 J=1,NJ
      MK=NK(I,J)
      DO 302 K=1,MK
      DE=RO(I,J,K)
      VOLUM=VSTAR(I)
      WRITE(6,250)I,J,K
  250 FORMAT(1H0,2X,2HI=,I3,5X,2HJ=,I3,5X,2HK=,I3)
      CALL CHAIN(DE,ENE,VOLUM,WMOL,NOSEG,THCON)
      TCOND(I,J,K)=THCON
  302 CONTINUE
  304 CONTINUE
      DO 305 I=1,NI



  650 WRITE(6,202)I,KIND(I),N(I),EPS(I)
  202 FORMAT(1HI,2X,2HI=,I2,3H,  ,5HTYPE ,I1,3X,6HNOSEG=,I2,3X,9HEPSILON
     1= ,E12.5)
      NJ=MJ(I)
      DO 305 J=1,NJ
      WRITE(6,204)PRESS(I,J),NK(I,J)
  204 FORMAT(1H0,2X,13H****PRESSURE=,I5,1X,2X,3HBAR,10X,I2,1X,5HTEMPS)
      WRITE(6,205)
  205 FORMAT(1H0,4X,4HTEMP,7X,7HTH,COND,9X,7HDENSITY,13X,1HI,5X,1HJ,5X,1
     1HK)
      WRITE(6,206)
  206 FORMAT(4X,3H(C),7X,12HJ/(K*CM*SEC),7X,7H(GM/CC))
      MK=NK(I,J)
      DO 305 K=1,MK
      WRITE(6,207)TEMP(I,J,K),TCOND(I,J,K),RO(I,J,K),I,J,K
  207 FORMAT(3X,F6.2,4X,E12.5,4X,E12.5,10X,I2,4X,I2,4X,I2)
  305 CONTINUE
      WRITE(6,217)
  217 FORMAT(1H0,2X,15HTHATS ALL FOLKS)
      CALL EXIT
      END
      SUBROUTINE CHAIN(DE,ENE,VOLUM,WMOL,NOSEG,THCON)
      B= 1.3800E-23
      F=.5
      CV=3.*B*F
      SR2=SQRT(2.0)
      AVO=6.02252E+23
      PIE=3.14159265
      WSEG= WMOL/(AVO*FLOAT(NOSEG))
      VAV= (WMOL/(DE*AVO*FLOAT(NOSEG)))
      ACUB=VAV*SR2
C     ALF  IS LOG OF A
      ALF=(ALOG(ACUB))/3.
      A=EXP(ALF)
```

```
      X=22.11
      Y=-10.56
      Z=12.
      V=VOLUM/VAV
      BRA1= X*(V**4)+Y*(V**2)
      ERA2=(2.*ENE*(Z-2.+(2./FLOAT(NOSEG))))/(A**2)
      B12= BRA1*BRA2
      BRA12=SQRT(B12)
      WSQ= SQRT(WSEG)
      BRA3=   (SR2*CV/A)/(2.*PIE*WSQ)
      THCON= BRA12*BRA3
      WRITE(6,207)NOSEG,WSEG,VAV,SR2,ACUB,ALF,A,V,WMOL
  207 FORMAT(I2,3X,E12.5,3X,E12.5,3X,E12.5,3X,E12.5,3X,E12.5,3X,E12.5,3X
     1,E12.5,3X,E12.5)
      WRITE(6,208)BRA1,BRA2,B12,BRA12,WSQ,BRA3,THCON,CV
  208 FORMAT(3X,3X,3X,E12.5,3X,E12.5,3X,E12.5,3X,E12.5,3X,E12.5,3X,E12.5
     1,3X,E12.5,3X,E12.5)
      RETURN
      END
```

APPENDIX IIIF

PROGRAM WRITTEN FOR CALCULATING XSI AND V1*/V

THESE RESULTS WERE USED IN CALCULATING VISCOSITIES AND THERMAL CONDUCTIVITIES OF DENSE HARD SPHERE FLUID MIXTURES

```
      DIMENSION P(20),R(20),X1(20),X2(20)
      COMMON /TR1/A,B,C,D,FR1,FR2,RAT,G
      P(1)=.04
      P(2)=.07
      P(3)=.1
      P(4)=.2
      P(5)=.3
      P(6)=.4
      P(7)=.5
      P(8)=.6
      P(9)=.7
      P(10)=.8
      P(11)=.9
      R(1)=.5
      R(2)=.66667
      R(3)=1.0
      R(4)=1.5
      X2(1)=1.0
      X1(1)=0.0
 1300 DO 300 I=2,11
      X1(I)=X1(I-1)+.1
      X2(I)=1.-X1(I)
  300 CONTINUE
C     I LOOP PVKT
C     J LOOP R
C     K LOOP COMP
      NI=11
      NJ=4
      NK=11
 1301 DO 301 I=7,NI
```

```
      WRITE(6,200)P(I)
  200 FORMAT(1H1,5X,3HP*=,F6.2)
      W=P(I)
 1302 DO 302 J=1,NJ
      WRITE(6,201)
  201 FORMAT(/13X,1HX,9X,3HXSI,11X,3HPHI,12X,1HA,13X,1HB,13X,1HC,13X,1HD
     1,8X,3HNTR,3X,2HIN,3X,2HNR)
      WRITE(6,202)R(J)
  202 FORMAT(5X,3HR =,F14.9)
 1303 DO 303 K=1,NK
      G =X1(K)+(X2(K)*(R(J)**3))
      GG=X1(K)+(X2(K)*(R(J)**2))
      Z1=(1.-R(J))**2
      Z2= (1.+R(J))
      A=      -(3.*X1(K)*X2(K)*Z1*R(J)*(GG/G))+((W*(G**2))+G)
      B=-(3.*X1(K)*X2(K)*Z1*Z2)+G-3.*W*(G**2)
      C=(3.*W*(G**2))+G



      D=-W*(G**2)
      DISC=(4.*(B**2))-(12.*A*C)
      IF(DISC .LT. 0.)GO TO 499
      AA=-A
      BB=-B
      CC=-C
      DD=-D
      F1=(-2.*B+SQRT((4.*(B**2))-(12.*A*C)))/(6.*A)
      F2=(-2.*B-SQRT((4.*(B**2))-(12.*A*C)))/(6.*A)
      DELTA=ABS(F2-F1)
      FR1=X1(K)
      FR2=X2(K*
      RAT=R(J)
      NGO=0
      IF(F1 .GT. 0. .AND. F1 .LT. 1.)GO TO 400
      NGO=1
      N2GO=2
  400 IF(F2 .GT. 0. .AND. F2 .LT. 1.)GO TO 401
      NGO=NGO+1
      N2GO=1
  401 IF(NGO-1)404,403,402
C**** ROUTE 1
  402 NR=1
      Q1=.3
      Q2=.32
      IN=1
      CALL TRIALS(Q1,Q2,IN,XX,PHI,NTR)
      GO TO 999
C
C**** ROUTE 88
C
  499 NR=88
      Q1=.3
      Q2=.32
      IN=1
      CALL TRIALS(Q1,Q2,IN,XX,PHI,NTR)
      GO TO 999
C
```

```
C**** ROUTE 2
C
  403 NR=2
      IF(N2GO .GT. 1)GO TO 405
      FD=F1
      FFD=A*(F1**3)+B*(F1**2)+C*F1+D
      GO TO 406
  405 FD=F2
      FFD=A*(F2**3)+B*(F2**2)+C*F2+D
  406 CONTINUE
      IF(FFD .GT. 0.)GO TO 407
      IN=2
      GO TO 408
  407 IN=1
  408 CONTINUE
      FD2=FD+(DELTA/4.)
      CALL TRIALS(FD,FD2,IN,XX,PHI,NTR)



      IF(XX .GT. 0. .AND. XX .LT. 1.)GO TO 409
      FD2=FD-(DELTA/4.)
      CALL TRIALS(FD,FD2,IN,XX,PHI,NTR)
  409 GO TO 999
C
C**** ROUTE 3
C
  404 CONTINUE
      FF1=A*(F1**3)+B*(F1**2)+C*F1+D
      FF2=A*(F2**3)+B*(F2**2)+C*F2+D
      FFF=FF2*FF1
      IF(FFF .GT. 0.)GO TO 420
C
C**** ROUTE 31
C
      NR=31
      IN=1
      CALL TRIALS(F1,F2,IN,XX,PHI,NTR)
      GO TO 999
C
C**** ROUTE 32
C
  420 CONTINUE
      NR=32
      IF(FF1 .GT. 0.)GO TO 421
      A2=AA
      B2=BB
      IN=2
      GO TO 422
  421 A2=A
      B2=B
      IN=1
  422 CONTINUE
      D2FDT1=(6.*A2*F1)+(2.*B2)
      D2FDT2=(6.*A2*F2)+(2.*B2)
      V=1.
      IF(D2FDT2 .LT. 0.)GO TO 423
      IF(F1 .GT. F2)GO TO 424
```

```
      V=-1.
  424 F3=F1+(V*(DELTA/4.))
      F4=F1
      GO TO 425
  423 IF(F1 .LT. F2)GO TO 426
      V=-1.
  426 F3=F2+(V*(DELTA/4.))
      F4=F2
  425 CONTINUE
      CALL TRIALS(F4,F3,IN,XX,PHI,NTR)
      GO TO 999
  999 CONTINUE
      WRITE(6,203)XI(K),XX,PHI,A,B,C,D,NTR,IN,NR
  203 FORMAT(1X,F6.3,6(2X,E12.5),3(2X,I3))
  303 CONTINUE
  302 CONTINUE
  301 CONTINUE
      STOP
      END



      SUBROUTINE TRIALS(P1,P2,IN,XX,PHI,NTR)
      COMMON /TRI/A,B,C,D,FR1,FR2,RAT,G
      IF(IN .LT. 2)GO TO 450
      A2=-A
      B2=-B
      C2=-C
      D2=-D
      GO TO 451
  450 A2=A
      B2=B
      C2=C
      D2=D
  451 CONTINUE
      XPD=0.0
      NTR=1
      Y2=A2*(P2**3)+B2*(P2**2)+C2*P2+D2
      Y1=A2*(P1**3)+B2*(P1**2)+C2*P1+D2
  453 S= (Y2-Y1)/(P2-P1)
      XX=P1-(Y1/S)
      DEL= ABS((XPD-XX)/XX)
      IF(DEL .LT. .000001)GO TO 452
      NTR=NTR+1
      XPD=XX
      P1=P2
      P2=XX
      Y1=Y2
      Y2=A2*(P2**3)+B2*(P2**2)+C2*P2+D2
      IF(NTR .LT. 4)GO TO 453
      IF(XX .GT. 0. .AND. XX .LT. 1.)GO TO 453
      XX=-1.
      PHI=1.
      RETURN
  452 CONTINUE
      PHI=XX/G
      RETURN
      END
```

```
C
C**** VISCOSITY
C
      DIMENSION P(20),RM(20),R(20),X1(20),X2(20),PHI(20,20)
      PIE=3.141592654
      Z1=4.*((4./25.)+(48./(25.*PIE)))
      P(1)= 1.
      P(2)= 2.
      P(3)= 4.
      P(4)= 8.
      P(5)=20.
      P(6)=30.
      RM(1)= .5
      RM(2)=1.
      RM(3)=2.
      R(1)= .5
      R(2)= .666667
      R(3)=1.0
      R(4)=1.5
      X1(1)=0.0
      X2(1)=1.0
 1300 DO 300 I=2,11
      X1(I)=X1(I-1)+.1
      X2(I)=X2(I-1)-.1
  300 CONTINUE
C**** I LOOP P      PV/KT
C**** J LOOP RM     MASS RATIO
C**** K LOOP R      RADIUS RATIO
C**** L LOOP X1     MOLE FRACTION
      NI=6
      NJ=3
      NK=4
      NL=11
 1301 DO 301 I=1,NI
      PP=P(I)
 1304 DO 304 K=1,NK
      READ(5,100)PHI(K,1),PHI(K,2),PHI(K,3),PHI(K,4),PHI(K,5)
  100 FORMAT(5(2X,E12.5))
      READ(5,101)PHI(K,6),PHI(K,7),PHI(K,8),PHI(K,9),PHI(K,10)
  101 FORMAT(5(2X,E12.5))
      READ(5,102)PHI(K,11)
  102 FORMAT(E12.5)
  304 CONTINUE
 1302 DO 302 J=1,NJ
      RRM=RM(J)
      BM1= 1./(1.+RRM)
      BM2=RRM/(1.+RRM)
      ZMU1= (40.)*((2./3.)+(.4*(BM1/BM2)))*(SQRT((BM1*BM2)/2.))
```

```
      ZMU2= (40.)*((2./3.)+(.4*(BM2/BM1)))*(SQRT((BM1*BM2)/2.))
      ZM15= SQRT(1./BM1)
      ZM25= SQRT(1./BM2)
      ZMU3=-(32./3.)*(SQRT((BM1*BM2)/2.))
      Z3S= ZMU3**2
      WRITE(6,200)P(I),RM(J)
  200 FORMAT(1H1,5X,3HP=,F6.3,2X,6HM2/M1=,F6.3)
 1303 DO 303 K=1,NK
      RR=R(K)
      WRITE(6,201)RR
  201 FORMAT(/12X,5HR2/1=,F10.7,6X,2HX1,10X,2HL*,12X,3HL**,12X,2HLK,12X,
     14HCOLL,12X,1HY)
      PHIP=PHI(K,NL)
      G=(2.+PHIP)/(2.*((1.-PHIP)**2))
      Z2=G*PHIP
      R1=((2.*RR)/(1.+RR))**2
      R2=(2./(1.+RR))**2
      NNL=NL-1
 1305 DO 305 L=1,11
      RX=X2(L)/X1(L)
      RXR=X1(L)/X2(L)
      OMR=1.-RR
      ZR3= X2(L)*(RR**3)
      ZXR= X1(L)+ZR3
      T=PHI(K,L)/ZXR
      F=T
      ZD=(1.-(T*ZXR))**2
      G1=(1.+(.5*T*ZXR)+(1.5*ZR3*T*(OMR/RR)))/ZD
      OPR=RR-1.
      G2=(1.+(.5*T*ZXR)+(1.5*X1(L)*T*OPR))/ZD
      G12=(1./(1.+RR))*((RR*G1)+G2)
      GG1=G1/G12
      GG2=G2/G12
      BRAX=1.+(1.6*X1(L)*T*G1)+(.4*BM2*G12*X2(L)*T*((1.+RR)**3))
      BRAY=1.+(1.6*ZR3*T*G2)+(.4*BM1*G12*X1(L)*T*((1.+RR)**3))
      CA=ZMU1+ (8.*RX*GG2*ZM25*R1)
      CB=ZMU2+ (8.*RXR*GG1*ZM15*R2)
      CAB=CA*CB
      DENOM=G12*(CAB-Z3S)
      A=(8.*RXR*R2*ZM15*CA)/DENOM
      B=(-16.*ZM15*R2*ZMU3)/DENOM
      C=(8.*RX*ZM15*R2*CB)/DENOM
      COEF=(768./(25.*PIE))*(T**2)
      FIRST=G1*(X1(L)**2)
      SECOND=(SQRT(BM2/32.))*G12*X1(L)*X2(L)*((1.+RR)**4)
      THIRD= (SQRT(BM2/BM1))*G2*(RR**4)*(X2(L)**2)
      D=COEF *(FIRST+SECOND+THIRD)
      COLL=D/F
      VRAT=((A*(BRAX**2)+B*BRAX*BRAY+C*(BRAY**2))+D)/F
      YY=(PP/T)-1.
      CIN=((A*BRAX)+((B/2.)*(BRAX+BRAY))+(C*BRAY))/F
      XDIST=BRAX-1.
      YDIST=BRAY-1.
      D1=XDIST*((A*BRAX)+((B/2.)*BRAY))
      D2=YDIST*((C*BRAY)+((B/2.)*BRAX))
```

```
      DIST=(D1+D2)/F
      DCOL=DIST+COLL
      TOTAL=CIN+DIST+COLL
      WRITE(6,202)X1(L),VRAT,TOTAL,CIN,DCOL,YY
  202 FORMAT(32X,F6.3,5(2X,E12.5))
  305 CONTINUE
  303 CONTINUE
  302 CONTINUE
  301 CONTINUE
      STOP
      END
```

APPENDIX IIIH

PROGRAM WRITTEN FOR CALCULATING THERMAL CONDUCTIVITY OF DENSE HARD SPHERE FLUID MIXTURES. FROM THE THORNE EXTENSION TO THE CHAPMAN-ENSKOG THEORY.

```
C
C**** THERMAL CONDUCTIVITY
C
      DIMENSION P(20),RM(20),R(20),X1(20),X2(20),PHI(20,20)
      PIE=3.141592654
      P(1)= 1.
      P(2)= 2.
      P(3)= 4.
      P(4)= 8.
      P(5)=20.
      P(6)=30.
      RM(1)= .5
      RM(2)=1.
      RM(3)=2.
      R(1)= .5
      R(2)= .666667
      R(3)=1.0
      R(4)=1.5
      X1(1)=0.0
      X2(1)=1.0
 1300 DO 300 I=2,11
      X1(I)=X1(I-1)+.1
      X2(I)=X2(I-1)-.1
  300 CONTINUE
C**** I LOOP P        PV/KT
C**** J LOOP RM       MASS RATIO
C**** K LOOP R        RADIUS RATIO
C**** L LOOP X1       MOLE FRACTION
      NI=6
      NJ=3
      NK=4
      NL=11
 1301 DO 301 I=1,NI
      PP=P(I)
 1304 DO 304 K=1,NK
```

```
      READ(5,100)PHI(K,1),PHI(K,2),PHI(K,3),PHI(K,4),PHI(K,5)
  100 FORMAT(5(2X,E12.5))
      READ(5,101)PHI(K,6),PHI(K,7),PHI(K,8),PHI(K,9),PHI(K,10)
  101 FORMAT(5(2X,E12.5))
      READ(5,102)PHI(K,11)
  102 FORMAT(E12.5)
  304 CONTINUE
 1302 DO 302 J=1,NJ
      RRM=RM(J)
      BM1= 1./(1.+RRM)
      BM2=RRM/(1.+RRM)
      ZM15=SQRT(1./BM1)
      ZM25=SQRT(1./BM2)
      Z12= 40.*(SQRT((BM1*BM2)/2.))
      BM1S=BM1**2
      BM2S=BM2**2
      SR2=SQRT(2.)
      ALFA=(Z12/BM1)*((.25*(6.*BM1S+5.*BM2S))-.6*BM2S+.8*BM1*BM2)
      BETA=(Z12/BM2)*((.25*(6.*BM2S+5.*BM1S))-.6*BM1S+.8*BM1*BM2)
      GAM= -(54./SR2)*BM1*BM2
      GS=GAM**2
      WRITE(6,200)P(I),RM(J)
  200 FORMAT(1HI,5X,3HP=,F6.3,2X,6HM2/M1=,F6.3)
 1303 DO 303 K=1,NK
      RR=R(K)
      WRITE(6,201)RR
  201 FORMAT(/12X,5HR2/1=,F10.7,6X,2HX1,10X,2HV=,12X,3HV=,12X,2HLK,12X,
     14HCOLL,12X,1HY)
      ZCON= 4.*((9./25.)+(32./(25.*PIE)))
      PHIP=PHI(K,11)
      G=(2.+PHIP)/(2.*((1.-PHIP)**2))
      Z2=G*PHIP
      R1=((2.*RR)/(1.+RR))**2
      R2=(2./(1.+RR))**2
      NNL=NL-1
 1305 DO 305 L=1,11
      RX=X2(L)/X1(L)
      RXR=X1(L)/X2(L)
      OMR=1.-RR
      ZR3=X2(L)*(RR**3)
      ZXR=X1(L)+ZR3
      T=PHI(K,L)/ZXR
      F=T
      ZD=(1.-(T*ZXR))**2
      G1=(1.+(.5*T*ZXR)+(1.5*ZR3*T*(OMR/RR)))/ZD
      OPR=RR-1.
      G2=(1.+(.5*T*ZXR)+(1.5*X1(L)*T*OPR))/ZD
      G12=(1./(1.+RR))*((RR*G1)+G2)
      GG1=G1/G12
      GG2=G2/G12
      BM12=BM1*BM2
      BRAX=1.+(2.4*G1*X1(L)*T)+(1.2*BM12*G12*X2(L)*T*((1.+RR)**3))
      BRAY=1.+(2.4*ZR3*T*G2)+(1.2*BM12*G12*X1(L)*T*((1.+RR)**3))
      CA=BETA+(8.*RX*GG2*R1*ZM25)
      CB=ALFA+(8.*RXR*GG1*ZM15*R2)
```

```
      DENOM=((CA*CB)-GS)*G12
      ZM125= ZM25/ZM15
      A=(8.*ZM15*R2*RXR*CA)/DENOM
      B=(-16.*R2*ZM25*GAM)/DENOM
      C=(8.*ZM125*R2*ZM25*CB*RX)/DENOM
      COEFF=(T**2)*(512./(25.*PIE))
      FIRST=G1*(X1(L)**2)
      SECOND=X1(L)*X2(L)*G12*BM1*(SQRT(BM2/8.))*((1.+RR)**4)
      THIRD=ZM125*(X2(L)**2)*(RR**4)*G2
      D=COEFF*(FIRST+SECOND+THIRD)
      COLL=D/F
      CRAT=((A*(BRAX**2))+(B*BRAX*BRAY)+(C*(BRAY**2))+D)/F
      YY=(PP/T)-1.
      CIN=((A*BRAX)+((B/2.)*(BRAX+BRAY))+(C*BRAY))/F
      XDIST=BRAX-1.
      YDIST=BRAY-1.



      D1=XDIST*((A*BRAX)+((B/2.)*BRAY))
      D2=YDIST*((C*BRAY)+((B/2.)*BRAX))
      DIST=(D1+D2)/F
      DCOL=DIST+COLL
      TOTAL=CIN+DIST+COLL
      WRITE(6,202)X1(L),CRAT,TOTAL,CIN,DCOL,YY
  202 FORMAT(32X,F6.3,5(2X,E12.5))
  305 CONTINUE
  303 CONTINUE
  302 CONTINUE
  301 CONTINUE
      STOP
      END
```

CHAPTER 1

1) Ziebland,H., "Thermal Conductivity," Edited by R.P.Tye, Academic Press, London, 1969. p.65.

2) Pittman,J.F.T., Ph.D. Thesis, University of London, 1968.

3) Horrocks,J.K. and McLaughlin,E., Trans.Far.Soc., 56, p.206, 1960.

4) Prigogine,I., "The Molecular Theory of Solutions," N.Holland Publishing Co., Amsterdam, 1957, Chapter 16.

5) Horrocks,J.K. and McLaughlin,E., Proc.Roy.Soc., 273A, p.259,1963.

6) Chapman,S. and Cowling,T.G., "The Mathematical Theory of Non-Uniform Gases," Cambridge University Press, 1953.a) p.292.

7) Lebowitz,J.L., Phys.Rev., 133, pA895, 1964.

8) Percus,J.K. and Yevick,G.J., Phys.Rev., 100, p1, 1958.

9) McLaughlin,E., Jour.Chem.Phys., 50, p1254, 1969.

10) Longuet-Higgins,H.C., Pople,J.A. and Valleau,J.P., "Transport Processes in Statistical Mechanics," Interscience Publishers Inc., London,1958, p.73.

CHAPTER 2

(1) Bird,R.B., Stewart,W.E. and Lightfoot,W.L., "Transport Phenomena," J.Wiley Inc., (1960)

(2) McLaughlin,E., Chem.Rev., 64, 389, 1964.

(3) Goldstein,P.J. and Briggs,D.G., Trans.ASME (Heat Transfer), 86, p 490, 1964.

(4) Pittman,J.F.T., Ph.D. Thesis, University of London, 1968.

a) 232 d) 135

b) 80 e) 290

c) 99 g) 111

(5) Carslaw,H.S. and Jaeger,J.C., "Conduction of Heat in Solids", 2nd Edition, Oxford University Press.

a) 261

b) 345

c) 152

(6) Jaeger,J.C., Jour.and Proc. of Roy.Soc. N.S.W., 74, 1940, p 342.

(7) Kudryashev,L.I. and Zhemkov,L.N., Izv.Vyssh. Uchhebn.Zav. Priborostr, 6, p 100, 1958.

(8) Fischer,J., Ann.Phys., Lpz., 34, p 669, 1939.

(9) Abramovitz,M and Stegun,I., Editors, "Handbook of Mathematical Functions," N.B.S., Washington,D.C. U.S.A.,1964; p360.

(10) Horrocks,J.K. and McLaughlin,E., Proc.Roy.Soc., A 273, 1963.

a) 262, c) 269

b) 259,

(11) Leidenfrost,W., Paper presented to the Thermal Conductivity Conference, Gatlinburg, Tennessee, 1963.

(12) Briggs,D.G., Ph.D. Thesis, University of Minnesota, Univ. Microfilms Inc., Ann Arbor, Michigan.

(13) Van der Held,E.F.M. and Van Drunen,F.G., Physica, 15, 865, 1949.

(14) Gebhart and Dring, Trans.ASME, (c), p 274, 1967.

(15) Viskanta,R., Ph.D. Thesis, University of Illinois, 1959.

(16) Poltz,H., Int.J.Heat and Mass Transf., 8, p 609, 1965.

(17) Ibid, 9, p 315, 1960

(18) Poltz,H. and Jugel,R., Int.J.Ht.M.Transf., V10, p 1075, 1967.

CHAPTER 3

(1) Horrocks,J.K. and McLaughlin,E., Proc.Roy.Soc.,1963, A273, a) p 259.

b) p 261.

(2) Fischer,J., Ann.Phys., Lpz., 34, p 669, 1939.

(3) Pittman,J.F.T., Ph.D. Thesis, University of London, 1968.

a) Chapter 3

b) p 140

(4) Goldstoin,R.J. and Briggs,D.G., Trans.ASME (Heat Transfer), 86, 490, 1964.

(5) International Critical Tables, V6, p 137.

CHAPTER 4

1) International Critical Tables, Vol, p115.

2) Francis,A.W., Chem.Eng.Sci., 10, p37, 1959.

3) Toohey,A.C., Ph.D. Thesis, Imperial College of Science and Technology, 1961, p208.

4) Bridgman, P.W., "The Physics of High Pressure", p129, G.Bell and Sons, London,1949.

5) Pittman,J.F.T., Ph.D. Thesis, University of London, 1968, p185.

CHAPTER 5

(1) Hays, D.F., "Non-Equilibrium Thermodynamics Variational Techniques and Stability", p.17, University of Chichago Press, 1966.

(2) Kudryashev, L.I. and Zhemkov, L.N., Izv.Vyssh. Uchhebn. Zav. Priborostr, 6, p.100, 1958.

(3) Carslaw, H.S. and Jaeger, J.C., "Conduction of Heat in Solids", p.97, Oxford University Press, 2nd Edition.

(4) Richtmyer, R.D., "Difference Methods for Initial Value Problems", Interscience Pub. Co., N.Y., 1957, p.101

(5) Smith, G.D., "Numerical Solution of Partial Differential Equations", Oxford University Press, London, 1965.

CHAPTER 6.

(1) Barker,J.A., "Lattice Theories of the Liquid State," Pergamon Press, 1963.

a) p 48 d) p 80

b) p 66 e) p 84

c) p 78

(2) Lennard-Jones,J.E. and Devonshire,A.F., Proc.Roy.Soc., A 163, p 53, 1937.

(3) Ibid, A 165, p 1, 1938.

(4) Prigogine,I., "The Molecular Theory of Solutions," N. Holland Pub.Co., Amsterdam, 1957.

a) p 130 c) p 337

b) Ch. 16 d) p 331

(5) Kirkwood,J.G., J.Chem.Phys., 18, p 380, 1950.

(6) Barker,J.A. Proc.Roy.Soc., A 237, p 63, 1956.

(7) Poplo, J.A., Phil.Mag., 42, p 459, 1951.

(8) Janssens,P. and Prigogine,I., Physica, 16, p 895, 1950.

(9) Hijmans,J., Physica, 27, p 433, 1961.

Chapter 7

1 Horrocks, J.K. and McLaughlin, E., Trans. Farad. Soc., 56 , 1960.

a) 206

b) 209

2 Prigogine, I., "The Molecular Theory of Solutions", N. Holland Pub. Co., Amsterdam, 1957, p 339.

3 International Critical Tables, V3 , pp 29-33.

4 I. Chem. E., Physical Data and Reaction Kinetics Committee, 1967.

5 Horrocks, J.K. and McLaughlin, E, Trans. Farad. Soc., 59,p 1709, 1963.

CHAPTER 8

1) Chapman, S. and Cowling, T.G., "The Mathematical Theory of Non-Uniform Gases", Cambridge University Press, Second Edition, 1952, London.

   a) P. 28

   b) P. 112

   c) P. 111

   d) P. 169

   e) Ch. 16

   f) P. 287

   g) P. 286

2) Dahler, J.S., Journ.Chem.Phys., 27, P. 1428, 1957.

3) Louguet-Higgins, H.C., and Pople, J.A., Jour.Chem.Phys, 25, P.884, 1956.

4) Rowlinson, J.S., Rep.Prog.Phys., 28, P.174, 1965.

5) Ornstein, L.S. and Zernike, F., Proc.Acad.Sci. Amsterdam, 17, P. 793, 1914.

6) Percus, J.K., and Yevick G.J., Phys.Rev., 110, P. 1, 1958.

7) Thiele, E., Jour.Chem.Phys., 39, P.474, 1963.

CHAPTER 9

(1) Chapman,S. and Cowling,T.G, "The Mathematical Theory of Non-Uniform Gases," Cambridge University Press, Second Edition, 1952, London.

a) Chapters 8 and 9.

b) p 166

c) p 167

d) pp 292-294

e) p 293

(2) Longuet-Higgins,H.C., Pople,J.A. and Valleau,J.P., 1958, "Transport Processes in Statistical Mechanics." (London, Interscience Publishers)

a) p 80

b) p 83

(3) Lebowitz,J.L., Phys.Rev., 133, p A895, 1964.

(4) Lebowitz,J.L. and Rowlinson,J.S., Jour.Chem.Phys., 41, p 133, 1964.

(5) McConalogue,D.J. and McLaughlin,E., Mol.Phys., 1969 to be published.

(6) McLaughlin,E., Chem.Rev., 64, p 403, 1964.

(7) Bearman,R.J. and Vaidhyanathan,V.S., Jour.Chem.Phys., 34, p 264, 1961.

(8) Boon,J.P. and Thomaes,G., Physica, 29, p 123, 1963.

(9) Wood,S.E. and Brusie,J.P., Journ.Amer.Chem.Soc., 65, p 1891, 1943.

(10) Klitz,W. and Sapper,A., Z.Anorg.Allgem.Chem., 203, p 277, 1932.

(11) Rowlinson,J.S., "Liquids and Liquid Mixtures." p 50 and 56, Butterworths, London, 1959.

(12) Lambert,M. and Simon,M., Physica, 28, p 1191, 1962.

(13) Dobbs,E.R., and Jones,G.O., Rep.Prog.Phys., 20, p 560, 1957.

(14) McLaughlin,E., Jour.Chem.Phys., 50, p 1254, 1969.

CHAPTER 10

1 Chapman, S. and Cowling T.G, "The Mathematical Theory of Non-Uniform Gases," Cambridge University Press, Second Edition, 1964.

a) p. 142

b) p. 144

c) p. 293

2 Lebowitz,J.L., Phys.Rev., 133, A895, 1964.

3 McLaughlin,E., J.Chem.Phys., 50, 1254, 1969.

4 Longuet-Higgins,H.C., Pople,J.A. and Valleau,J.P., "Transport Processes in Statistical Mechanics," p.80. Interscience Pub.Ltd., London, 1958.

5 Tung,L.H. and Drickamer,H.G., J.Chem.Phys., 18, p 1031, 1950.

6 Horne,F.F. and Bearman,R.J., J.Chem.Phys., 37, p 2842, 1962.

7 Thomaes,G., Physica, 17, 885, 1951.

8 Wood,S.E., and Gray,J.A., III, J.Am.Chem.Soc., 74, 3729, 1952.

9 Blitz,W. and Sapper,A.,Z.Anorg.Allgem.Chem., 203, p.277, 1932.

10 Furry,W.H., Jones,R.C. and Onsager, Phys.Rev., 55, p 1083, 1939.

11 Drickamer,H.G., Mellow,E.W. and Tung,L.H., J.Chem.Phys., 18, P 945, 1950.

12 Dobbs,E.R., and Jones,G.D., Rep.Prog.Phys., 20, p 516, 1957.